A DISSERTATION ON

"EFFICACY OF ULTRASOUND ELASTOGRAPHY IN CHARACTERIZING FOCAL LIVER LESIONS WITH HISTOPATHOLOGIC CORRELATION"

Submitted to

THE TAMIL NADU Dr.M.G.R. MEDICAL UNIVERISTY

CHENNAI

In Partial fulfillment of the Regulations

For the Award of the degree

M.D. DEGREE BRANCH VIII

RADIODIAGNOSIS

MADRAS MEDICAL COLLEGE

CHENNAI

MAY - 2019

CERTIFICATE

This is to certify that the dissertation titled **"EFFICACY OF ULTRASOUND ELASTOGRAPHY IN CHARACTERIZING FOCAL LIVER LESIONS WITH HISTOPATHOLOGIC CORRELATION"** submitted by **Dr. NAGARAJAN.K. B,** appearing for **M.D. RADIODIAGNOSIS** degree examination in May 2019, is a bonafide record of work done by him, under my guidance and supervision in partial fulfillment of requirements of The Tamilnadu Dr. M.G.R Medical University, Chennai. I forward this to The Tamilnadu Dr. M.G.R Medical University, Chennai.

PROF.E. MANIMEKALA, MDRD, DNB,
Guide,
Associate Professor,
Barnard Institute of Radiology,
Madras Medical College &
Rajiv Gandhi Government
General Hospital,
Chennai – 600 003.

PROF.R. RAVI, M.D., D.M.R.D.,
Director & Professor,
Barnard Institute of Radiology,
Madras Medical College &
Rajiv Gandhi Government
General Hospital,
Chennai - 600 003.

PROF.R. JAYANTHI, M.D., FRCP(Glasg),
The Dean,
Madras medical college &
Rajiv Gandhi Government General Hospital,
Chennai - 600 003.

DECLARATION

I, **Dr. NAGARAJAN.K.B.,** certainly declare that this dissertation titled, **"EFFICACY OF ULTRASOUND ELASTOGRAPHY IN CHARACTERIZING FOCAL LIVER LESIONS WITH HISTOPATHOLOGIC CORRELATION**", represent a genuine work of mine, done at the Barnard Institute of Radiology, Madras Medical College and Rajiv Gandhi Government General Hospital, under the supervision of **PROF.Dr.E.MANIMEKALA, MDRD,DNB,** Associate Professor, Barnard Institute of Radiology, Madras Medical College and Rajiv Gandhi Government General Hospital.

I, also affirm that this bonafide work or part of this work was not submitted by me or any others for any award, degree or diploma to any other university board, neither in India or abroad. This is submitted to The Tamil Nadu Dr.MGR Medical University, Chennai in partial fulfillment of the rules and regulations for the award of M.D Degree in Radiodiagnosis (Branch VIII).

Date:

Place: Chennai **Dr. NAGARAJAN.K. B.**

ACKNOWLEDGEMENT

I would like to express my deep sense of gratitude to **the Dean**, **Professor.Dr. R. Jayanthi, M.D., FRCP(Glasg),** Madras Medical College and **Professor.Dr.R.Ravi, M.D.R.D., D.M.R.D., our Director, Barnard Institute of radiology, MMC & RGGGH,** for allowing me to undertake this study on "**EFFICACY OF ULTRASOUND ELASTOGRAPHY IN CHARACTERIZING FOCAL LIVER LESIONS WITH HISTOPATHOLOGIC CORRELATION"** and utilize the Institutional facilities.

I was able to carry out my study to my fullest satisfaction, thanks to the guidance, encouragement, motivation and constant supervision extended to me, by my beloved **Head of the Department, Professor Dr.K.Malathi, M.D.R.D., D.M.R.D.** Hence my profuse thanks are due for her.

I would like to express my deep gratitude and respect to my guide **Professor Dr.E. Manimekala,** whose advice and insight was invaluable to me. This work would not have been possible without her guidance, support and encouragement.

My sincere thanks to **Professor Dr.S. Kalpana, Dr.S. Babu Peter** for their valuable support throughout the study and I also thank **Professor Dr.D. Ramesh** for his practical comments and guidance.

I am bound by ties of gratitude to my respected Associate Professor, **Dr.Sivashankar.K.** and Assistant Professors, **Dr.Geetha.G, Dr.Iyengaran.H, Dr.Mohideen Ashraf, Dr.Saranya.M, Dr.Balan.M.P, Dr.Dheebha, Dr.Karthik,** in general, for placing and guiding me on the right track from the very beginning of my career in Radiodiagnosis till this day.

I also thank **my past and present fellow postgraduates** who helped me in carrying out my work and preparing this dissertation. I thank **all the Radiology technicians, Staff Nurses and all the Paramedical staff members** in Barnard Institute of Radiology, for their fullest co-operation. I thank my statistician **Mr.Venkatesan**, who rendered his valuable timely help in completing this study.

My heartfelt thanks to **my wife**, for her endless support, continued and unfailing love, which helped me to overcome the difficulties encountered in the pursuit of this degree.

I would be failing in my duty if I don't place on record my sincere thanks to those **patients and their relatives** who inspite of their sufferings extended their fullest co-operation to this study.

Dr.NAGARAJAN.K.B.

TABLE OF CONTENTS

"EFFICACY OF ULTRASOUND ELASTOGRAPHY IN CHARACTERIZING FOCAL LIVER LESIONS WITH HISTOPATHOLOGIC CORRELATION"

1. INTRODUCTION

Focal liver lesions (FLL) are solid or cystic masses or areas of tissue that are identified as an abnormal part of the liver. The term "lesion" rather than "mass" was chosen because "lesion" is a term that has a wider application, including solid and cystic masses [1 – 3]. The increasing and widespread use of imaging studies has led to an increase in detection of incidental FLL.

Characterizing focal liver masses comprises a significant component of health care costs with substantial impact on patient management both in health and disease. Metastatic liver cancers are the most frequently encountered malignant liver tumours. Primary liver cancer is the fifth most common cancer in the world [5] and its detection and management place a large demand on imaging, which allows for improved detection of lesions while they are still at a small size and amenable to treatment.

It is important to consider not only malignant liver lesions, but also benign liver lesions in the differential diagnosis. Therefore, a thorough and systematic approach to the management of FLLs is of utmost importance.

The critical components of evaluating an FLL are a detailed history, physical exam, radiological tests, and pathology. A radiological test is the most important aspect in the evaluation of a liver lesion.

Conventional ultrasonography (US) is often the first imaging modality performed to screen for, or to study hepatic lesions because of its low cost and wide availability. Colour-Doppler, Contrast Enhanced Ultrasound (CEUS) have significantly improved the characterization of FLL.

Computed Tomography (CT) and Magnetic Resonance Imaging (MRI) are second line imaging methods able to accurately characterize previously detected lesions, but they are more expensive and less available. Contrast enhanced imaging modalities, such as contrast-enhanced US, contrast enhanced-CT and contrast-MRI, assess lesion morphology and vascularization, with a high diagnostic accuracy owing to their specific features. Nevertheless, percutaneous biopsy is required to make a definite diagnosis, which is invasive [4].

Ultrasound elastography is a novel imaging technique to characterize the focal liver lesions better. It is an easily applicable, non–contrast-enhanced, non-invasive and fast imaging method that can be performed during the primary sonographic examination of the patient.

2. RATIONALE OF THE STUDY

FLLs frequently pose a diagnostic challenge for clinicians. FLLs of the liver may arise from hepatocytes, biliary epithelium, mesenchymal tissue, or metastases from extrahepatic tumours.

FLLs are classified as benign or malignant.

Benign (noncancerous) FLLs can be solid or cystic (meaning that the lesions are fluid filled). Within these types, the subtypes include haemangiomas (the most common), focal nodular hyperplasia (FNH), hepatic adenoma, focal fatty changes, and hydatid cysts and bile duct cysts.

Malignant liver tumours can be primary liver cancers or secondary liver lesions (metastases). The most common primary malignant liver tumour is hepatocellular carcinoma (HCC) and the second most common type of liver malignancy is cholangiocarcinoma. Other rare liver cancers are: angiosarcomas and hepatoblastomas.

Historically, the type of liver lesion was diagnosed by either their surgical excision or biopsy. In the last four decades, however, there has been a progressive trend away from such invasive procedures. We now live in an era of non-invasive liver mass diagnosis. This has been accomplished largely on the basis of information acquired with the use of advanced imaging modalities.

The identification of liver lesion type, firstly discriminating between malignant and benign, could represent an important diagnostic goal in order to choose the best management.

For example, Haemangioma, the most common benign liver tumor is present in as many as 20% of patients on autopsy studies [6,7], which can often precisely be diagnosed by a quality imaging modality alone. Non-invasive confirmation of their benign nature allows them to be removed from consideration for clinical management and avoids unnecessary painful biopsy, risk of bleeding and anxiety.

While routine ultrasonography, CECT and MRI provide information on the size, morphology and vascularity of focal liver lesions, a newer imaging technique like ultrasound elastography provides new perspectives in imaging of focal liver lesions.

Elastography, or elasticity imaging, measures the natural tendency of tissue to resume its original size and shape after being subjected to a deforming force or stress [8,9,10]. Neoplastic and inflammatory diseases can change the tissue's composition/structure, and thus parenchyma stiffness of an organ. The provision of these stiffness measurements is established as a method of assessing focal liver lesions and the differentiation of those that are malignant from those that are benign.

Considering all these, this study aimed at prospectively evaluating if ultrasound elastography could be an additional useful tool in the characterisation of focal liver lesions, thereby aiding in further management.

3.REVIEW OF LITERATURE

EMBRYOLOGY OF LIVER

The liver primordium appears in the 3rd week of gestation as an outgrowth from endodermal epithelium at the distal end of distal foregut. This outgrowth, the hepatic diverticulum, or liver bud, penetrate the septum transversum, that is, the mesodermal plate between the pericardial cavity and the stalk of the yolk sac. While hepatic cells continue to penetrate the septum, the connection between the hepatic diverticulum and the foregut (duodenum) narrows, forming the bile duct. A small ventral outgrowth formed by the bile duct gives rise to the gallbladder and the cystic duct. During further development, epithelial liver cords intermingle with the vitelline and umbilical veins, which form hepatic sinusoids. Liver cords differentiate into the parenchyma (liver cells) and form the lining of the biliary ducts.

Hematopoietic cells, Kupffer cells, and connective tissue cells are derived from mesoderm of the septum transversum. When liver cells have invaded the entire septum transversum, so that the organ bulges caudally into the abdominal cavity, mesoderm of the septum transversum lying between the liver and the foregut and the liver and the ventral abdominal wall becomes membranous, forming the lesser omentum and falciform ligament respectively. They are known as the ventral mesentery.

Mesoderm on the surface of the liver differentiates into visceral peritoneum except on its cranial surface. In this region, the liver remains in contact with the rest of the original septum transversum. This portion of the septum will form the central tendon of the diaphragm. The surface of the liver that is in contact with the future diaphragm is never covered by peritoneum is the bare area of the liver.

Around 10th week of intrauterine life, the liver occupies 10% of the total body weight. Another important factor is haematopoiesis. Large number of proliferating cells, which produce red and white blood cells, lie between hepatic cells and walls of the vessels. This activity gradually subsides during the last 2 months of intrauterine life, and only small hematopoietic islands remain at birth. The weight of the liver is then only 5% of the total body weight.

Another important function of the liver begins at approximately the 12th week, when bile is formed by hepatic cells. Meanwhile, since the gallbladder and cystic duct have developed and the cystic duct has joined the hepatic duct to form the bile duct, bile can enter the gastrointestinal tract. As a result, its contents take on a dark green colour. Because of positional changes of the duodenum, the entrance of the bile duct gradually shifts from its initial anterior position to a posterior one, and consequently, the bile duct passes behind the duodenum.

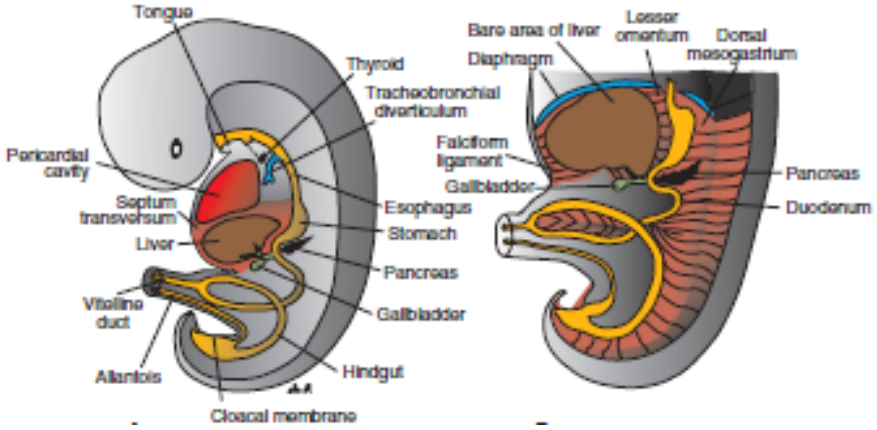

Fig.3.1. Embryological development of liver

LIVER ANATOMY

A human liver normally weighs 1.44–1.66 kg (3.2–3.7 lb) [14], and has a width of about 15 cm. The liver is usually described as having diaphragmatic and visceral surfaces, and has an inferior border. On the diaphragmatic surface, apart from a triangular bare area where it connects to the diaphragm, the liver is covered by a thin, double-layered membrane, the peritoneum, that helps to reduce friction against other organs. This surface covers the convex shape of the two lobes where it accommodates the shape of the diaphragm. The peritoneum folds back on itself to form the ligament and the right and left triangular ligaments[18].The falciform ligament, divides the liver into a left and right lobe. From below, the two additional lobes are located between the right and left lobes, one in front of the other. A line can be imagined running from the left of the vena cava and all the way forward to divide the liver and gallbladder into two halves [15]. The visceral surface or inferior surface, is uneven and concave, which is covered by peritoneum apart from its attachment with the gallbladder and the porta hepatis [17].

There are two prominent regions seen to the right of the groove for ligamentum venosum. Porta hepatis separates these into caudate lobe(posterior) and quadrate lobe(anterior). The gallbladder fossa lies to the right of the quadrate lobe.

The left lobe is the smaller than the right lobe in adults, although it is nearly as large as the right lobe in children. The caudate lobe is a separate structure that receives blood flow from both the right- and left-sided vascular branches [24].

Functional anatomy of the liver:

The most widely used system to describe functional liver anatomy is the Couinaud classification. The liver is divided into eight functional segments based upon the distribution of portal venous branches and the hepatic veins in the parenchyma. From the parietal view, seven segments can be seen, because the eighth segment is only visible in the visceral view [16]. The liver is divided into four portal sectors by the four main branches of the portal vein. These are right lateral, right medial, left medial and left lateral. The three main hepatic veins lie in the portal fissures(scissures) between these sectors as intersectoral veins. The tertiary divisions of the vascular biliary sheaths divide each sector into two segments.

The liver is divided into right and left halves by the main fissure. Segments V and VIII lie to the right and segment IV to the left of the fissure. The left fissure divides the left hemi-liver into medial (anterior) and lateral (posterior) sectors. It contains the left hepatic vein and separates the left anterior and left posterior sectors: segment III lies anteriorly and segment II posteriorly. The right

portal fissure divides the right hemiliver into lateral (posterior) and medial (anterior) sectors. The fissure divides the right anterior sector to its left (segments V and VIII) from the right posterior sector to its right (segments VI and VII), and contains the right hepatic vein. The umbilical fissure separates segment III from segment VI within the left anterior sector and contains a main branch of the left hepatic vein (the umbilical fissure vein). It contains the umbilical portion of the left portal vein and the final divisions of the left hepatic duct and the left hepatic artery branches. The venous fissure is a continuation of the umbilical fissure on the under surface of the liver and contains the ligamentum venosum. It lies between the caudate lobe and segment IV. The deeper continuation of this plane is the dorsal fissure.

The central area or hepatic hilar area of the liver is described in terms of three plates that contain the bile ducts and blood vessels. The contents of the whole plate system are surrounded by a sheath [23]. The three plates are the hilar plate, the cystic plate and the umbilical plate.

Impressions:

Several impressions on the surface of the liver accommodate the various adjacent structures and organs. Underneath the right lobe and to the right of the gallbladder fossa are two impressions, one behind the other and separated by a ridge. The one in front is a shallow colic impression, formed by the hepatic flexure and the one behind is a deeper renal impression accommodating part of the right kidney and part of the suprarenal gland.[19]

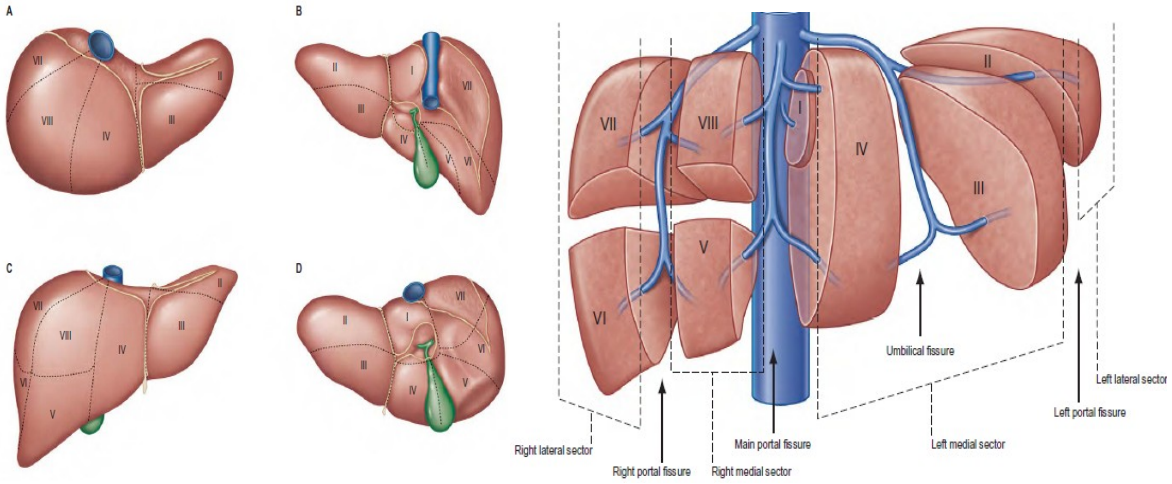

Fig.3.2. COUINAD'S SEGMENTS OF LIVER

Arterial supply and venous drainage:

The hepatic portal vein delivers around 75% of the liver's blood supply, and carries venous blood drained from the spleen, gastrointestinal tract, and its associated organs. The hepatic arteries supply arterial blood to the liver, accounting for the remaining quarter of its blood flow. Oxygen is provided from both sources; about half of the liver's oxygen demand is met by the hepatic portal vein, and half is met by the hepatic arteries [30]. The hepatic artery carries oxygen-rich blood from the aorta, whereas the portal vein carries blood rich in digested nutrients from the entire gastrointestinal tract and also from the spleen and pancreas[19] .The branches arising from hepatic artery are right gastric, gastroduodenal and cystic branches as well as direct branches to the bile duct from the right hepatic and sometimes the supraduodenal artery .It is subdivided into the common hepatic artery(from the coeliac trunk to the origin of the gastroduodenal artery), and the hepatic artery 'proper'(from that point to its bifurcation).

The portal vein starts at the level of L_2 vertebra and is formed from the confluence of the superior mesenteric and splenic veins. It lies between neck of the pancreas(anteriorly)and the inferior vena cava (posteriorly). It runs obliquely to the right and ascends posterior to the first part of the duodenum, the common bile duct and gastroduodenal artery. The coronary or the left gastric vein (ending in the left margin of the portal vein), and the posterior superior pancreatoduodenal vein (nearer to the head of the pancreas) are the main extrahepatic tributaries of the portal vein.

At hilum, it divides into right and left main branches which accompany the corresponding branches of the hepatic artery into the liver supplying each lobe of liver.

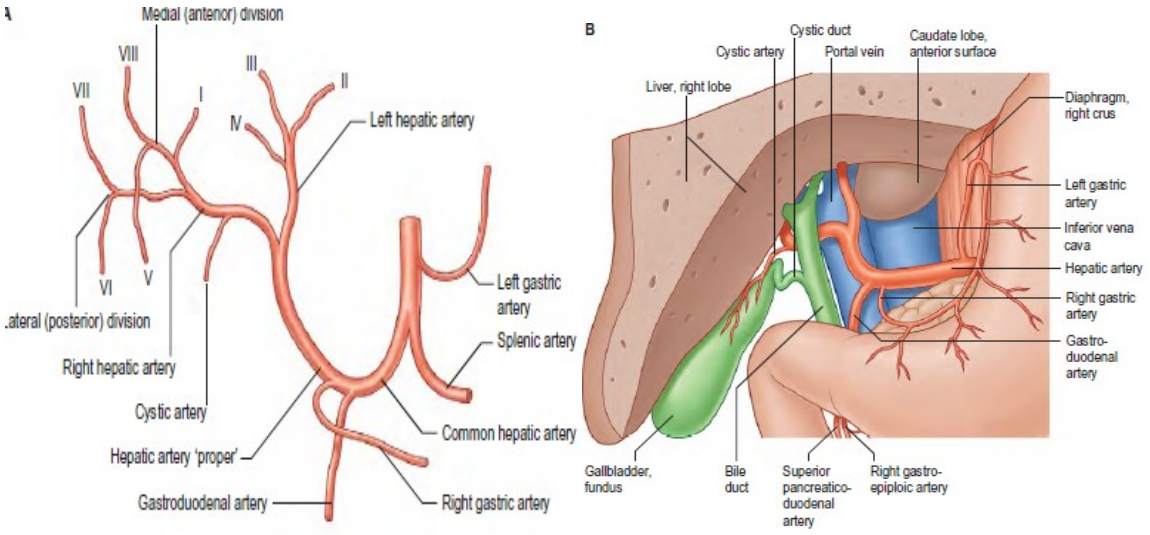

Fig.3.3. Arterial supply to the liver

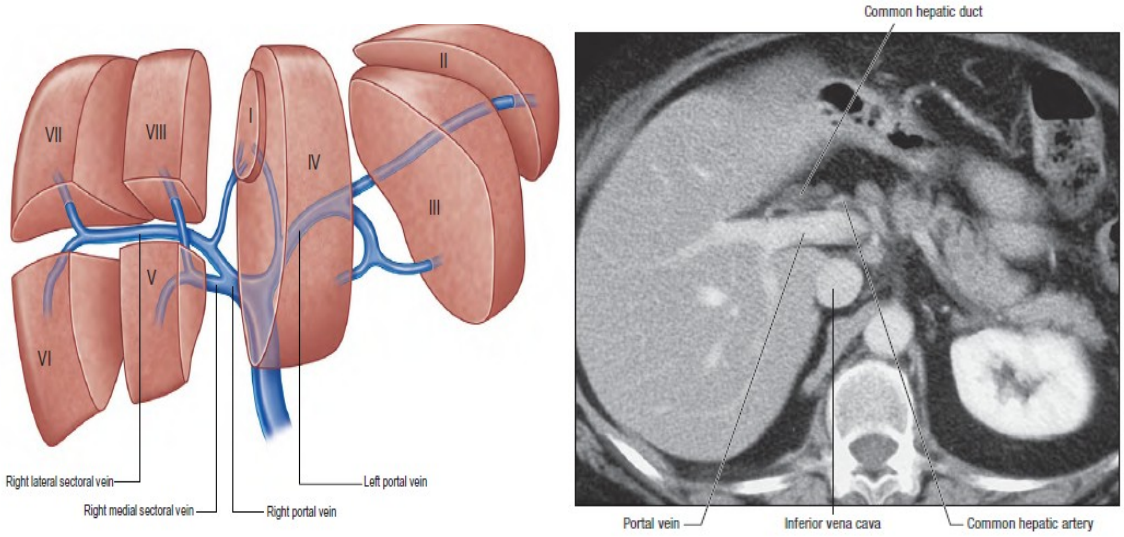

Fig.3.4. Venous drainage of the liver

LIVER HISTOLOGY AND PHYSIOLOGY

All nutrients and liquids that are absorbed in the intestines enter the liver through the hepatic portal vein, except the complex lipid products, which are transported by the lymph vessels. The absorbed products first percolate through the liver capillaries called sinusoids. Because venous blood from the digestive organs in the hepatic portal vein is poor in oxygen, the hepatic artery from the aorta supplies liver cells with oxygenated blood, forming a dual blood supply to the liver.

The liver exhibits repeating hexagonal units called liver (hepatic) lobules. In the centre of each lobule is the central vein, from which radiate plates of liver cells, called hepatocytes, and sinusoids toward the periphery. Here, the connective tissue forms portal canals or portal areas, where branches of the hepatic artery, hepatic

portal vein, bile duct, and lymph vessels can be seen. In human liver, three to six portal areas can be seen per lobule.

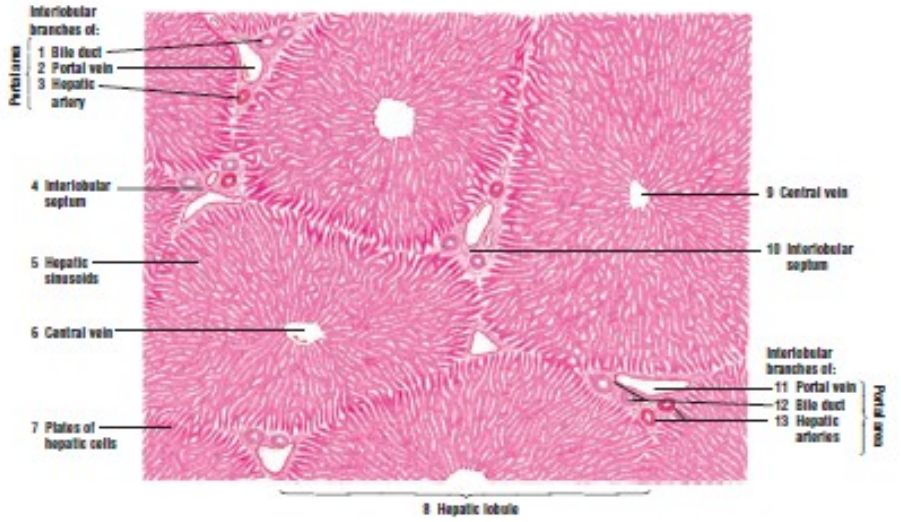

Fig.3.5. Histology of the liver

Between the hepatocyte plates are liver sinusoids, which are enlarged capillaries through which blood from the hepatic portal vein and hepatic artery enters via the portal triads, then drains to the central vein [22]. The blood enters the general circulation through the hepatic veins and enter the inferior vena cava. The hepatic sinusoids are tortuous, dilated blood channels lined by a discontinuous layer of fenestrated endothelial cells and discontinuous basal lamina. The hepatic sinusoids are separated from the underlying hepatocytes by a subendothelial perisinusoidal space (of Disse). The structure and the tortuous path of sinusoids through the liver allows for an efficient exchange of materials between hepatocytes and blood. In addition to the endothelial cells, the hepatic sinusoids also contain macrophages, called Kupffer cells, located on the luminal side of endothelial cells.

Hepatocytes secrete bile into tiny channels called bile canaliculi located between individual hepatocytes. The canaliculi converge at the periphery of liver lobules in the portal areas as bile ducts. The bile ducts drain into larger hepatic ducts that carry bile out of the liver. Within the liver lobules, bile flows in bile canaliculi toward the bile duct in the portal area, whereas blood in the sinusoids flows toward the central vein. As a result, bile and blood do not mix. Cholangiocytes are the epithelial lining cells of the bile ducts [35].

In the human liver, at the centre of each hepatic lobule is the central vein. The hepatic sinusoids appear between the plates of hepatic cells that radiate from the central veins toward the periphery of the hepatic lobule. The branches of the interlobular vessels and bile ducts are seen within the portal areas of a hepatic lobule.

The cytoplasm of liver cells varies in appearance depending on nutritional status. After a meal, liver hepatocytes store increased amounts of glycogen in their cytoplasm. With the periodic acid-Schiff stain, the glycogen granules in the hepatocyte cytoplasm stain bright red and exhibit an irregular distribution within the cytoplasm.

Fine reticular fibres provide most of the supporting connective tissue of the liver. The reticular fibres line the sinusoids, support the endothelial cells, and form a denser network of reticula fibres in the wall of the central vein. Hepatic stellate cells are nonparenchymal cells found in the perisinusoidal space, between a

sinusoid and a hepatocyte[20]. Hepatic stellate cells are derived from mesenchyme [27].

FUNCTIONS OF LIVER

The liver detoxifies various metabolites, synthesizes proteins, and produces biochemicals necessary for digestion[11,12]. The liver performs hundreds of functions. Hepatocytes perform more functions than any other cell in the body, and perform both endocrine and exocrine roles. Its roles in metabolism include the regulation of glycogen storage, decomposition of red blood cells and the production of hormones. Terminology related to the liver often starts in hepat- from the Greek word for liver [14]. The gallbladder, a small pouch that sits just under the liver, stores bile produced by the liver [13]. About 20,000 protein coding genes are expressed in human cells and 60% of these genes are expressed in a normal, adult liver. Over 400 genes are more specifically expressed in the liver [25].

Exocrine Functions:

One major exocrine function of hepatocytes is to synthesize and release 500 to 1,200mL of bile into the bile canaliculi per day. From these canaliculi, bile flows through a system of ductules and ducts to enter the gallbladder, where it is stored and concentrated by removal of water. Release of bile from the liver and gall bladder is primarily regulated by hormones

Bile salts in the bile emulsify fats in the small intestine (duodenum). This process allows for more efficient digestion of fats by the fat-digesting pancreatic lipases produced by the pancreas.

Hepatocytes also excrete bilirubin, a toxic chemical formed in the body after degradation of worn-out erythrocytes by liver macrophages, called Kupffer cells. Bilirubin is taken up by hepatocytes from the blood and excreted into bile.

Endocrine Functions:

The endocrine functions of the liver hepatocytes involve synthesis of numerous plasma proteins, including albumin and the blood-clotting factors prothrombin and fibrinogen. The liver also stores fats, various vitamins, and carbohydrates as glycogen. Adipose and liver cells produce glycerol by breakdown of fat, which the liver uses for gluconeogenesis [28].

The liver sinusoids are lined with two types of cell, sinusoidal endothelial cells, and phagocytic Kupffer cells[21]. In the foetus, the liver is the site of hemopoiesis, or blood cell production. The liver is a major site of production for thrombopoietin, a glycoprotein hormone that regulates the production of platelets by the bone marrow[29].

FOCAL LIVER LESIONS

CLASSIFICATION OF FOCAL LIVER LESIONS

- Benign FLL
  - Serous cyst
  - Biliary hamartoma
  - Hemangioma (cavernous and capillary)
  - Focal nodular hyperplasia
  - Nodular regenerative hyperplasia
  - Hepatocellular adenoma
  - Inflammatory lesions (abscess, cholangitis)
- Malignant FLL
  - Fibrolamellar hepatocarcinoma
  - Cholangiocarcinoma
  - Metastases
- FLL of the cirrhotic liver
  - Regenerative nodule
  - Dysplastic nodule
  - Hepatocellular carcinoma

FLL: Focal liver lesion.

Fig.3.6. Classification of focal liver lesions

HAEMANGIOMA

Cavernous haemangiomas are the most common benign tumours of the liver [46]. They are composed of vascular channels of varying size (cavernous to capillary), lined with endothelium, with intervening fibrous tissue. Usually liver cavernoma patients are asymptomatic [47].

Liver haemangiomas are typically hyperechoic on ultrasound though may occasionally be hypoechoic; ultrasound is not diagnostic. Computed tomography (CT) [44], magnetic resonance imaging (MRI) [45] or single-photon emission

computed tomography (SPECT) using autologous labelled Red Blood Cells (RBC) with Tc-99m is diagnostic.

USG:

On USG, capillary haemangiomas are typically well-defined, lobular, homogeneous lesions showing increased echo reflectivity. There is usually no detectable Doppler signal within the lesion due to the slow flow, although signals may be detected in adjacent feeding vessels or within the lesion with better sensitive harmonic imaging techniques.

Fig.3.7. USG showing multiple haemangioma liver

CT and MRI:

MRI is the most sensitive and specific imaging examination for the diagnosis of haemangioma. Using extended echo time (e.g. TE of 120 to 160 ms)

T2w spin-echo sequences at 1.5 T, haemangiomas appear as well-defined lesions with a lobular outline and homogeneously high signal on T2w, in excess of the spleen and approaching that of fluid. During the arterial phase following IV enhancement with Gd-DTPA, haemangiomas have rapidly enhancing vessels at the periphery. Over a period of minutes, the lesion will 'fill in' centripetally to become isointense or slightly hyperintense with the adjacent parenchyma.

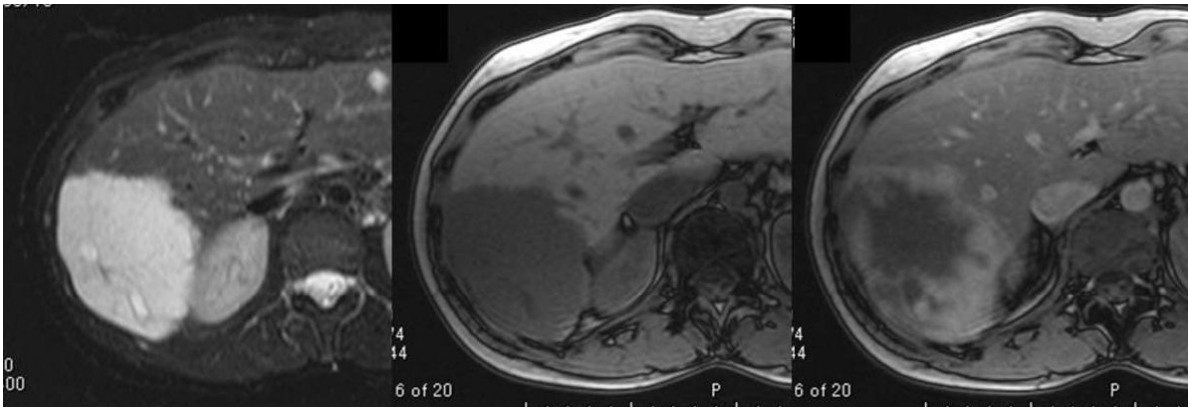

Fig.3.8. MRI demonstrating haemangioma liver.

CT examination demonstrates a well-defined, lobulated lesion with attenuation close to blood values before enhancement. The pattern of enhancement follows that for MRI, with centripetally infilling and eventually merging with the background parenchyma. Small (<1.5 cm) lesions are frequently difficult to characterise and may fail to demonstrate either the characteristic signal changes on T2w MRI (partial volume effects) or the typical enhancement pattern on CT or MRI.

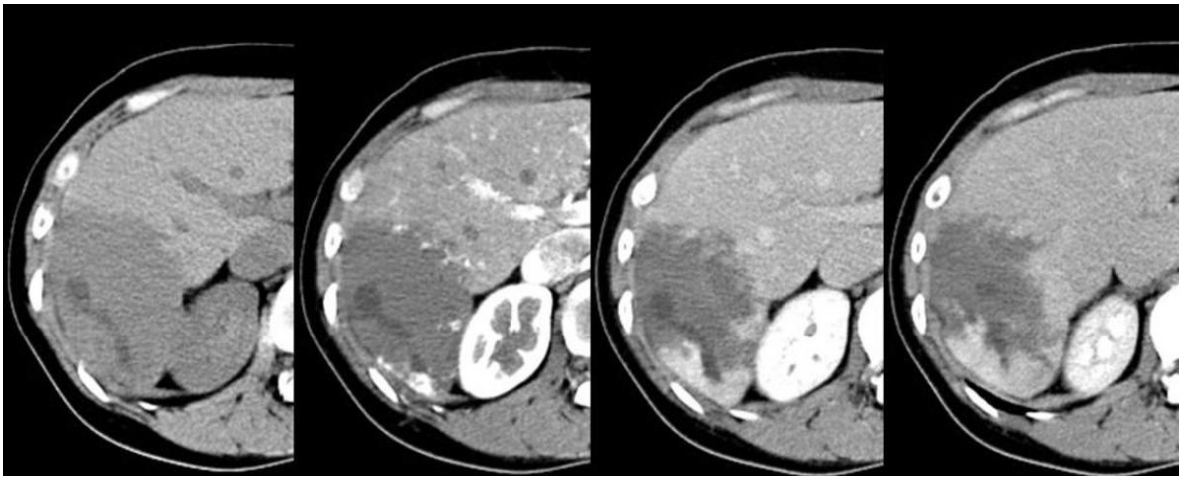

Fig.3.9. CT scan showing peripheral nodular enhancement of hypodense lesion with delayed centripetal filling suggestive of haemangioma.

ATYPICAL HAEMANGIOMA

On US atypical lesions may appear heterogeneous. Small lesions may fill in relatively rapidly and be confused with other arterial enhancing solid lesions. Larger lesions (>4 cm) often have atypical internal features such as an area of central fibrosis that does not enhance on MRI or CT.

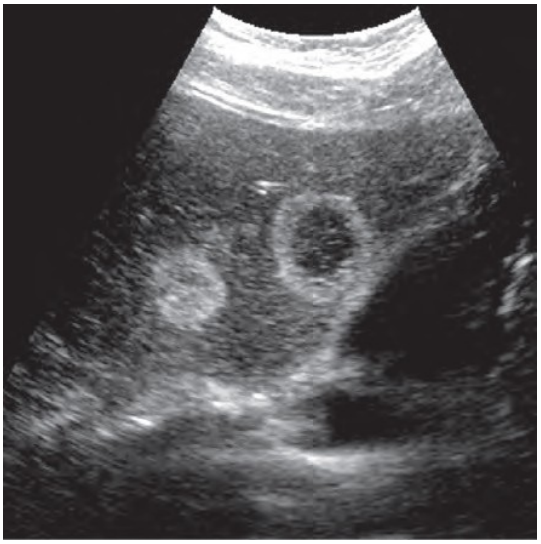

Fig.3.10. USG image showing atypical haemangioma liver

FOCAL NODULAR HYPERPLASIA

Focal nodular hyperplasia (FNH) is the second most frequent benign liver lesion after haemangioma and it is the most common solid benign liver lesion, comprising ~8 % of all primary hepatic tumours [36-38]. This benign tumour occurs most commonly in women aged 20–50 years, but can occur in men and women at any age. It is usually asymptomatic. FNH is considered to be the result of a vascular malformation, which leads to hepatocellular hyperplasia [39,40]. FNH's do not have the potential for malignant transformation and they are not known to cause bleedings like adenoma [41].

USG:

USG findings are usually non-specific with subtle lesions of similar reflectivity to adjacent liver. Central scars are rarely seen, although Doppler signals are often detected at the centre and edge of the lesion. Overall the features overlap substantially with those of other benign lesions such as adenoma and malignant vascular lesions such as hepatocellular carcinoma making further imaging studies necessary.

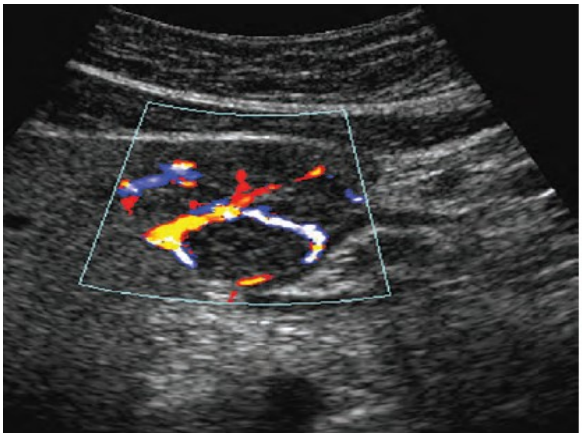

Fig.3.11.USG image showing an isoechoic and subtle mass with a stellate arterial pattern suggestive of FNH

CT:

On unenhanced CT studies, FNH are subtle and well defined and may exhibit mass effect, displacing adjacent vessels. Their attenuation is similar to surrounding liver parenchyma, and they may have a central focal low attenuation scar. During the hepatobiliary phase, progressive contrast uptake is observed in normal functioning liver parenchyma, followed by enhancement of the bile-duct system, as the contrast is transported to the biliary canaliculi and subsequently to the extrahepatic bile-ducts [42]. There is contrast enhancement during the hepatobiliary phase in ~90 % of FNHs [43]; as opposed to other focal liver lesions, such as metastases, hepatocellular carcinoma or adenoma, which generally do not show enhancement during the hepatobiliary phase.

MRI:

On MRI the lesions are also subtle, being either isointense or of minimally reduced signal on T1w and increased signal on T2w images. The central scar is hypointense on T1w and hyperintense on T2w images. Hepatocyte-specific contrast

agents such as gadoxetic acid, taken up by hepatocytes and partially excreted into the biliary system, may differentiate FNH and adenoma. On delayed phase T1w images using these agents, substantial hepatocellular enhancement occurs within the lesion, unlike most adenomas.

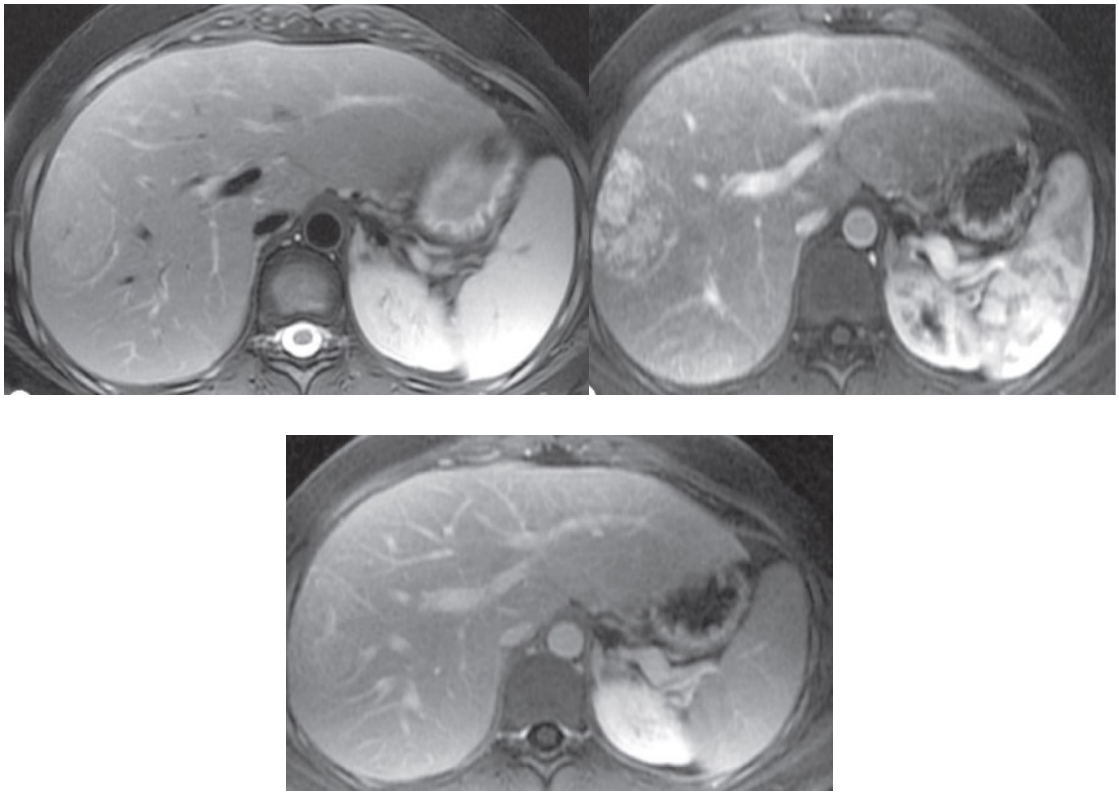

Fig.3.12. A subtle lesion is demonstrated on fat-suppressed multi-shot T2w FSE. There is avid arterial phase enhancement, becoming isointense in the portal and delayed phases. A central scar is evident on some of the images, which enhances on the delayed image.

METASTASIS

The liver is the most common site of metastases that arise from gastrointestinal malignancies; other primary sites of origin including breast, lung, pancreas, and melanoma [48,49]. GIT tumours metastasise to the liver via the portal vein, and tumours elsewhere via the hepatic artery. Liver metastases derive their blood supply from the hepatic artery but the majority are less vascular than adjacent liver parenchyma. Metastatic tumours that may have increased vascularity compared with normal liver parenchyma include breast, kidney, thyroid, neuroendocrine and melanoma.

USG:

On US metastases may be homogeneous and of increased or decreased reflectivity. They may have a surrounding rim of reduced reflectivity, giving a target-type appearance. Central necrosis may result in a partly cystic appearance. Contrast-enhanced US has been demonstrated to be useful for differentiating among hepatic tumours by their differing enhancement patterns [52].

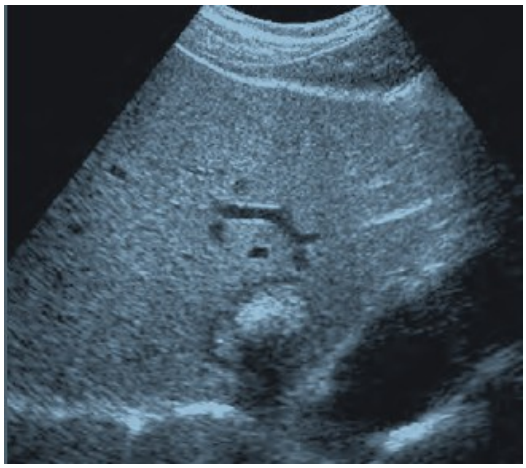

Fig.3.13. USG showing metastasis to liver from colon cancer.

CT:

Computed tomography during arterial portography (CTAP) has been used primarily when considering hepatic resection [53]. On CT most metastases are low attenuation on plain CT images. Hypervascular tumours may enhance transiently in the arterial phase, some becoming invisible in the portal phase. CT is the most sensitive method for detecting the subtle calcification that may occur within mucin-secreting metastases of GI tract origin. Central necrosis and rim enhancement can also be clearly demonstrated on CT. Hypervascular metastases including neuroendocrine tumours, melanoma, sarcoma, and renal cell carcinoma enhance more rapidly than normal liver parenchyma, resulting in greater conspicuity better detected in the hepatic arterial phase [50,51].

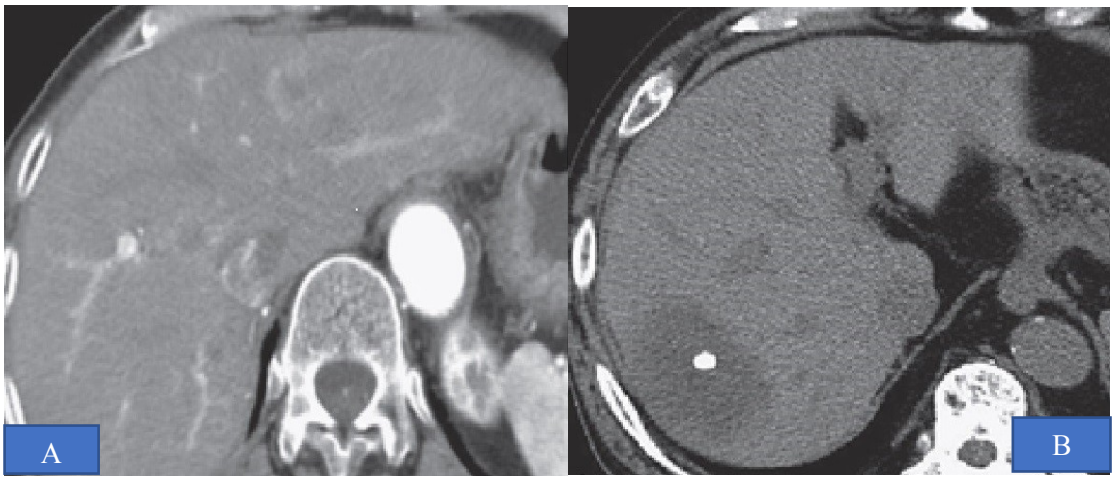

Fig.3.14. A. CECT showing liver metastasis with peripheral ring enhancement.

B. Plain CT showing liver metastasis from colon cancer with calcific foci

MRI:

More recent comparisons of non-invasive imaging modalities, primarily MDCT and MRI, have shown equally accurate if not better lesion detection with lower false-positive rates [54,55]. On MRI most metastases are of low signal on T1w and high signal on T2w images, their signal approximately matching that of the spleen. Contrast- enhanced MR studies give similar appearances to CT. On T2w studies with paramagnetic iron oxide agents there is reduction of normal parenchymal signal due to Kupffer cell uptake, making the metastases (and any other lesions that do not take up the iron oxide) more obvious. Paramagnetic hepatocyte-specific contrast media increase the normal liver signal on T1w imaging, whereas metastases (and other lesions) are unable to metabolise hepatocyte specific contrast agents and appear hypointense on delayed phase. In DWI, there is high signal intensity on intermediate b-values and reduced ADC values.

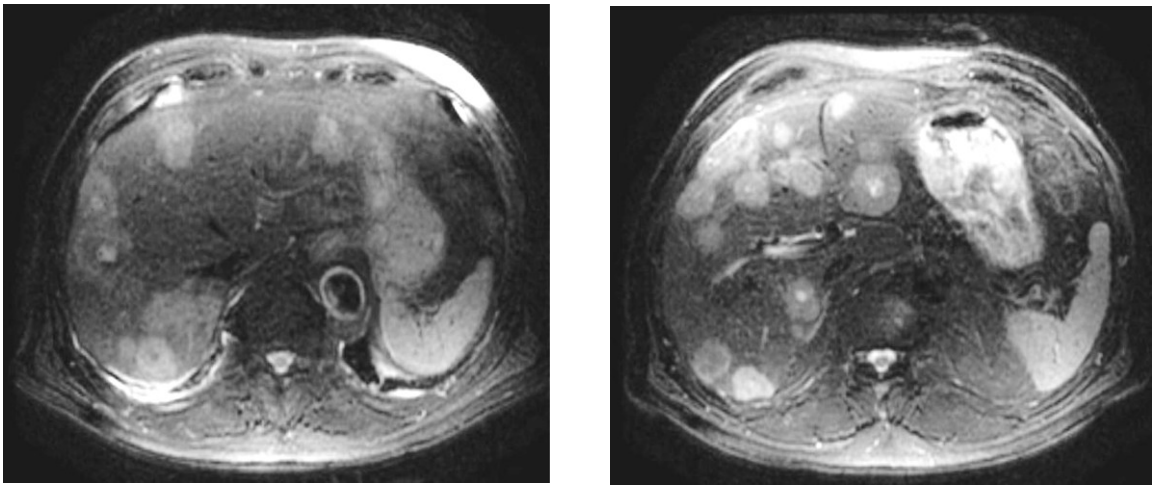

Fig.3.15. MRI showing multiple liver metastasis from prostatic cancer showing bull's eye appearance

INTRAHEPATIC CHOLANGIOCARCINOMA

Known risk factors for cholangiocarcinoma include primary sclerosing cholangitis (an inflammatory disease of the bile ducts)[56], infection with the parasitic liver flukes Opisthorchis viverrini or Clonorchis sinensis, some congenital liver malformations, and exposure to Thorotrast (thorium dioxide), a chemical formerly used in medical imaging. Patients with chronic liver disease, whether in the form of viral hepatitis (e.g. hepatitis B or hepatitis C)[57,58,59], alcoholic liver disease, or cirrhosis of the liver due to other causes, are at significantly increased risk of cholangiocarcinoma[60,61]. Caroli's syndrome (a specific type of five recognized choledochal cysts), have been associated with an approximately 15% lifetime risk of developing cholangiocarcinoma [62,63]. The rare inherited disorders Lynch syndrome II and biliary papillomatosis have also been found to be associated with cholangiocarcinoma[64,65]. Intrahepatic stones (called hepatolithiasis), which are rare in the West but common in parts of Asia, have been strongly associated with cholangiocarcinoma [66,67,68].

Intrahepatic cholangiocarcinomas include peripheral and hilar cholangiocarcinomas. Most peripheral cholangiocarcinomas are the mass-forming type, whereas the majority of hilar cholangiocarcinomas are the periductal-infiltrating type. The peripheral intrahepatic cholangiocarcinoma on imaging is a well-defined single hypovascular mass with wavy borders. Owing to intrahepatic metastasis via the portal vein, satellite or daughter nodules are frequent.

USG:

USG of the liver and biliary tree is often used as the initial imaging modality in patients with suspected obstructive jaundice[69,70].Ultrasound can identify obstruction and ductal dilatation and, in some cases, may be sufficient to diagnose cholangiocarcinoma[71]. The sonographic appearance is often that of a hypovascular solid mass with heterogeneous echotexture, and it may appear hypoechoic, isoechoic, or hyperechoic. A clue to the differentiation from hepatocellular carcinoma (HCC) is a much higher incidence of ductal obstruction.

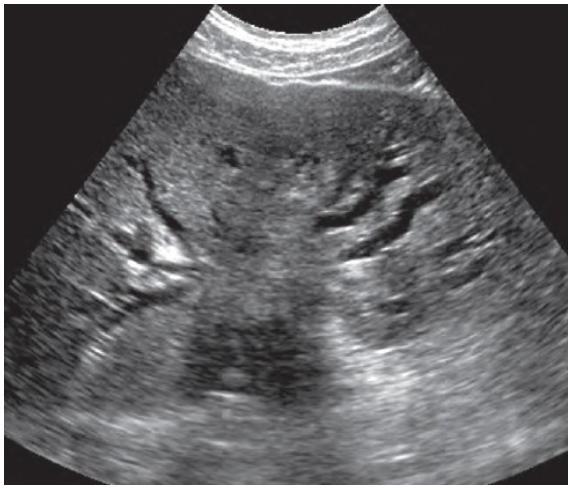

Fig.3.16. USG showing hilar cholangiocarcinoma with IHBR dilatation

CT and MRI:

On contrast-enhanced CT or MRI, thin or thick rim like enhancement is frequently seen around the periphery of the tumours on arterial-phase images, and there is gradual centripetal enhancement on delayed-phase images. The entire mass may be enhanced only on delayed-phase images some hours after contrast administration. These findings reflect the desmoplastic nature. Capsular retraction is relatively frequent. Bile duct dilatation peripheral to the tumour is common.

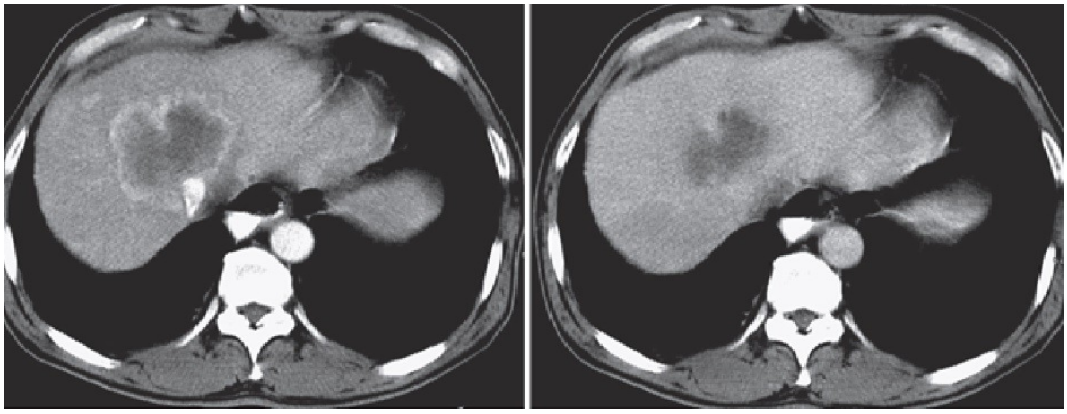

Fig.3.17. CT image showing peripheral cholangiocarcinoma

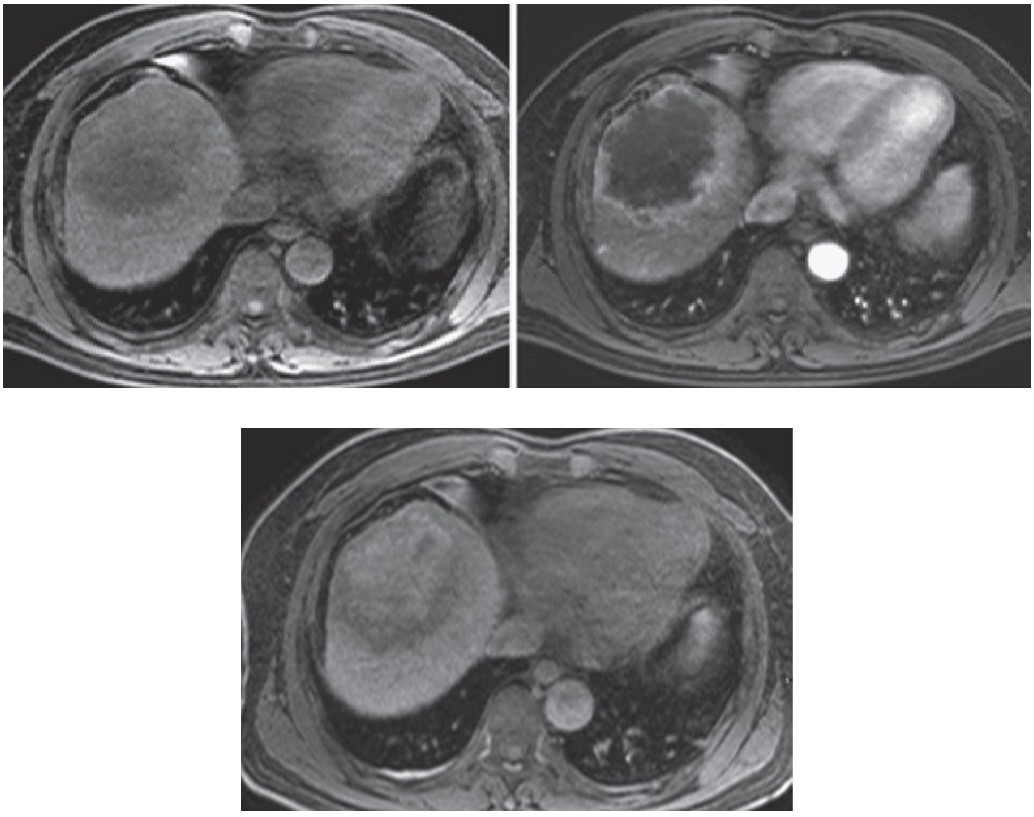

Fig.3.18. MRI showing peripheral hilar cholangiocarcinoma showing centripetal delayed enhancement.

HEPATOCELLULAR CARCINOMA

Hepatocellular carcinoma (HCC) is the most common type of primary liver cancer in adults, and is the most common cause of death in people with cirrhosis[72]. There are many predisposing factors, including aflatoxin, chronic hepatitis and cirrhosis, particularly post-necrotic cirrhosis and haemochromatosis. Globally, about 248 million individuals are chronically infected with HBV [31] and 142 million are chronically infected with HCV [32]. Hepatitis D virus is a "satellite" of hepatitis B virus (can only infect in the presence of hepatitis B), and co-infects nearly 20 million people with hepatitis B, globally [33]. Serum alpha-fetoprotein (AFP) can be helpful in diagnosis. Metabolic syndrome and NASH are also increasingly recognized as risk factors for HCC[73].HCC can be solitary, multifocal or rarely, diffuse.

USG:

The masses may be hypoechoic, complex, or echogenic. A thin, peripheral hypoechoic halo, which corresponds to a fibrous capsule, is seen most often in small HCCs.With time and increasing size, the masses tend to become more complex and inhomogeneous as a result of necrosis and fibrosis. Calcification is uncommon. Liver biopsy will be necessary, and a tissue sample is taken through a needle inserted into the skin just below the rib cage. This procedure may be helped by a sonographer providing ultrasound guidance to an interventional radiologist [34].

CT:

With triple-phase helical CT, the sensitivity was 90% or higher, but these data have not been confirmed with autopsy studies [74]. MRI is more sensitive and specific than CT[75]. Nonenhanced CT usually reveals a hypodense area. Calcification is rare. When copper accumulation or haemorrhage is associated, slight hyper density can be seen [76]. In the arterial phase of dynamic CT, enhancement of the entire lesion is seen, and its intensity differs in accordance with its mosaic architecture. However, when the lesions are small or predominantly well differentiated, they may appear hypoattenuating or isoattenuating even in the arterial phase. CTHA or contrast ultrasonography may be valuable for visualizing the increased arterial vascularity.

Drainage flow from these HCCs into the surrounding hepatic sinusoids is through the connections between intratumoral blood sinusoids and hepatic sinusoids or tiny portal venules in the pseudocapsule. This drainage flow results in "corona enhancement" surrounding the tumour in the arterial or portal phase of dynamic CT and is a very useful imaging feature for differentiating benign hypervascular hepatic nodules such as cavernous haemangioma, Arterioportal shunting, FNH, angiomyolipoma, and peliosis hepatis, which seldom show this kind of corona enhancement [77,78,79].

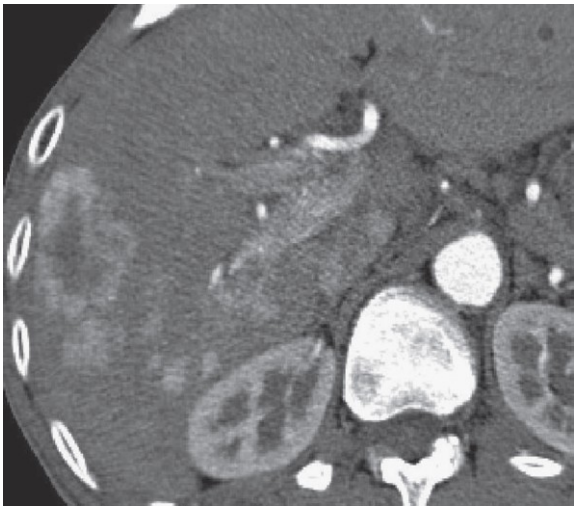

Fig.3.19. Portal vein tumour thrombus-The arterial phase of dynamic CT demonstrates multiple well-enhanced HCCs and marked enhancement showing a thread- and streak-like pattern in the proximal right portal vein.

MRI:

On T1-weighted images, classic HCC usually shows hypointensity. However, one third of nodular-type HCCs demonstrate hyperintensity relative to the surrounding liver on T1W images. Almost all classic hypervascular HCCs show hyperintensity on T2W images. This combination is unique among hepatic malignant tumours except for metastatic malignant melanoma; it is almost diagnostic for HCC, especially in high-risk patients. The fibrous capsule is demonstrated as a hypodense rim surrounding the tumour on nonenhanced CT; it is hyperdense on postcontrast CT, hypointense on T1-weighted images, and hyperintense on both T2-weighted and postcontrast MRIs. The internal mosaic architecture is visualized as components of variable density or intensity separated by fibrous septa, with imaging features similar to those of the fibrous capsule. Tumour thrombus—whether in the main portal vein, the first and second branches

of the intrahepatic portal vein, or the major branches of the hepatic vein—is visualized as an intravascular solid mass lesion. Differentiation from blood thrombus is usually possible by enhancement on contrast-enhanced CT or MRI.

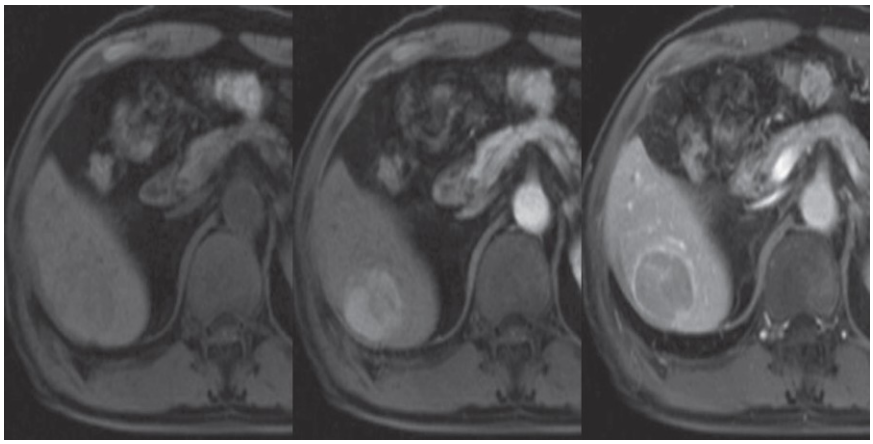

Fig.3.20. Moderately differentiated HCC with an internal mosaic pattern enhancement in the arterial phase and washout of contrast in the equilibrium phase

FIBROLAMELLAR CARCINOMA

On nonenhanced CT, a hypodense solitary mass is seen; central calcification is present. On dynamic CT inhomogeneous enhancement is observed during the arterial phase. A poorly enhanced hypodense area generally reflects necrosis. In the equilibrium (or delayed) phase, delayed enhancement of the central scar is seen in about 25% of cases. On MRI the signal intensity is variable but is essentially hypointense on T1- and hyperintense on T2-weighted images. The central scar characteristically shows hypointensity on both T1- and T2-weighted images. Superparamagnetic iron oxide and hepatobiliary agents do not accumulate.

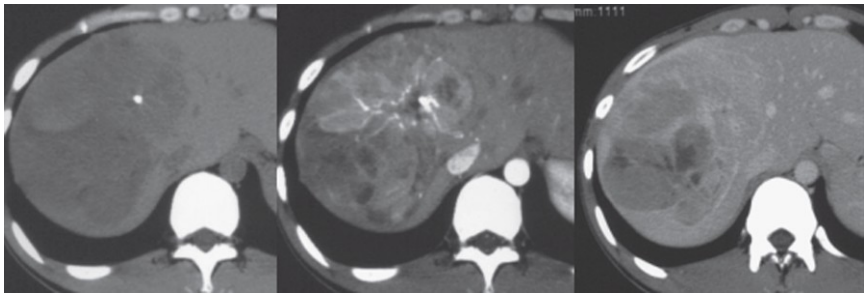

Fig.3.21. CECT showing fibrolamellar carcinoma.

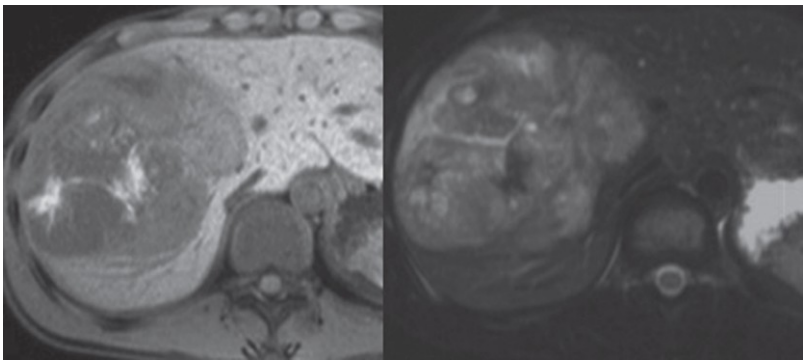

Fig.3.22. MRI. T1-weighted image demonstrates an inhomogeneous hypointense mass with a more hypointense central scar. On the T2-weighted image the mass shows inhomogeneous hyperintensity and the scar remains hypointense

HEPATIC ADENOMA

Adenomas are rare benign tumours of liver. The risk factors are Oral contraceptives and anabolic steroid use, glycogen storage disease type 1, maturity-onset diabetes of the young and Klinefelter's syndrome. They are vascular lesions composed primarily of hepatocytes, with no portal tracts or bile ducts. Kupffer cells are usually absent but their activity has been observed in up to 20% of cases. These hepatocytes also tend to accumulate both fat and glycogen. Patients may present with pain or life-threatening haemorrhage. There is a small (1–5%) but definite risk of malignant change.

USG:

The lesions are isoreflective with adjacent parenchyma or, if they accumulate fat, are well-defined increased echo-reflectivity lesions that mimic haemangiomas. Alternatively, where there is hepatic steatosis and the adenoma does not accumulate fat they may be of reduced echo reflectivity and confused with metastases.

CT:

On CT adenomas may be isodense, hypo or hyperdense depending on both the amount of fat in the background liver and within the adenoma. They are usually homogeneous with a well-defined margin and enhance markedly and uniformly during the arterial phase, then rapidly merge with surrounding liver during the portal phase.

MRI:

The lesions are well-defined isointense or slightly hyperintense lesions on T2w and T1w images. They typically enhance markedly and uniformly during the arterial phase and disappear in the portal phase following gadolinium enhancement on T1w imaging. Persisting delayed enhancement is seen in the telangiectatic histological variant of adenoma. They may undergo haemorrhage or necrosis. On delayed imaging following IV hepatocyte-specific contrast agents adenomas appear hypointense due to the absence of biliary ducts which helps to differentiate hepatic adenomas from FNH.

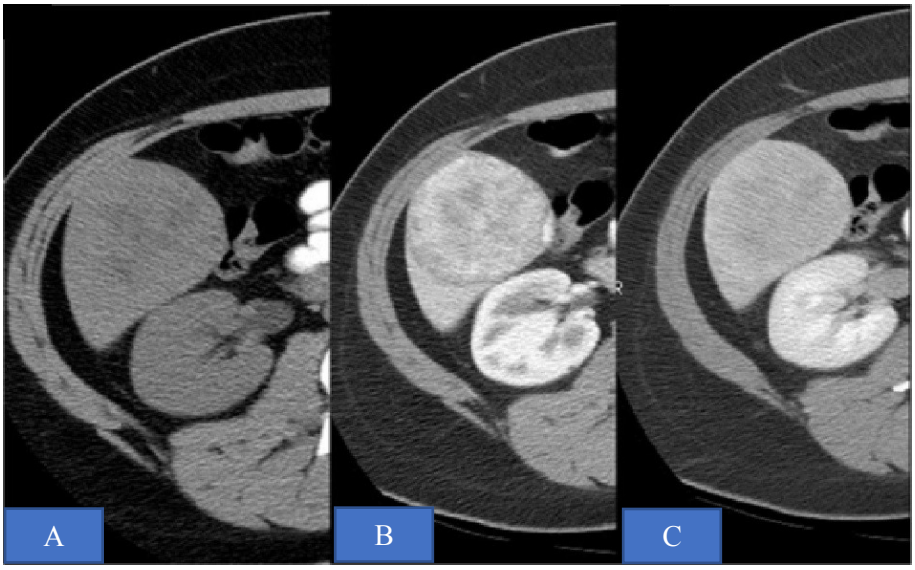

Fig.3.23. Hepatic adenoma. (A) Axial unenhanced CT scan shows a low-density hepatic mass with focal areas of fat. This lesion exhibits moderate, inhomogeneous contrast enhancement on hepatic arterial-phase image (B) that shows gradual washout on delayed phase (C).

ULTRASOUND ELASTOGRAPHY

Ultrasound elastography (USE) is an imaging technology sensitive to tissue stiffness that was first described in the 1990s [80]. It has been further developed and refined in recent years to enable quantitative assessments of tissue stiffness.

PHYSICS

Elastography assesses tissue elasticity, which is the tendency of tissue to resist deformation with an applied force, or to resume its original shape after removal of the force. Assuming that a material is entirely elastic and its deformation has no time dependency (i.e. viscosity), elasticity can be described by Hooke's Law:

Stress = (Elastic modulus) x (Strain) (Eqn. 1)

where stress is the force per unit area with units' kilopascals (i.e. N/m^2) (**Fig.3.24.**, top row), strain is the expansion per unit length which is dimensionless (**Fig.3.24.**, second row), and the elastic modulus relates stress to strain with units' kilopascals (**Fig.3.24.**, third row).

There are three types of elastic moduli defined by the method of deformation: Young's modulus (E), shear modulus (G), and bulk modulus (K).

1) Young's modulus E is defined by the following equation when a normal stress produces a normal strain, where normal is perpendicular to the surface (**Fig.3.24.**, first column):

Normal Stress = Normal Strain (Eqn. 2)

2) Shear modulus G is defined by the following equation when a shear stress produces a shear strain, where shear is tangential to the surface (**Fig.3.24.**, second column):

Shear stress = (Shear modulus) x (Shear strain) (Eqn. 3)

3) Bulk modulus K is defined by the following equation when a normal inward force or pressure produces a bulk strain or change in volume (**Fig.3.24.**, third column):

Normal inward force or pressure = (Bulk modulus) x (Bulk strain) (Eqn. 4)

The higher the elastic modulus, the more a material tends to resist deformation, which can be thought of as increased stiffness.

In strain imaging, the normal strain is measured after application of normal stress to yield estimates of Young's modulus E via Equation 2.

In addition to the above equations which describe static deformations, the elastic modulus also characterizes the propagation speed of waves:

Wave speed = Square root of (Elastic modulus/Material density) (Eqn. 5)

There are two types of wave propagation in ultrasound: longitudinal waves and shear waves.

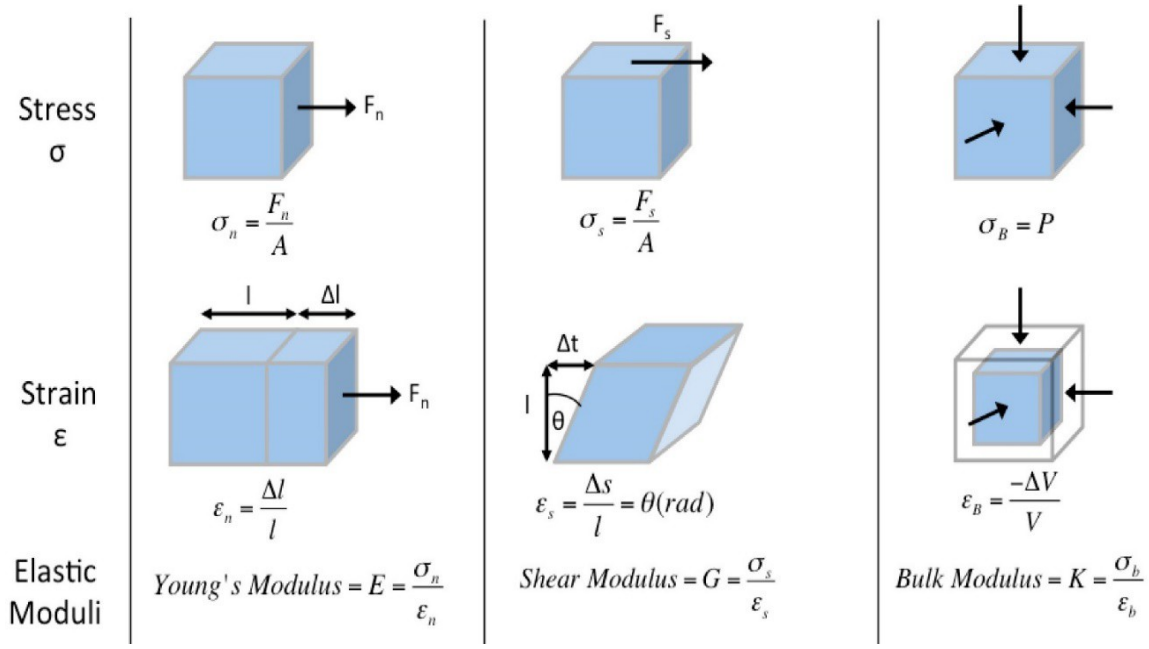

Fig.3.24. Ultrasound elastography physics, deformation models. Static deformations of entirely elastic materials can be described by stress (force per unit area, top row), strain (expansion per unit length, middle row), and elastic modulus (stress divided by strain, bottom row). This is applied to normal (perpendicular to surface, first column), shear (tangential to surface, second column), and bulk (normal inward or pressure, third column) forces used in ultrasound elastography.

Shear waves have particle motion perpendicular to the direction of wave propagation and are defined using the shear modulus G as:

Shear wave speed = Square root of (Shear modulus/Material density)

where the shear wave speed is approximately 1-10 m/s in soft tissues. The low wave speed in soft tissues allows for high differences in G between tissues, giving suitable tissue contrast for elastography measurements.

The relationships between Young's modulus E, shear modulus G, and shear wave speed are important because different parameters are reported. Ultrasound shear wave imaging directly measures shear wave speed, which is either reported or converted to Young's modulus E.

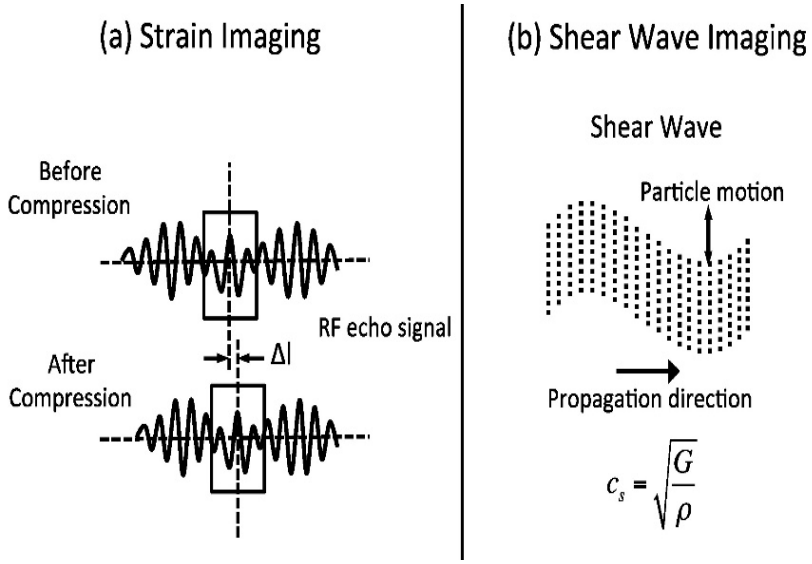

Fig.3.25. Ultrasound elastography physics, measurement methods. In strain imaging (a), tissue displacement is measured by correlation of Radio Frequency echo signals between search windows (boxes) in the states before and after compression. In shear wave imaging (b), particle motion is perpendicular to the direction of wave propagation, with shear wave speed (c_s) related to shear modulus G.

USE techniques can be classified by the measured physical quantity.

1) Strain imaging: In this technique, a normal stress is applied to tissue and the normal strain is measured.
2) Shear wave imaging (SWI): In this technique, a dynamic stress is applied to

tissue by using a mechanical vibrating device in 1D transient elastography (1D-TE) or acoustic radiation force in point shear wave elastography (pSWE) and 2D shear wave elastography (2D-SWE). Shear waves created by the excitation are measured perpendicular to the acoustic radiation force application or parallel to the 1D transient elastography excitation.

STRAIN IMAGING

In addition to visualization of elasticity on color-coded elastographic images, the strain of tissues can be defined as numerical strain values and compared by cross-correlation of radiofrequency signals. Strain values may be obtained by different mechanisms such as acoustic radiation force impulse imaging or semiquantitative strain elastography [81].

There are two approaches for strain imaging using ultrasound: Strain elastography (SE) and acoustic radiation force impulse (ARFI) strain imaging.

Strain elastography can be further subdivided by the excitation method:

1) In the first method, the operator exerts manual compression on the tissue with the ultrasound transducer [9]. Manual compression works fairly well for superficial organs such as the breast and thyroid but is challenging for assessing elasticity in deeper located organs such as the liver [82].

2) In the second excitation method, the ultrasound transducer is held steady, and tissue displacement is generated by internal physiologic motion (e.g. cardiovascular, respiratory). Since this method is not dependent on superficially applied compression, it may be used to assess deeper located organs [80].

Process of the investigation:

After fitting the semiquantitative strain elastographic image box to fully cover the lesion in the liver, a compressive and decompressive force was applied, keeping the same area of the lesion in the field of view. We applied the probe with vertical pressure, avoiding lateral movement. Subcostal scanning was used for all elastographic examinations. During probe movement, gray-scale images of the lesions were shown on the sonographic screen. The elasticity images were produced automatically on the ultrasound machine by comparing two adjacent frames during compression and relaxation by continuously moving the probe. After 7 to 8 compression-relaxation cycles, the elastographic examinations were finalized, and strain value measurements were obtained. Compression and relaxation waveforms were shown on the elastographic screen as above and below the baseline of the waveform scale, respectively.

The color-coded image scale ranged from red for components with highest strain (i.e., softest components) to blue for those with lowest strain (i.e., hardest components). Green indicated intermediate strain in the region of interest. On semiquantitative strain elastography, strain represents the degree of tissue displacement as a response to induced pressure. The ratio of displacement (strain) of the normal tissue and lesion in response to the induced pressure is defined as the strain index value. The strain index value represents the ratio of the strain of focal solid liver lesions to that of normal liver parenchyma. The strain index value

increases when the lesion is harder (stiffer) than the parenchyma. In cirrhotic patients, the strain of the liver is decreased; therefore, one may expect a considerable decrease in the strain index value of focal solid liver lesions [83].

Strain values of tissues were measured by putting equal or near-equal-sized regions of interest in the lesion and liver parenchyma. Regions of interest were intended to be at the same level as possible to perform the measurements. The sizes of the regions of interest were determined as large enough to place within the confines of the lesion to represent elasticity of the lesion appropriately.

After the strain measurements were obtained, the strain index values of the lesions were compared. Comparison of mean strain index values in the benign lesion group (haemangiomas, focal nodular hyperplasia, and nodular regenerative hyperplasia) and the malignant lesion group (metastases, hepatocellular carcinomas, and cholangiocarcinomas) was performed.

SHEAR WAVE ELASTOGRAPHY(SWE)

It relies on the measurement of the shear wave propagation speed in soft tissue; Like ARFI, it does not require an external vibrator to generate the shear wave. It is based on the generation of a radiation force in the tissue to create the shear wave.

The ultrasound probe of the device produces a very localized radiation force deep in the tissue of interest. This acoustic radiation force/push induces a shear wave, which then propagates from this focal point. Several focal points are then

generated almost simultaneously, in a line perpendicular to the surface of the patient's skin. This creates a conical shear wave front, which sweeps the image plane, on both sides of the focal point. A high-speed acquisition is necessary to capture the shear wave as it moves at a speed in the order of 1 to 10 m/s. The propagation speed of the shear wave is then estimated in meters per second (m/s), or the elasticity of the medium in kilopascals (kPa). In contrast to strain imaging, which measures physical tissue displacement parallel to the applied normal stress, SWI employs a dynamic stress to generate shear waves in the parallel or perpendicular dimensions. Measurement of the shear wave speed results in qualitative and quantitative estimates of tissue elasticity. The shear wave velocity depends on tissue elasticity because the speed of the shear wave traveling through a region of interest increases as tissue stiffness increases [81].

Process of the investigation:

SWE acquisition can be performed just after a complete morphological and Doppler vascularization examination of the liver. Patients are placed in the supine position, with the right arm in maximum abduction to make the right hypochondrium accessible and to increase intercostal space (to improve the acoustic window). The probe is placed parallel to the intercostal space within the space with sufficient gel in order to minimize rib shadowing. To insure reliable SWE acquisition and contrary to what has been recommended as a rule for most of the organs, a pressure must be applied to the probe when scanning the liver. It allows a better acoustic coupling by opening the rib space and decreasing tissue thickness

between the probe and the ribs (The ribs will absorb the pressure and the elasticity of the liver will not be impacted). The window is positioned within the liver parenchyma, avoiding artifact from vessels and 2 cm beneath the Glisson's capsule. It is essential that the operator waits for 2 to 3 seconds in order for the signal to stabilize before freezing. Measurements are taken with patients holding their breath gently, without deep inspiration.

Advantages:

- It is an easy, painless, rapid technique.
- The result is immediately available.
- SWE is incorporated onto a conventional ultrasound diagnostic imaging device, which allows the combination, in one exam, of quantitative elastography assessment of the liver fibrosis and/or tumour after the morphological ultrasound examination of the liver.
- Quantitative assessment of soft tissue elasticities in kPa or in m/s;
- The ability to select the measurement depth, and an area free of SWE artifact (due to vessels, Glisson's capsule, or other lesions).

Technical approaches:

There are currently three technical approaches for SWI:

1) 1 dimensional transient elastography (1D-TE),

2) point shear wave elastography (pSWE), and

3) 2-dimensional shear wave elastography (2D-SWE)

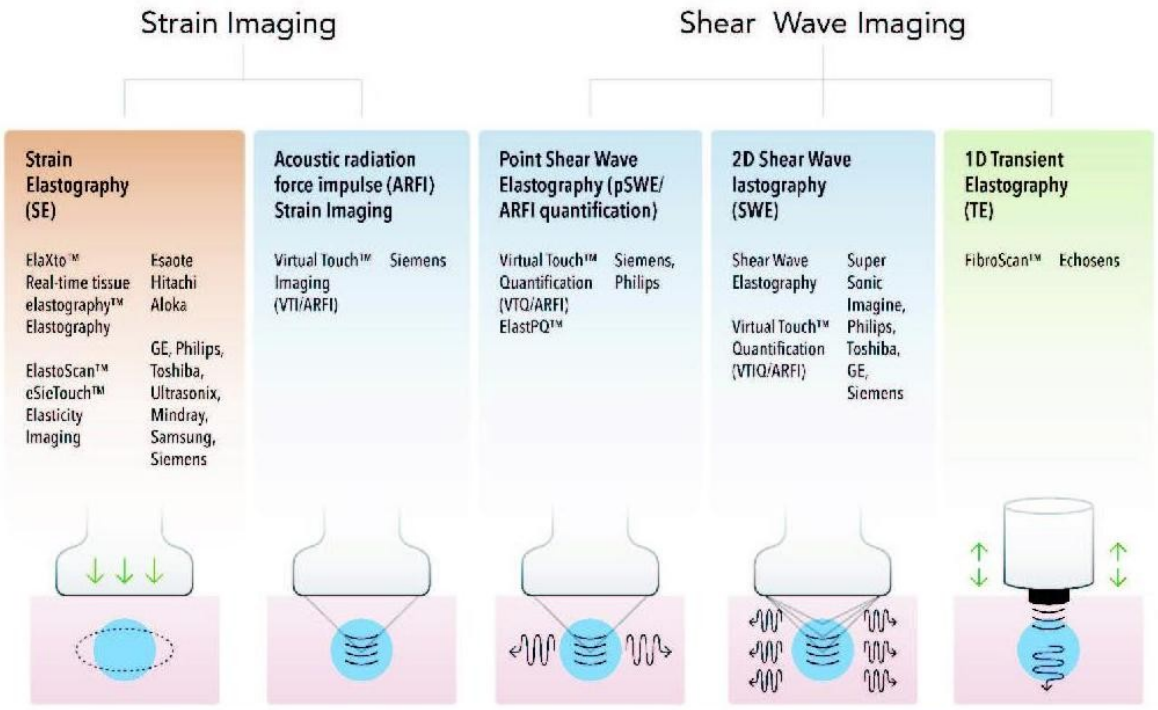

Fig.3.26. Ultrasound Elastography Techniques. Currently available USE techniques can be categorized by the measured physical quantity: 1) strain imaging (left), and 2) shear wave imaging (right). Excitations methods include quasi-static mechanically-induced displacement via active external compression or passively-induced physiologic motion (orange), dynamic mechanically-induced compression via a "thumping" transducer at the tissue surface to produce shear waves (green), and dynamic ultrasound-induced tissue displacement and shear waves by acoustic radiation force impulse excitation (blue).

1D Transient Elastography:

It is the most widely used and validated technique for assessment of liver fibrosis. Dynamic stress is given by a mechanical vibrating device. Shear waves are measured parallel to excitation.

Point shear wave elastography(pSWE):

In this technique, ARFI is used to induce tissue displacement in the normal direction in a single focal location. The longitudinal waves generated by ARFI is intra-converted to shear waves through the absorption of acoustic energy [84].

In liver applications, there are several advantages of pSWE compared to 1D-TE. The operator can use B-mode US to directly visualize the liver to select a uniform area of liver parenchyma without large vessels or dilated bile ducts. Also, unlike 1D-TE where the shear waves are produced by excitation at the body surface, pSWE produces shear waves which originate locally inside the liver, making pSWE less affected by ascites and obesity [85,86,87].

Two-dimensional (2D) Shear wave elastography:

Instead of a single focal location as in ARFI strain imaging and pSWE, multiple focal zones are interrogated in rapid succession, faster than the shear wave speed.

ELASTOGRAPHY PARAMETERS:

Several parameters obtained from these elastography techniques have been studied in the literature in order to characterise a nodule or a tissue overall. All these parameters are not age specific.

These parameters can be divided into three major groups:

- Qualitative,
- Semi-Quantitative and
- Quantitative

Qualitative parameters:

Qualitative parameters are obtained from a visual analysis of parameter maps showing the distribution of deformities or elasticities, which are known as elastograms. These representations are available on most machines regardless of the technique used. They may be presented in grey scales or in colour and the representation scales vary between manufacturers: the hard structures may be coded, for example, in red or blue depending on the manufacturer (**Fig.3.27.**). The ratio between the diameter of nodules on B-mode and on elastography can be calculated.

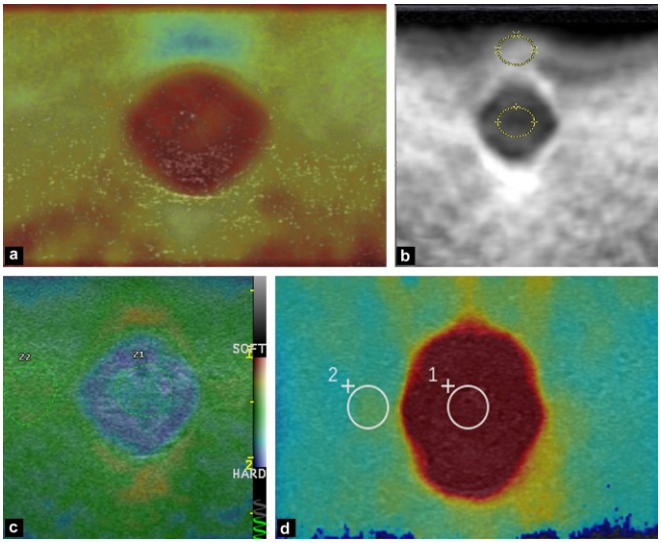

Fig.3.27. Elastograms obtained from the same hard inclusion (type 4) with four systems: a-c by real time elastography, and d by shear wave elastography. Note that the colourimetric hardness scale varies depending on the manufacturer with a hard inclusion coded blue in one (c) and red in the other 2 (a and d). Manufacturer b uses a grey scale coding in which structures of increasing hardness are coded in darker grey and less hard structures are coded in lighter grey.

Semi-quantitative analysis or evaluation of deformations or relative hardness:

Semi-quantitative parameters are calculations of deformation ratios or elasticity ratios between two regions of interest (ROI). These can be calculated with any of the techniques most malignant tissues are harder than the surrounding healthy tissues. The relative hardness of a lesion compared to the adjacent tissue has been studied in different organs, calculating the hardness or deformation ratio between the ROI in the nodule and the surrounding tissue [88,89,90,91,92].

The phantom analysis results show that the ratios obtained vary according to several parameters:

- the system used,
- the position of the ROI in the surrounding tissue compared to the nodule,
- the hardness of the nodule.

Quantitative parameters:

Quantitative parameters are only available from techniques which measure shear wave propagation speed, the values of which are given either in m/s or by calculating the Young module in kPa. Only shear wave elastography techniques can be used for quantitative analysis.

TECHNICAL LIMITATIONS OF ULTRASOUND ELASTOGRAPHY:

With a growing clinical interest in developing new USE applications, or refining existing ones, it is essential to understand current technical limitations that hinder reproducibility of measurements. Several technical confounders are known to affect USE.

A number of these can be traced back to general sonography limitations such as shadowing, reverberation, and clutter artifacts, or the operator-dependent nature of free-hand ultrasound systems [87,93].

Similarly, tissue attenuation decreases ultrasound signal as a function of depth, limiting accurate assessment of deeper tissue or organs.

Fluid or subcutaneous fat also attenuates propagation of the external stimulus applied at the skin surface, which can invalidate measurements in the setting of obesity or abdominal ascites [93].

Of the USE methods described above, measurements from methods that utilize external stimuli, such as strain elastography, are the most challenging to reproduce. Measurements in these modes are highly subjective since the magnitude of the applied stress is difficult to control with operator dependent manual compression and the inherent variability of physiologic motion when used as a stimulus.

Selection of the ROI is also operator dependent and can introduce variability [88]. In addition, the extent of stress induced by an operator can result in strain concentration artifacts around specific structures, which then distort the strain field and generate artifacts in images or erroneous measurements [87,94,95].

Liver USE measurements can be confounded by both pathologic and normal physiologic processes (**Fig.3.28.**).

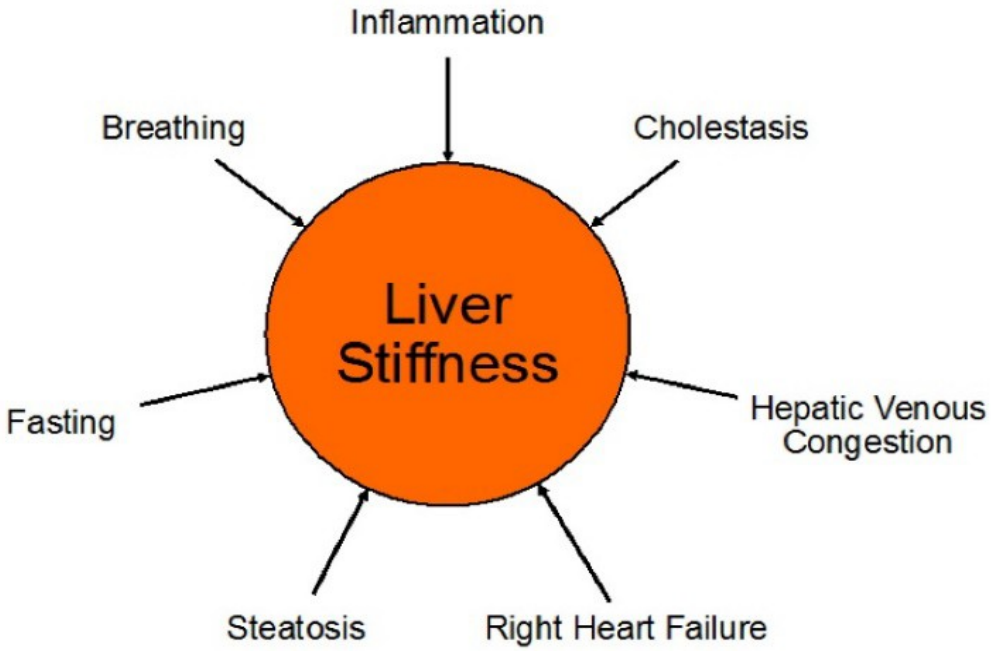

Fig.3.28. Pathologic and normal physiologic processes which can be confounders of liver stiffness measurements. Among other causes, right heart failure can lead to hepatic venous congestion with consecutive elevation of liver stiffness due to the increased venous pressure. Increased levels of inspiration and expiration (Valsalva manoeuvre) can also increase liver stiffness and, therefore, patients need to be coached regarding breathing instructions when obtaining liver stiffness measurements.

Elastography measurements are very dependent on the composition of the tissue (necrosis, haemorrhagic change, the presence of a colloid component, congestion, sinus distension, peliosis fibrosis, etc.), which is often seen, in variable proportions in benign and malignant tumours. Treatments (chemotherapy, anti-angiogenesis etc.) can also change the stiffness of tumour and of the adjacent liver.

PREVIOUS STUDIES ON ULTRASOUND ELASTOGRAPHY IN FOCAL LIVER LESIONS

Park et al [96] evaluated patients with focal liver lesions by ARFI technique using shear wave velocity (SWV) as the parameter. The results showed that significant difference in SWV values was observed between malignant and benign masses (mean 2.31 ± SD m/s vs 1.51 SD m/s, $p = 0.047$), as well as between HCCs and benign masses (mean 2.48 ± SD m/s vs 1.51 ± SD m/s, $p = 0.006$).

Gallotti et al [4] demonstrated a great variability in stiffness of haemangiomas (mean wave velocity value of 2.30 m/s), FNH (mean wave velocity value of the lesion 2.75 m/s), adenomas (mean wave velocity value was 1.25 m/s and HCCs (mean wave velocity value of 2.17 m/s).

Guo et al [97] reported a significant difference of the mean velocity of the mass between malignant and benign liver lesions (SWV of malignant and benign masses being 2.95 ± 1.00 m/s and 1.69 ± 0.89 m/s, respectively) with $p < 0.001$. They also gave cut-off values of 2.13 m/s for the SWV value of focal lesion for the differential diagnosis of malignant and benign masses.

Zhang et al [98] performed ARFI on patients with FLLs. The virtual touch tissue quantification (VTTQ) median values resulted: 1.30, 1.80, 2.52, 3.08 and 3.89 m/s for haemangiomas, FNH, HCC, metastasis and CCC, respectively, from the softest to stiffest one ($p < 0.001$).

Ronot et al [99] demonstrated that there was no difference between the benign and the malignant focal liver lesions in terms of mean stiffness value(kPa) ($p = 0.64$).

The study done by Choi et al [81] showed that there were no statistical differences among the different groups of focal liver lesions in terms of tumour stiffness as seen on ARFI-based shear wave elastography images ($p > 0.05$).

Shuang-Ming et al [100] demonstrated that ARFI could differentiate benign and malignant liver lesions. For a cut-off value of 2.22 m/sec, 89.7% sensitivity, 95% specificity and 92.2% accuracy were observed for the diagnosis of malignancy.

Yu and Wilson [101] found significant differences between quantitative acoustic radiation force impulse values (SWV) of benign and malignant liver masses. A threshold acoustic radiation force impulse value of 1.9 m/s in their study yielded lower sensitivity and higher specificity for differentiation between benign and malignant liver masses.

Kapoor et al [102] reported that SWV showed significant differences in the strain velocities of benign, metastatic and hepatocellular carcinoma nodules $p < 0.0001$ and $p < 0.008$ respectively.

Lu et al [103] demonstrated that diagnostic performance with stiffness values was significantly lower than that with stiffness ratio for discrimination of metastasis from primary liver cancers.

Heide et al [104] evaluated 62 liver lesions by using ARFI quantitative elastography. Mean velocity(m/s) was assessed for each group of lesions, which showed no significant difference between benign and malignant tumour groups.

Davies and Koenen [105] performed a study on 45 liver tumours by using ARFI Quantitative elastography. The mean velocity measurements showed significant difference between angiomas and metastases. The cut-off value to differentiate benign (Angiomas) from malignant (Metastases) was 2.5 m/s.

Frulio et al [106] proposed a hypothesis that there was no significant difference between benign and malignant tumour groups in terms of mean shear wave velocity due to large tissue heterogeneity for the same type of tumour and between tumour types.

4.AIM OF THE STUDY

1. To acquire ultrasound elastographic parameters (Stiffness value, Stiffness Ratio, Shear wave velocity & Strain Ratio) in persons with focal liver lesions.
2. To study the differences among the elastographic parameters obtained from various focal liver lesions and to correlate with the histopathological results.
3. To find out the sensitivity and specificity of the elastographic parameters that can be used to differentiate malignant tumours from other benign tumours of the liver.

5. MATERIALS AND METHODS

5.1 Study Area : Barnard Institute of Radiology,
Madras Medical College, Chennai.

5.2 Study Period : 6 months (March 2018 – August 2018)

5.3 Sample Size : 50

5.4 Study Design : Prospective study

5.5 Inclusion Criteria:

- Age between 20 and 80 years, both sexes.
- The presence of focal liver lesions identified by USG / Conventional CT/MRI.

5.6 Exclusion Criteria:

Lactating and pregnant females whatever the gestational age.

Patients with focal liver lesions which have been treated previously.

Patients with gross ascites.

Patients with simple hepatic cysts.

Uncooperative patients / patients unable to hold breath.

5.7 METHODOLOGY:

This prospective study was performed after obtaining clearance from our Institutional Ethics Committee and institutional informed consent guidelines were observed.

5.7.1 Study Population:

Patients with focal liver lesions referred for image guided biopsy/ planned for surgical resection were included in this study during the period from March 2018 to August 2018.

The patients were screened using the drawn inclusion/ exclusion criteria. Relevant entries in the proforma for each patient were made after reviewing his/her case sheet & previous medical records.

The final population enrolled in this study composed of 50 patients diagnosed as having focal liver lesion by ultrasound / Conventional CT/MRI, planned for image guided biopsy/scheduled for surgery.

All patients were required to provide written informed consent before study participation.

5.7.2 Elastographic Examination:

Patients with focal liver lesions underwent abdominal sonographic examination and elastography using 3.5MHz convex probe in Hitachi Aloka Arietta S70 machine.

Scanning was performed as follows:

Shear Wave Elastography:

SWE acquisition was performed just after a complete morphological and Doppler vascularization examination of the liver. Patients were placed in the supine position, with the right arm in maximum abduction to make the right hypochondrium accessible and to increase intercostal space (to improve the acoustic window). The probe was placed parallel to the intercostal space within the space with sufficient gel in order to minimize rib shadowing. The size of the region of interest was approximately 1.0 cm by 1.5 cm at a depth of 4 cm. The maximum penetration depth was 7 cm. The liver stiffness measurement was performed in areas without blood vessels during a 5-second breath hold at inspiration. For patients with multiple lesions, the largest lesion was chosen as the index lesion. Liver stiffness was measured in two locations: in the peripheral area of the largest lesion, in the liver at greater than 2 cm from the lesion periphery (background liver). From which, stiffness value (kPa), stiffness ratio and shear wave velocity(m/s) were obtained. The measurements were performed five times for each group. The mean value of five measurements for each individual was used in the statistical analysis.

Strain Elastography:

After fitting the strain elastographic image box to fully cover the lesion in the liver, we applied the probe with vertical pressure, avoiding lateral movement. Subcostal scanning was used for all elastographic examinations. On strain elastography, strain represents the degree of tissue displacement as a response to induced pressure.

Strain values of tissues were measured by putting equal or near-equal sized regions of interest in the lesion and liver parenchyma. Regions of interest were intended to be at the same level as possible to perform the measurements. The sizes of the regions of interest were determined as large enough to place within the confines of the lesion to represent elasticity of the lesion appropriately. The strain ratio value was obtained which represents the ratio of the strain of focal solid liver lesions to that of normal liver parenchyma. All the patients were followed up and histopathological reports were collected from the pathology department except patients with haemangiomas, for whom other imaging modalities were used as the confirmation study.

The mean of the observed values was calculated for each group of lesions. These values were correlated with histopathological results. The ability of these values to differentiate between benign and malignant focal liver lesions was assessed.

Case:1

50-year-old male with upper abdominal pain diagnosed to have focal liver lesion on USG. Histopathology showed- hepatocellular carcinoma.

Shear wave elastography:

Lesion:

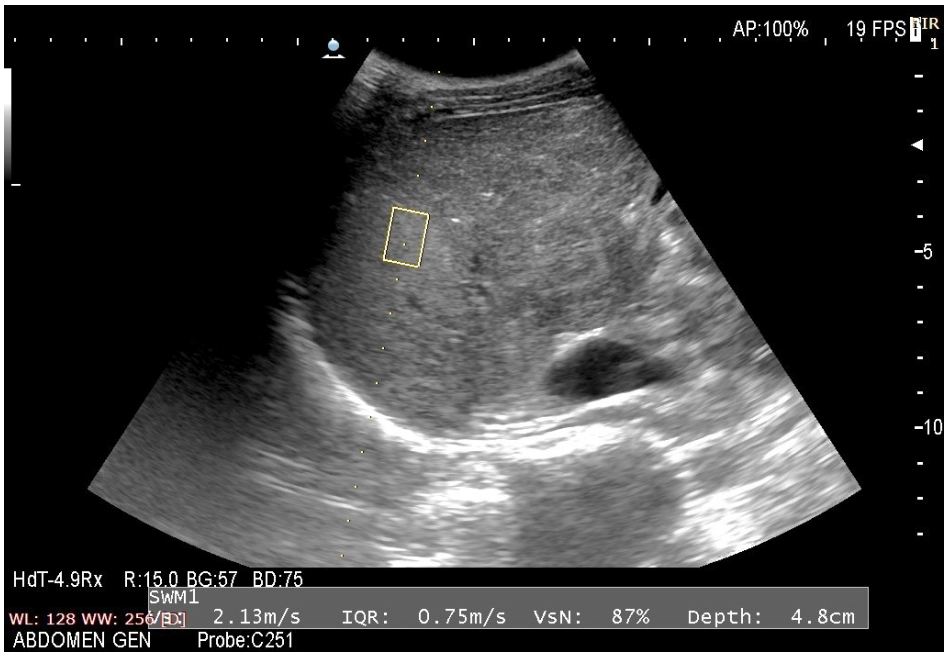

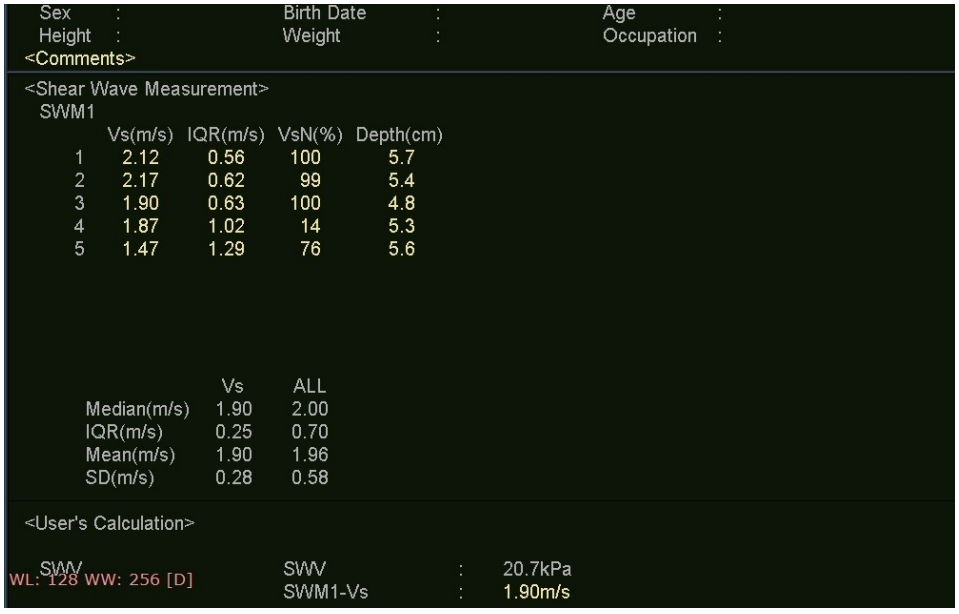

Background Liver:

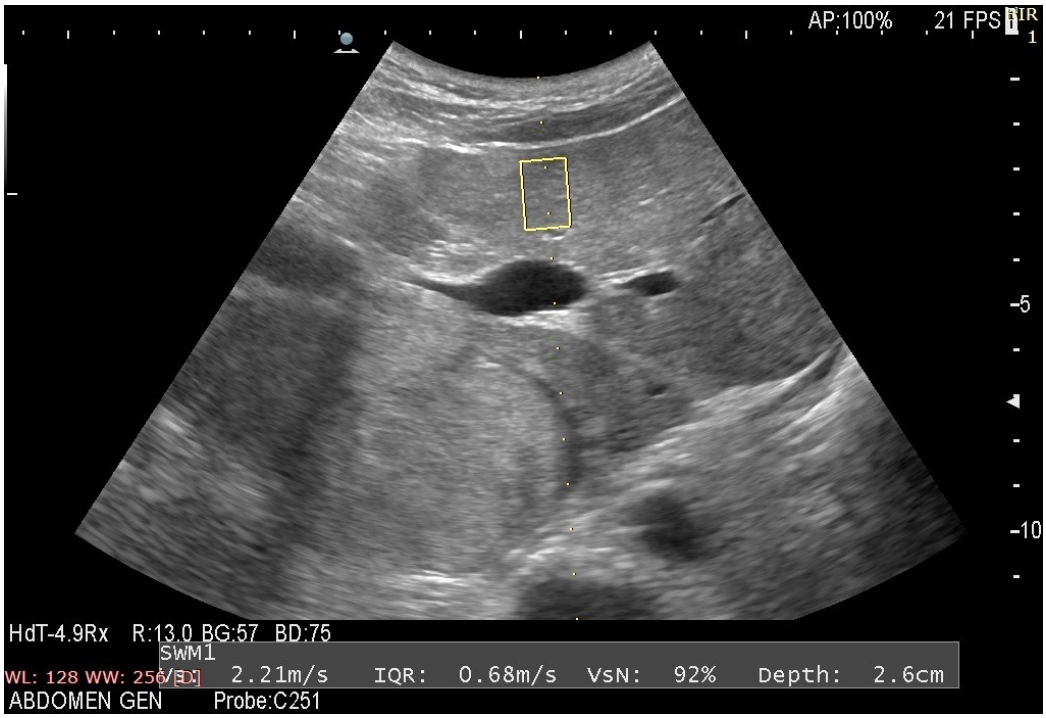

Sex : Birth Date : Age :
Height : Weight : Occupation :
<Comments>

<Shear Wave Measurement>
SWM1

	Vs(m/s)	IQR(m/s)	VsN(%)	Depth(cm)
1	2.30	0.70	84	2.4
2	2.62	0.85	77	2.3
3	2.21	0.68	92	2.6
4	1.87	0.53	99	2.6
5	2.17	0.47	98	2.6

	Vs	ALL
Median(m/s)	2.21	2.18
IQR(m/s)	0.13	0.66
Mean(m/s)	2.23	2.21
SD(m/s)	0.27	0.52

<User's Calculation>

SWV SWV : 33.4kPa
SWM1-Vs : 2.23m/s

Strain Elastography:

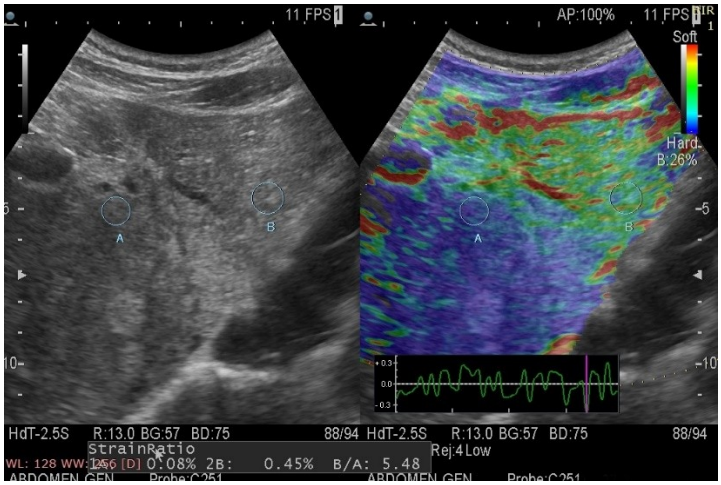

Elastography Parameters:

HCC	
Parameter	**Values**
Stiffness Value of lesion(kPa)	20.70
Stiffness Value of background liver(kPa)	33.40
Stiffness Ratio	0.62
Shear wave velocity of lesion(m/s)	1.90
Shear wave velocity of background liver(m/s)	2.23
Strain Ratio	5.50

HPE- HEPATOCELLULAR CARCINOMA

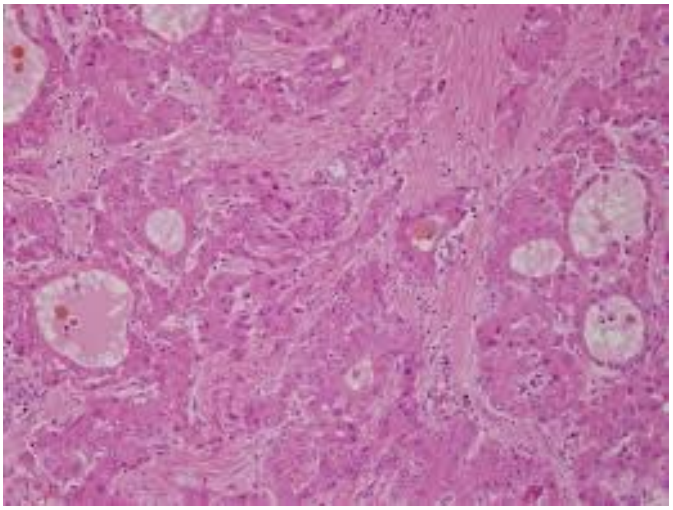

Case:2

65-year-old male with right upper quadrant pain diagnosed to have few focal liver lesions on USG. Histopathology showed- well differentiated adenocarcinoma metastasis.

Shear wave elastography:

Lesion:

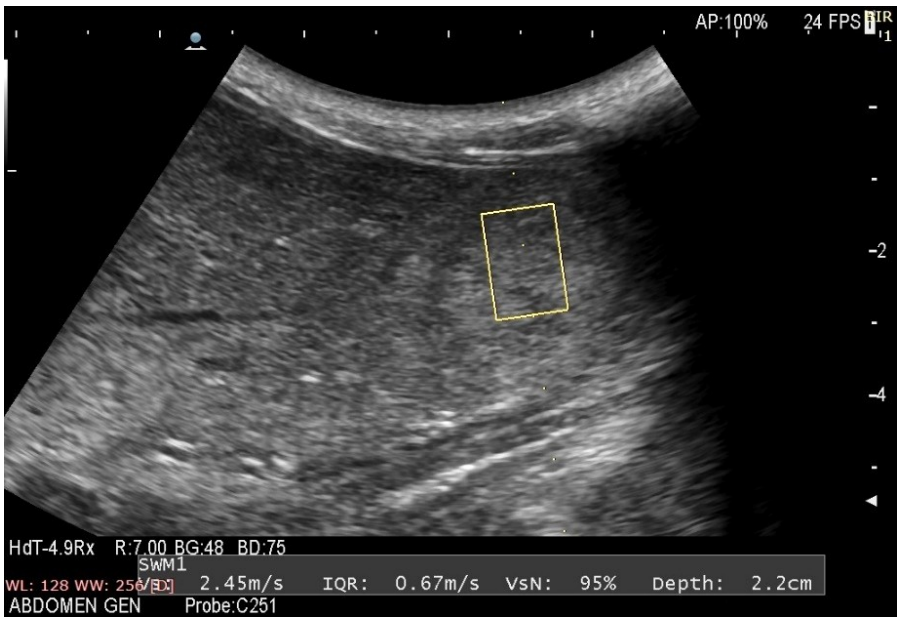

Background Liver:

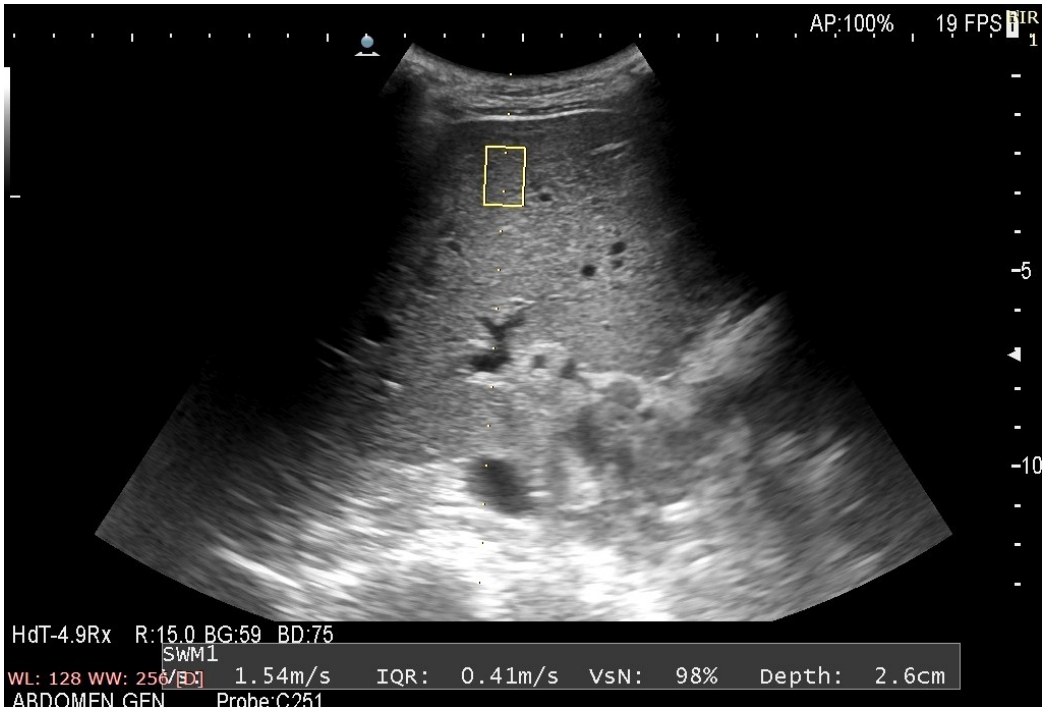

Sex : Birth Date : Age :
Height : Weight : Occupation :
<Comments>

<Shear Wave Measurement>
SWM1

	Vs(m/s)	IQR(m/s)	VsN(%)	Depth(cm)
1	1.50	0.22	100	2.7
2	1.51	0.46	100	2.8
3	1.50	0.49	99	2.7
4	1.54	0.40	100	3.0
5	1.54	0.41	98	2.6

	Vs	ALL
Median(m/s)	1.51	1.52
IQR(m/s)	0.03	0.36
Mean(m/s)	1.52	1.52
SD(m/s)	0.02	0.29

<User's Calculation>

SWV SWV : 10.5kPa
SWM1-Vs : 1.52m/s

WL: 128 WW: 256 [D]

Strain Elastography:

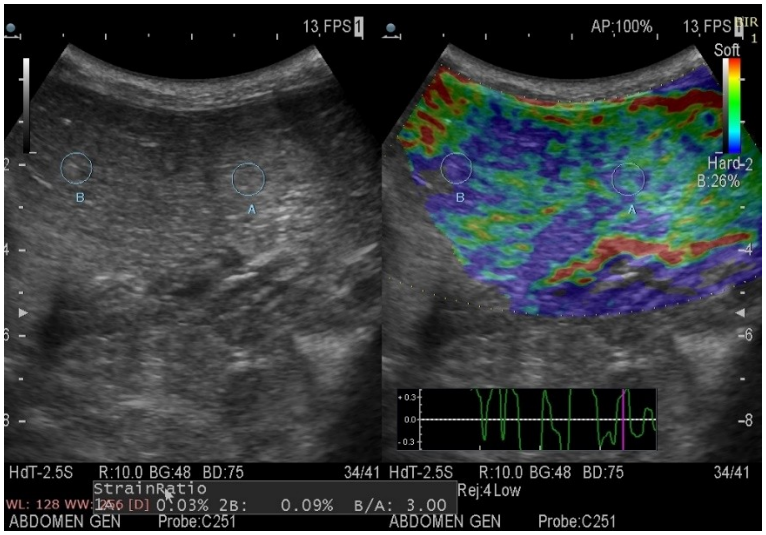

Elastography Parameters:

METASTASIS	
Parameter	**Values**
Stiffness Value of lesion(kPa)	52.90
Stiffness Value of background liver(kPa)	10.50
Stiffness Ratio	5.03
Shear wave velocity of lesion(m/s)	2.60
Shear wave velocity of background liver(m/s)	1.52
Strain Ratio	3.00

HPE- METATSTASIS TO LIVER

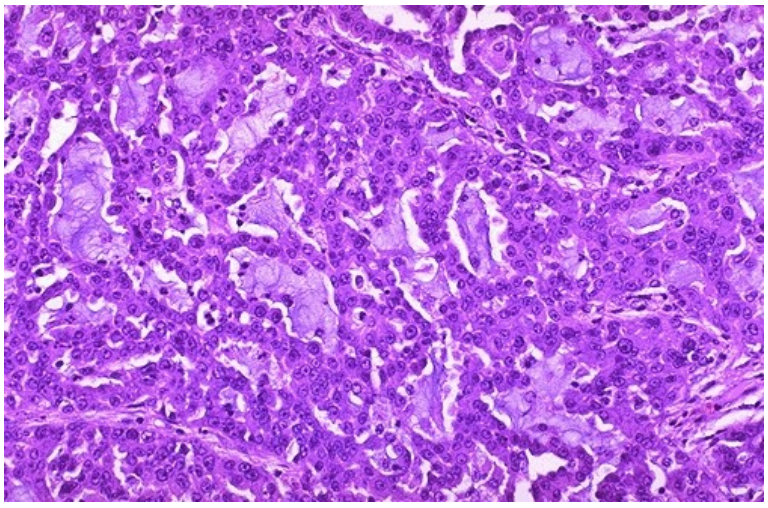

Case:3

35-year-old female with upper abdominal pain diagnosed to have few focal liver lesions on USG. Histopathology showed- haemangioma.

Shear wave elastography:

Lesion:

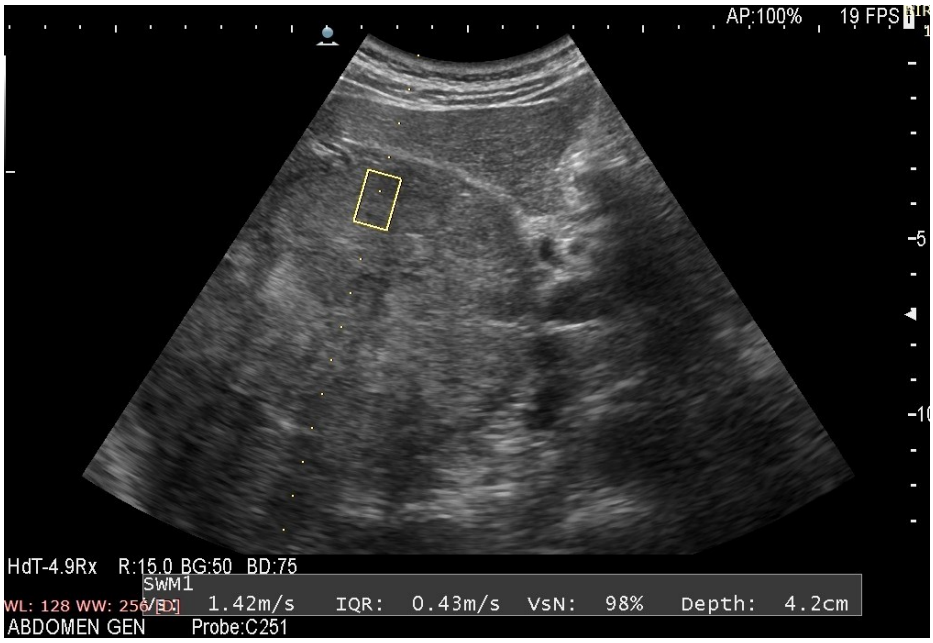

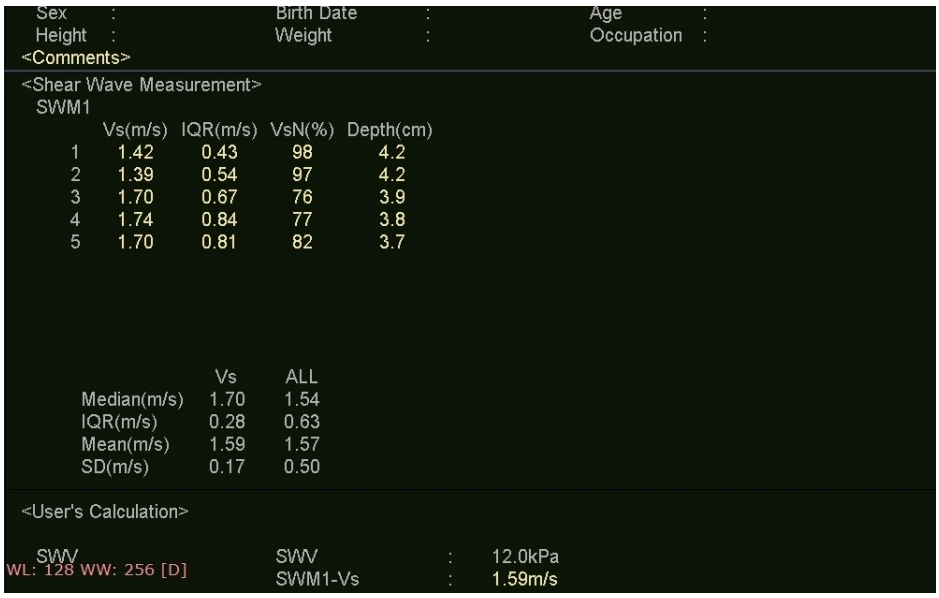

Background Liver:

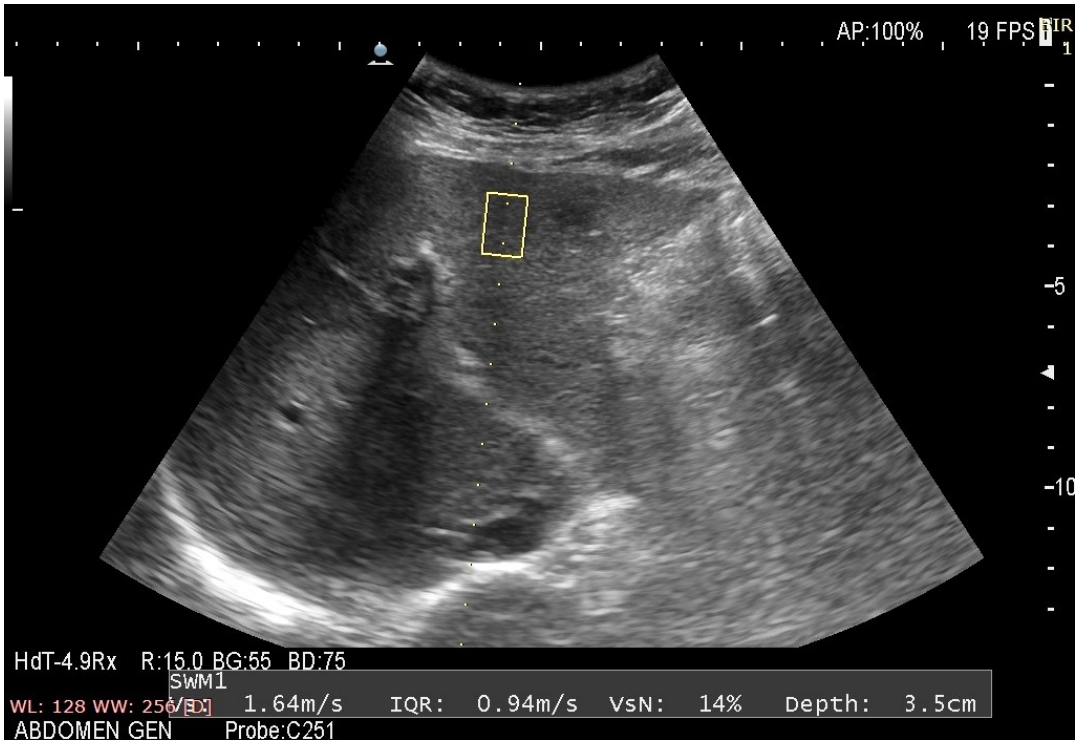

Sex : Birth Date : Age :
Height : Weight : Occupation :
<Comments>

<Shear Wave Measurement>
SWM1

	Vs(m/s)	IQR(m/s)	VsN(%)	Depth(cm)
1	1.05	0.22	10	3.9
2	1.74	1.39	45	3.8
3	1.02	1.01	53	3.8
4	1.57	1.02	72	3.9
5	1.64	0.94	14	3.5

	Vs	ALL
Median(m/s)	1.57	1.43
IQR(m/s)	0.59	1.04
Mean(m/s)	1.40	1.51
SD(m/s)	0.34	0.77

<User's Calculation>

SWV : 8.3kPa
SWM1-Vs : 1.40m/s

Strain Elastography:

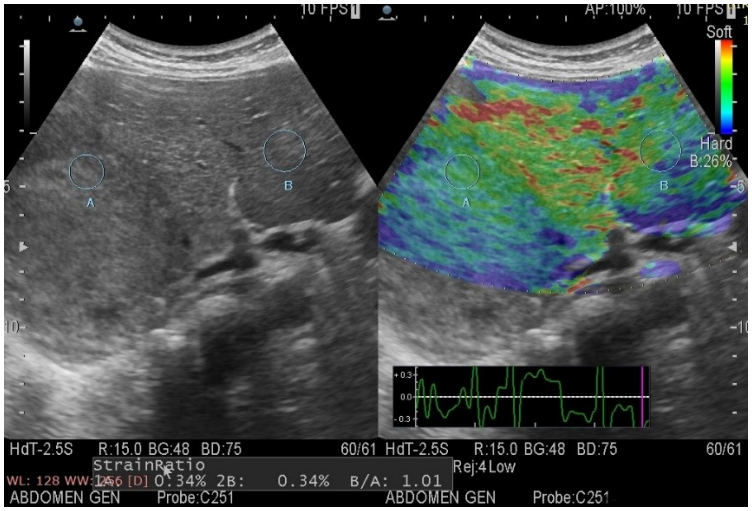

Elastography Parameters:

HAEMANGIOMA	
Parameter	**Values**
Stiffness Value of lesion(kPa)	12.00
Stiffness Value of background liver(kPa)	8.30
Stiffness Ratio	1.44
Shear wave velocity of lesion(m/s)	1.59
Shear wave velocity of background liver(m/s)	1.40
Strain Ratio	1.01

HPE- HAEMANGIOMA LIVER

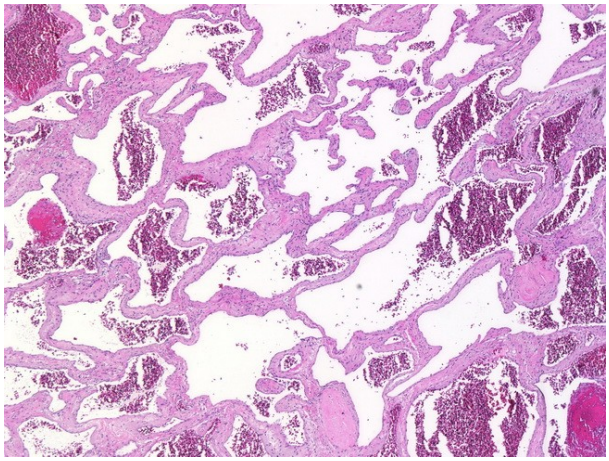

Case:4

57-year-old male with right upper abdominal pain and jaundice diagnosed to have few focal liver lesions on USG. Histopathology showed- cholangiocarcinoma

Shear wave elastography:

Lesion:

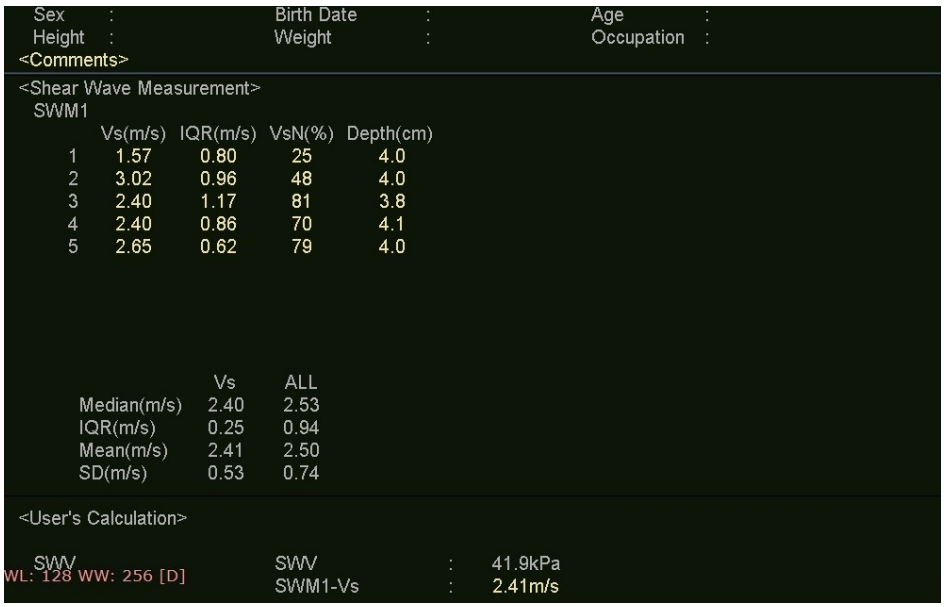

Background Liver:

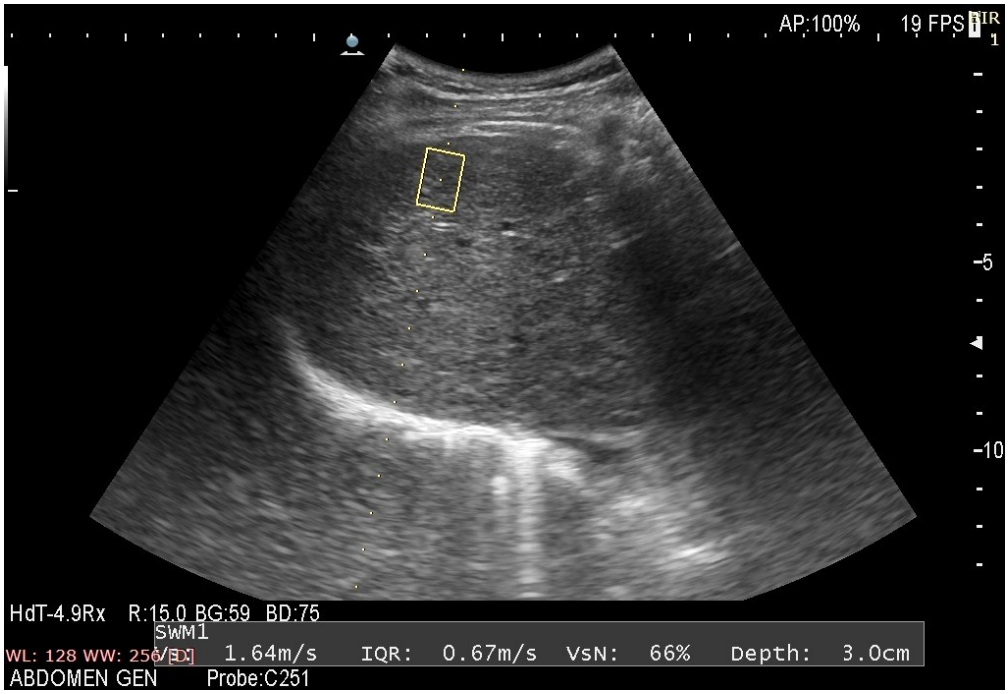

Sex : Birth Date : Age :
Height : Weight : Occupation :
<Comments>

<Shear Wave Measurement>
SWM1

	Vs(m/s)	IQR(m/s)	VsN(%)	Depth(cm)
1	1.72	1.23	14	2.3
2	1.64	0.67	66	3.0
3	1.56	0.94	59	3.5
4	1.01	1.16	57	3.2
5	1.25	0.65	53	3.6

	Vs	ALL
Median(m/s)	1.56	1.45
IQR(m/s)	0.39	0.83
Mean(m/s)	1.44	1.45
SD(m/s)	0.30	0.63

<User's Calculation>

SWV

WL: 128 WW: 256 [D]

SWV : 8.9kPa
SWM1-Vs : 1.44m/s

Strain Elastography:

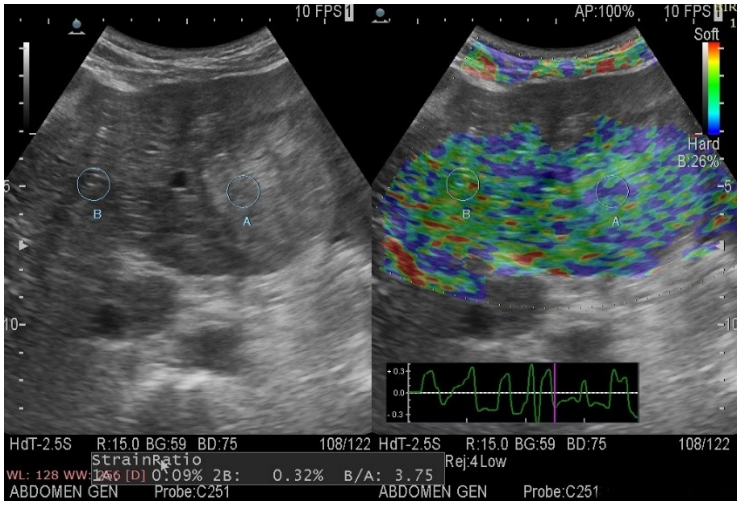

Elastography Parameters:

CHOLANGIOCARCINOMA	
Parameter	**Values**
Stiffness Value of lesion(kPa)	41.90
Stiffness Value of background liver(kPa)	8.90
Stiffness Ratio	4.71
Shear wave velocity of lesion(m/s)	2.41
Shear wave velocity of background liver(m/s)	1.44
Strain Ratio	3.75

HPE- CHOLANGIOCARCINOMA

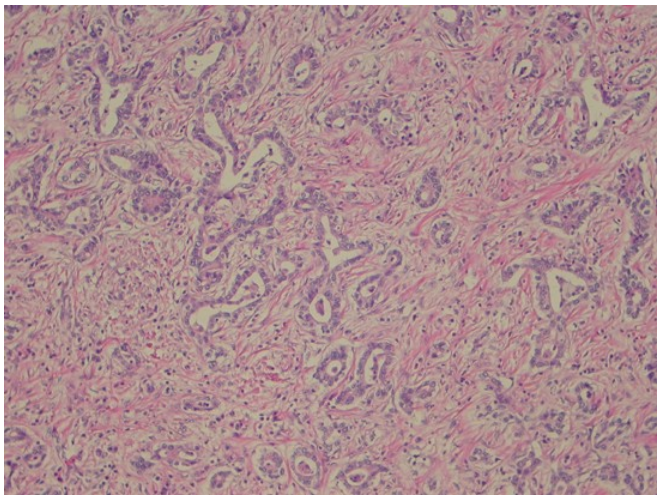

Case:5

40-year-old female with upper abdominal pain diagnosed to have few focal liver lesions on USG. Histopathology showed- FNH

Shear wave elastography:

Lesion:

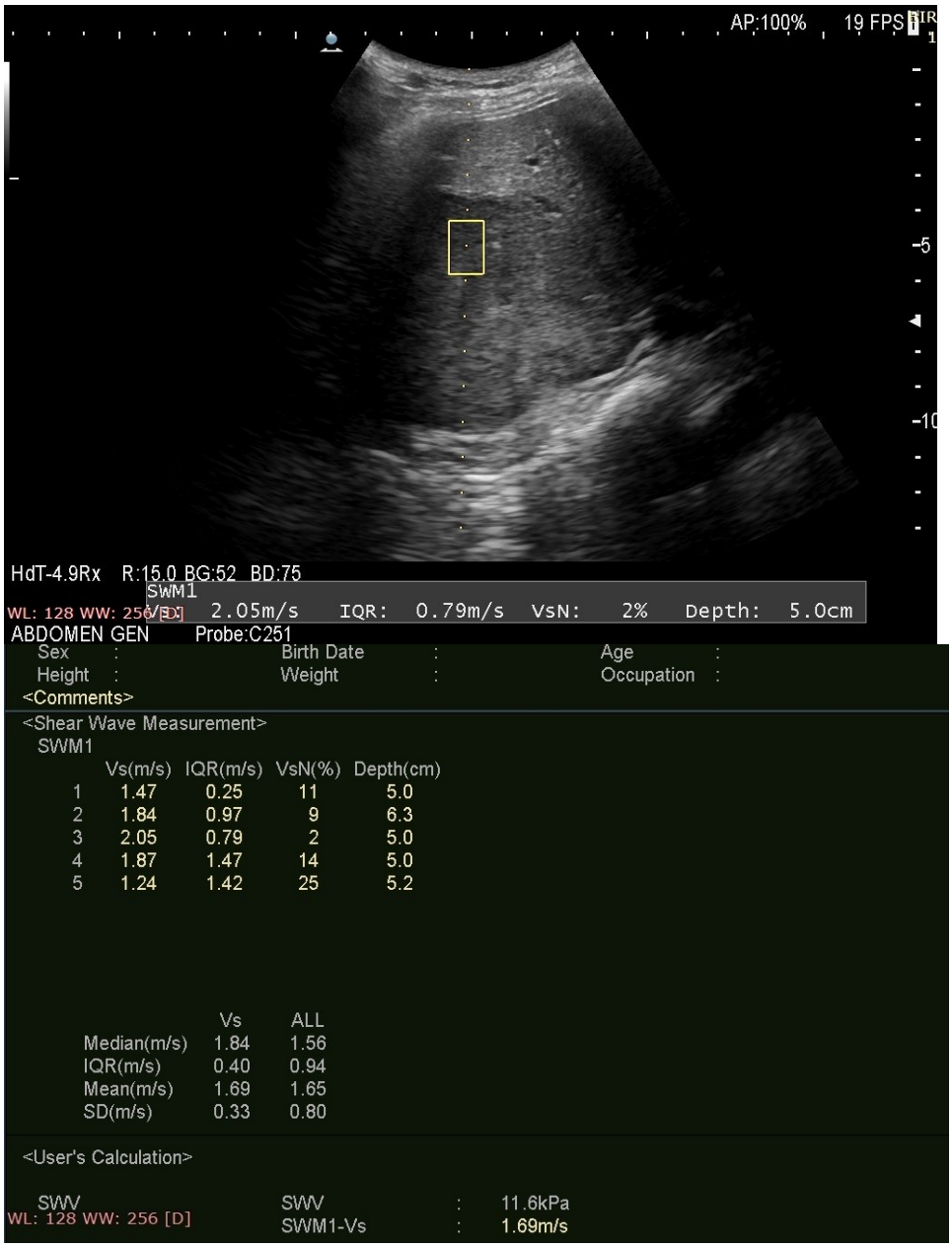

Background Liver:

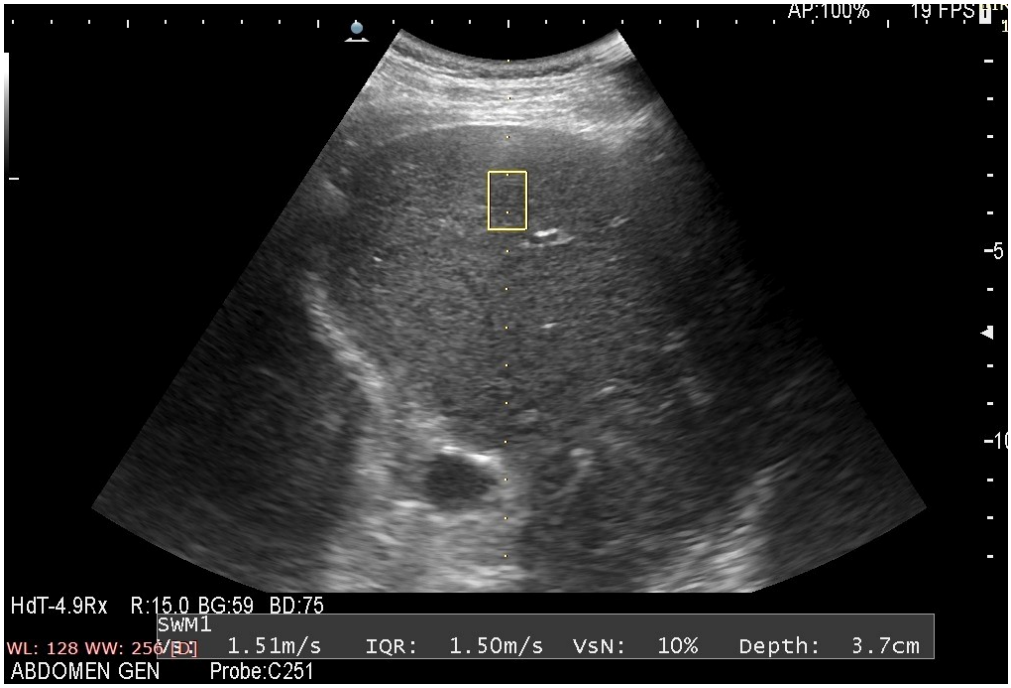

Sex : Birth Date : Age :
Height : Weight : Occupation :
<Comments>

<Shear Wave Measurement>
SWM1

	Vs(m/s)	IQR(m/s)	VsN(%)	Depth(cm)
1	1.29	1.13	54	4.0
2	1.21	0.65	65	4.0
3	1.35	0.74	55	4.1
4	1.45	1.48	43	4.1
5	0.96	0.39	63	4.1

	Vs	ALL
Median(m/s)	1.25	1.19
IQR(m/s)	0.13	0.65
Mean(m/s)	1.24	1.26
SD(m/s)	0.17	0.57

<User's Calculation>

WL: 128 WW: 256 [D]
SWV : 5.8kPa
SWM1-Vs : 1.24m/s

Strain Elastography:

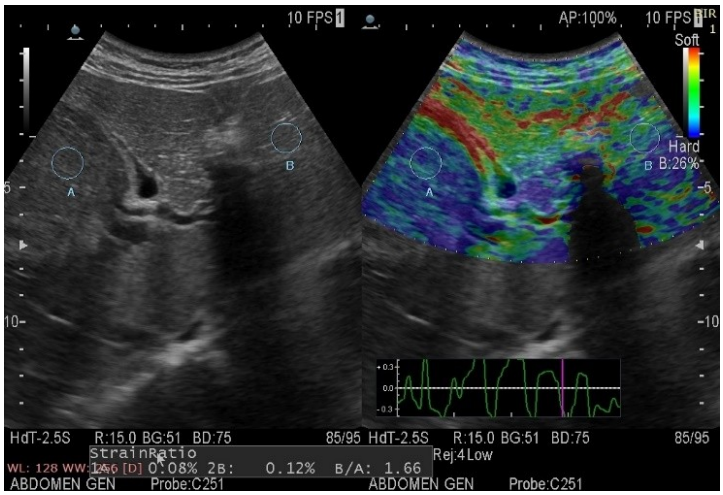

Elastography Parameters:

FNH	
Parameter	**Values**
Stiffness Value of lesion(kPa)	11.60
Stiffness Value of background liver(kPa)	5.80
Stiffness Ratio	2.00
Shear wave velocity of lesion(m/s)	1.69
Shear wave velocity of background liver(m/s)	1.24
Strain Ratio	1.66

HPE- FOCAL NODULAR HYPERPLASIA

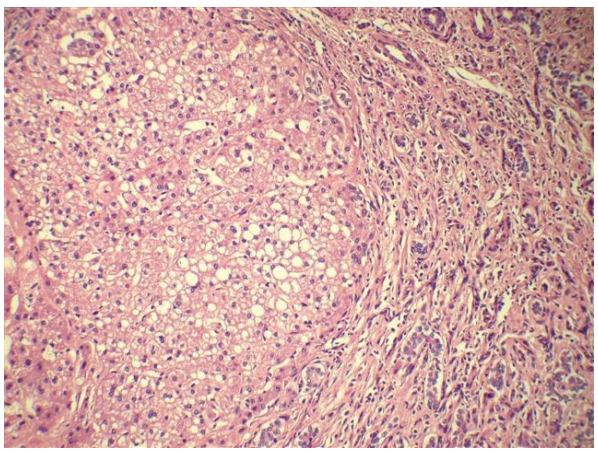

6.STATISTICAL ANALYSIS

The collected data were analysed with IBM.SPSS statistics software 23.0 Version.

To describe about the data descriptive statistics, frequency analysis & percentage analysis were used for categorical variables and the mean & Standard Deviation were used for continuous variables.

To find the significant difference between the bivariate samples in Independent groups the Unpaired sample t-test was used.

The Receiver Operator Characteristic (ROC) curve analysis was used to find the Sensitivity, Specificity.

To find the significance in categorical data Chi-Square test was used similarly if the expected cell frequency is less than 5 in 2×2 tables then the Fisher's Exact was used.

In all the above statistical tools the probability value .05 is considered as significant level.

7.OBSERVATION & RESULTS

7.1.AGE DISTRIBUTION

In this study, benign liver lesions are more common in people up to 4th decade (~63%), whereas malignant liver lesions are more common in 6th to 7th decade (~66%).

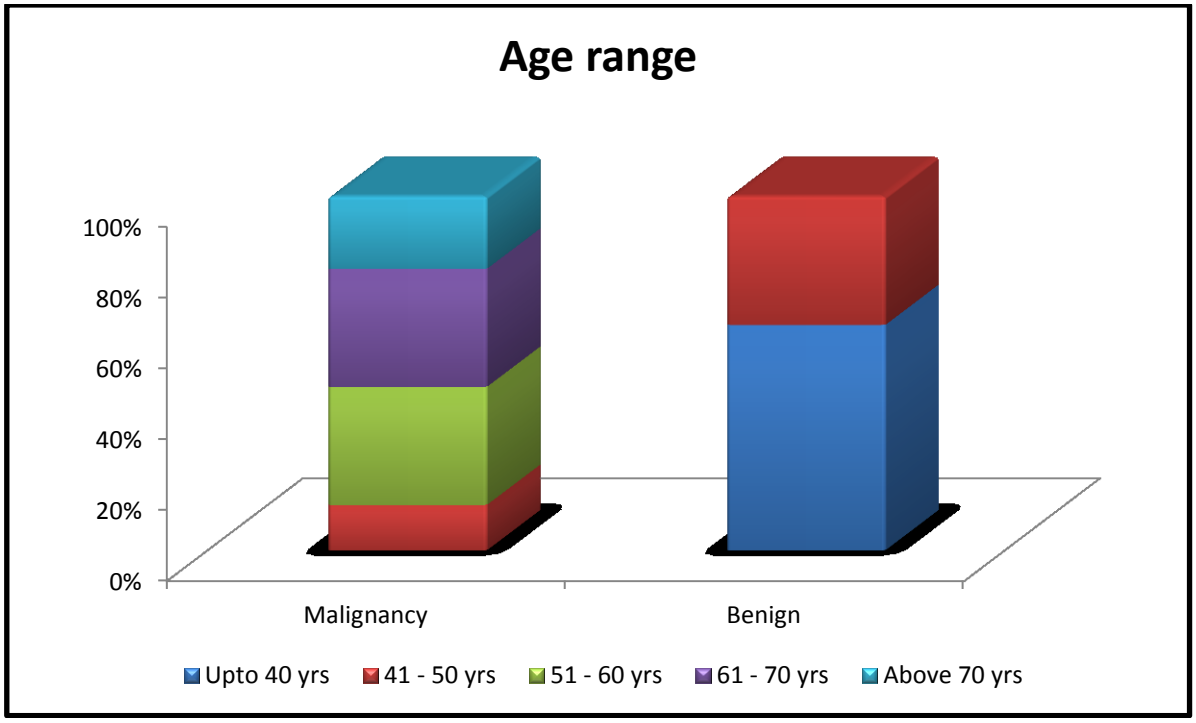

Fig.7.1.1. Bar diagram showing mean age range distribution of benign and malignant liver lesion among the study group

	Malignancy	Benign
Upto 40 yrs	0.0%	63.6%
41 - 50 yrs	12.8%	36.4%
51 - 60 yrs	33.3%	
61 - 70 yrs	33.3%	
Above 70 yrs	20.5%	

Table.7.1.1. Mean age range distribution of benign and malignant liver lesion among the study group

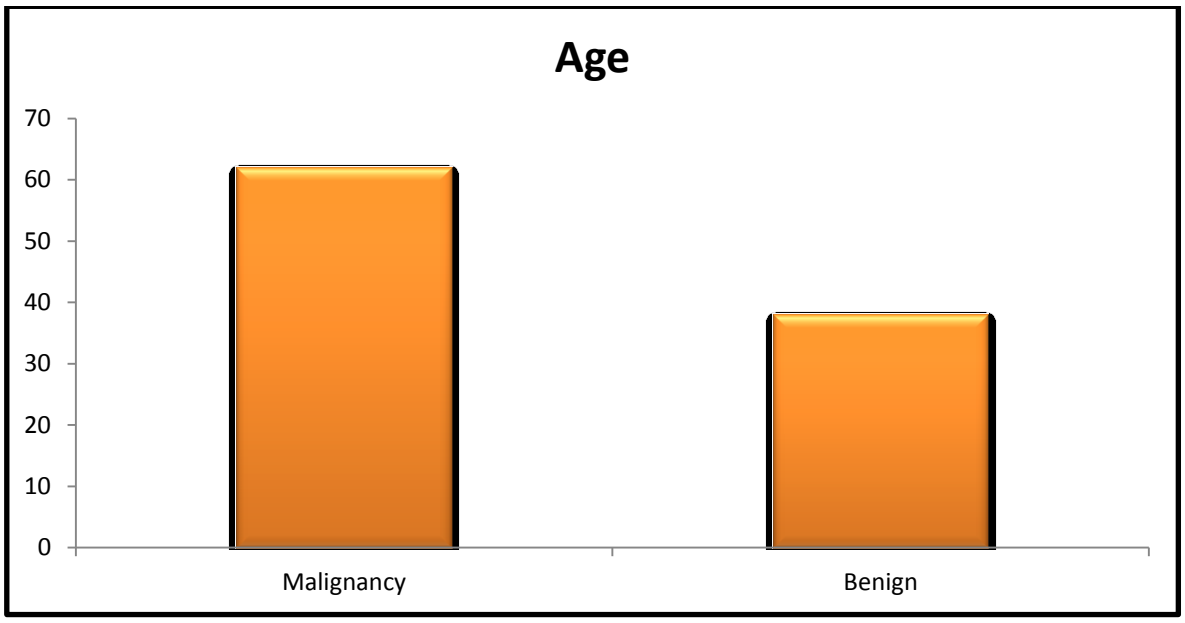

Fig.7.1.2. Bar diagram showing mean age range distribution of benign and malignant liver lesion among the study group

	Age
Malignancy	62
Benign	38

Table.7.1.2. Mean age range distribution of benign and malignant liver lesion among the study group

7.2. GENDER DISTRIBUTION

In this study, out of 50 patients, 37 (74%) were males and 13(26%) were females. Out of 39 patients of malignant liver lesion 30(76.9 %) were males and 9 were females (23.1 %). Out of 11 patients of benign liver lesion 7 (63.6%) were males and 4 (36.4%) were female.

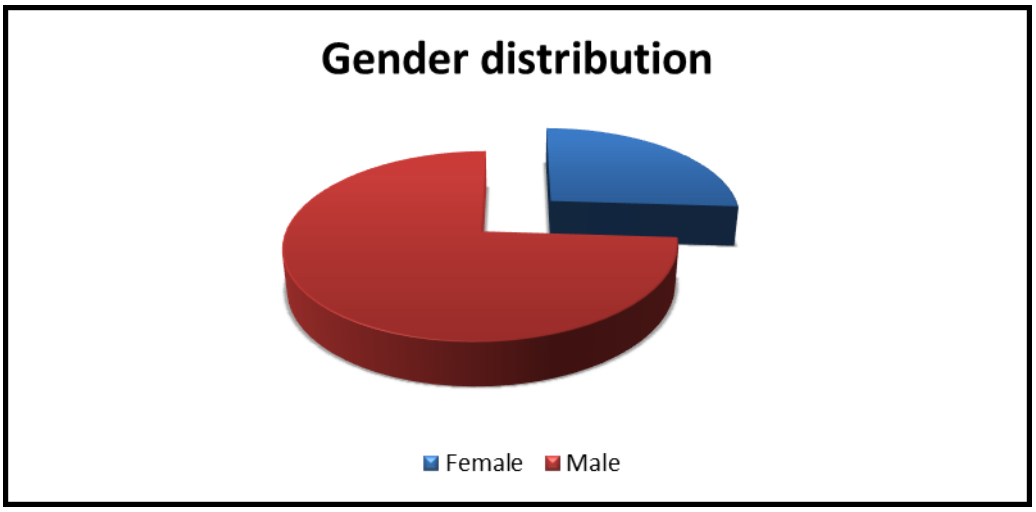

Fig.7.2.1. Pie chart shows gender distribution of liver lesions

GENDER			
		Frequency	Percent
Valid	Female	13	26.0
	Male	37	74.0
	Total	50	100.0

Table.7.2.1. Cross tabulation showing gender distribution of liver lesions

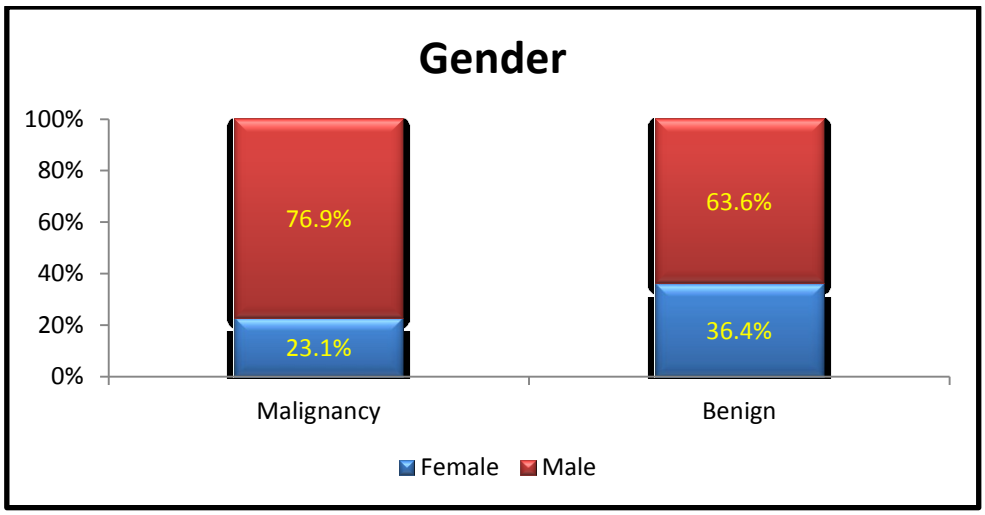

Fig.7.2.2. Bar diagram shows gender distribution of benign and malignant liver lesion among the study group

Crosstab					
			HPE		Total
			Malignancy	Benign	
SEX	F	Count	9	4	13
		% within HPE	23.1%	36.4%	26.0%
	M	Count	30	7	37
		% within HPE	76.9%	63.6%	74.0%
Total		Count	39	11	50
		% within HPE	100.0%	100.0%	100.0%

Table.7.2.2. Gender distribution of benign and malignant liver lesion among the study group

7.3. FREQUENCY DISTRIBUTION OF FOCAL LIVER LESIONS

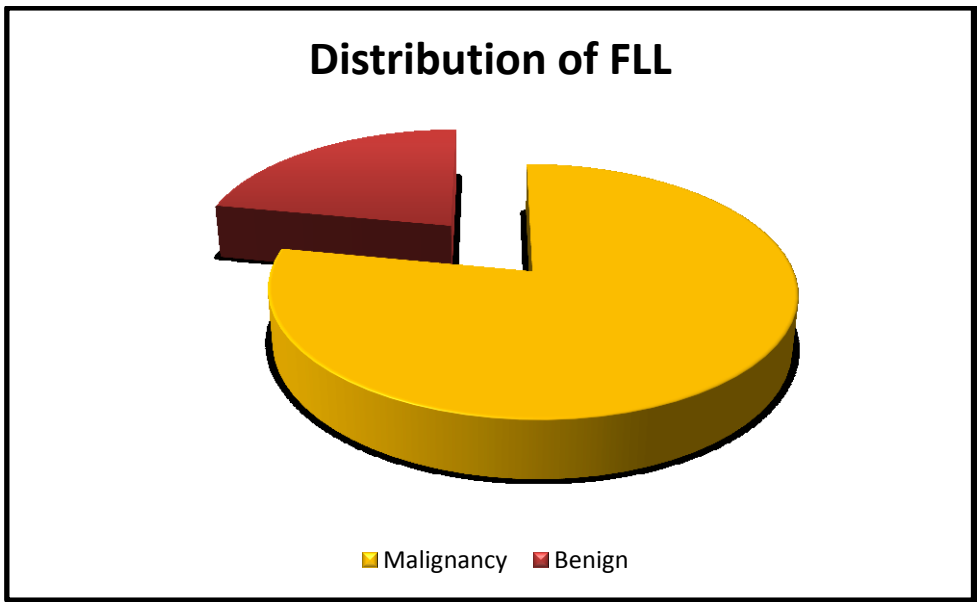

Fig.7.3.1. Pie chart showing the distribution of malignant & benign liver lesions among the study group.

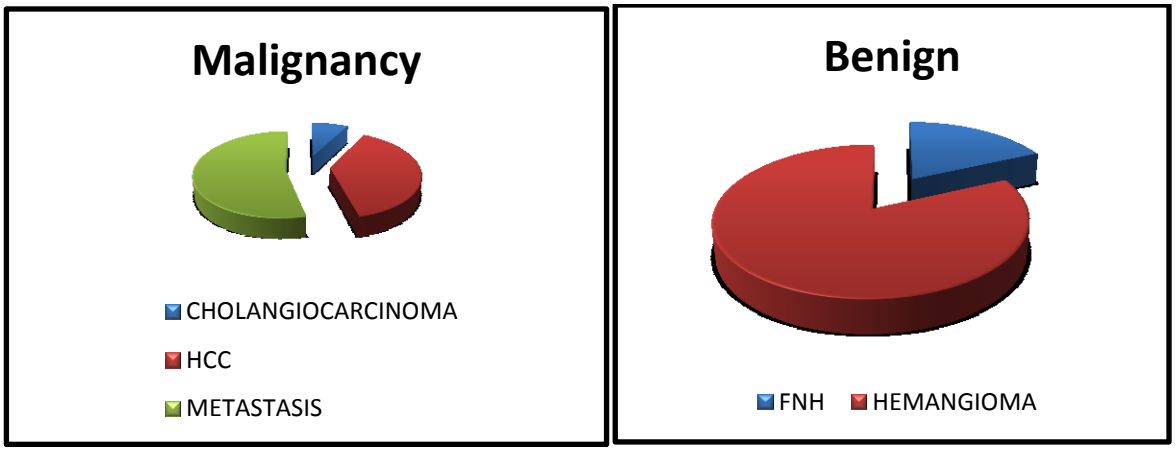

Fig.7.3.2. Pie charts showing the distribution of various malignant and benign FLL.

DISTRIBUTION OF FLL			
		Frequency	Percent
Valid	CHOLANGIOCARCINOMA	3	6.0
	FNH	2	4.0
	HCC	15	30.0
	HEMANGIOMA	9	18.0
	METASTASIS	21	42.0
	Total	50	100.0

Table.7.3.1. Overall frequency distribution of FLL in the study group.

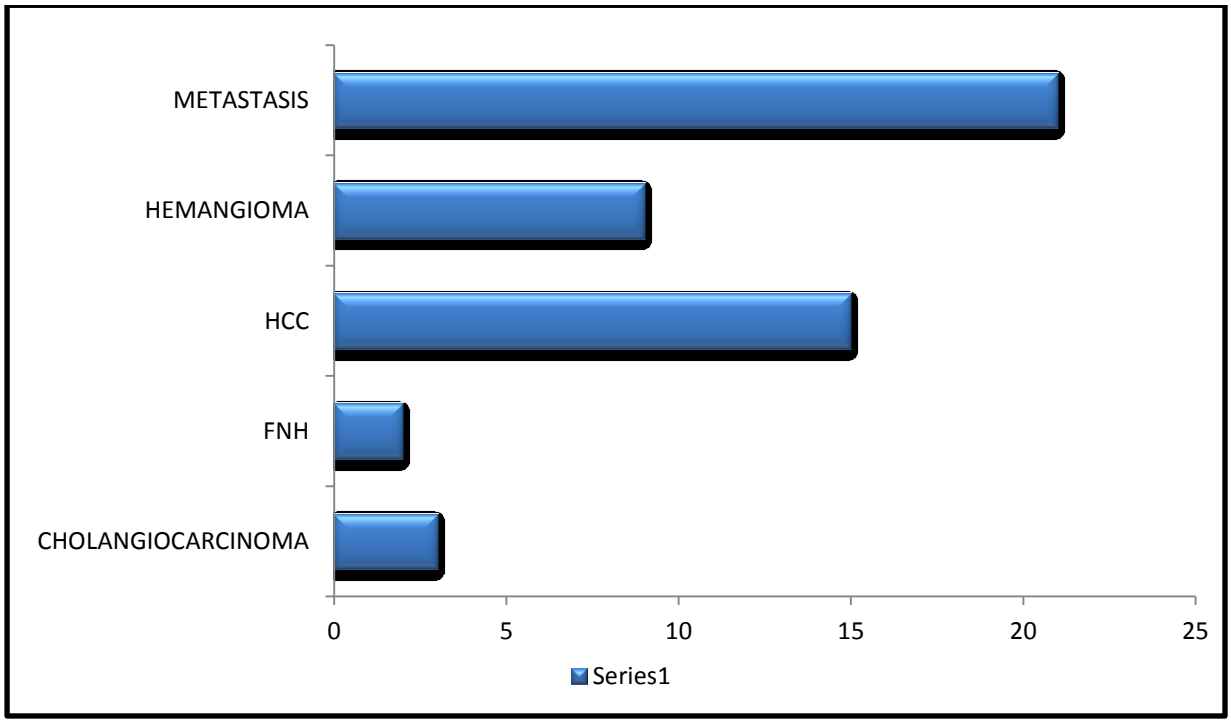

Fig.7.3.3. Bar diagram showing overall frequency distribution of FLL in the study group.

7.4.USG CHARACTERISTICS OF LESIONS

Multiplicity of lesions in each group:

		NO. OF LESIONS		Total
		MULTIPLE	SINGLE	
CHOLANGIOCARCINOMA	Count	0	3	3
	%	0.0%	100.0%	100.0%
FNH	Count	0	2	2
	%	0.0%	100.0%	100.0%
HCC	Count	3	12	15
	%	20.0%	80.0%	100.0%
HEMANGIOMA	Count	2	7	9
	%	22.2%	77.8%	100.0%
METASTASIS	Count	21	0	21
	%	100.0%	0.0%	100.0%

Table.7.4.1. Multiplicity of lesions in each group

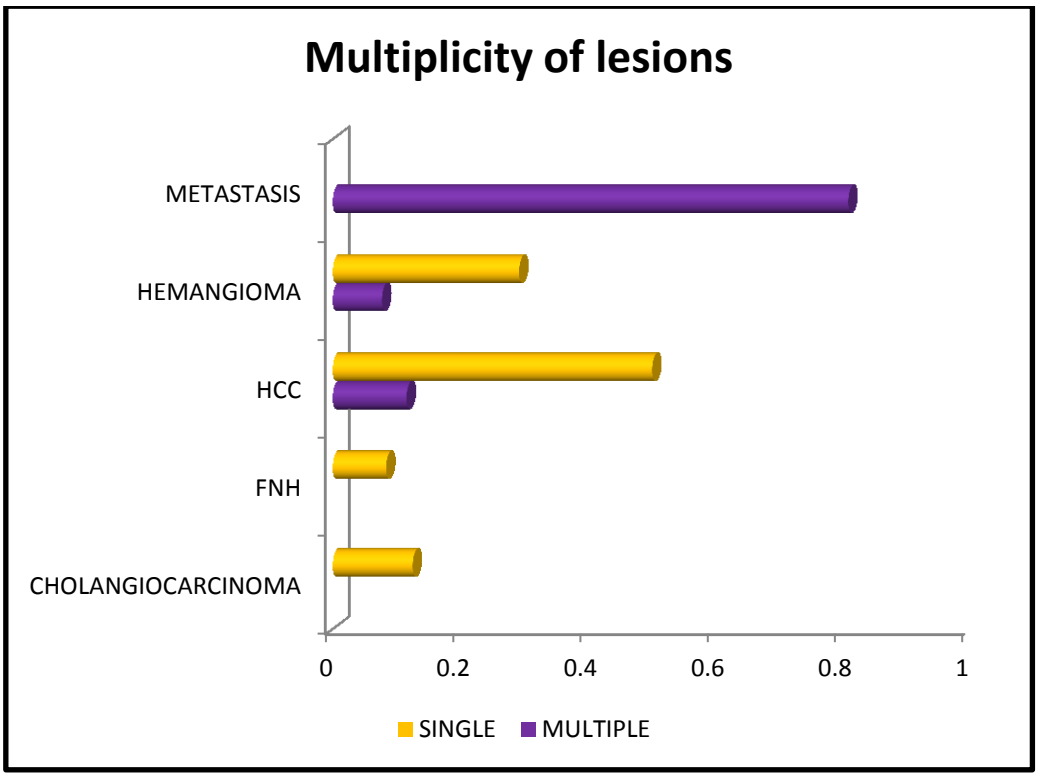

Fig.7.4.1. Bar diagram showing multiplicity of lesions in each group

Background liver in each group:

		BACKGROUND LIVER		Total
		CIRRHOSIS	NORMAL	
CHOLANGIOCARCINOMA	Count	0	3	3
	%	0.0%	100.0%	100.0%
FNH	Count	0	2	2
	%	0.0%	100.0%	100.0%
HCC	Count	11	4	15
	%	73.3%	26.7%	100.0%
HEMANGIOMA	Count	0	9	9
	%	0.0%	100.0%	100.0%
METASTASIS	Count	0	21	21
	%	0.0%	100.0%	100.0%

Table.7.4.2. Background liver in each group

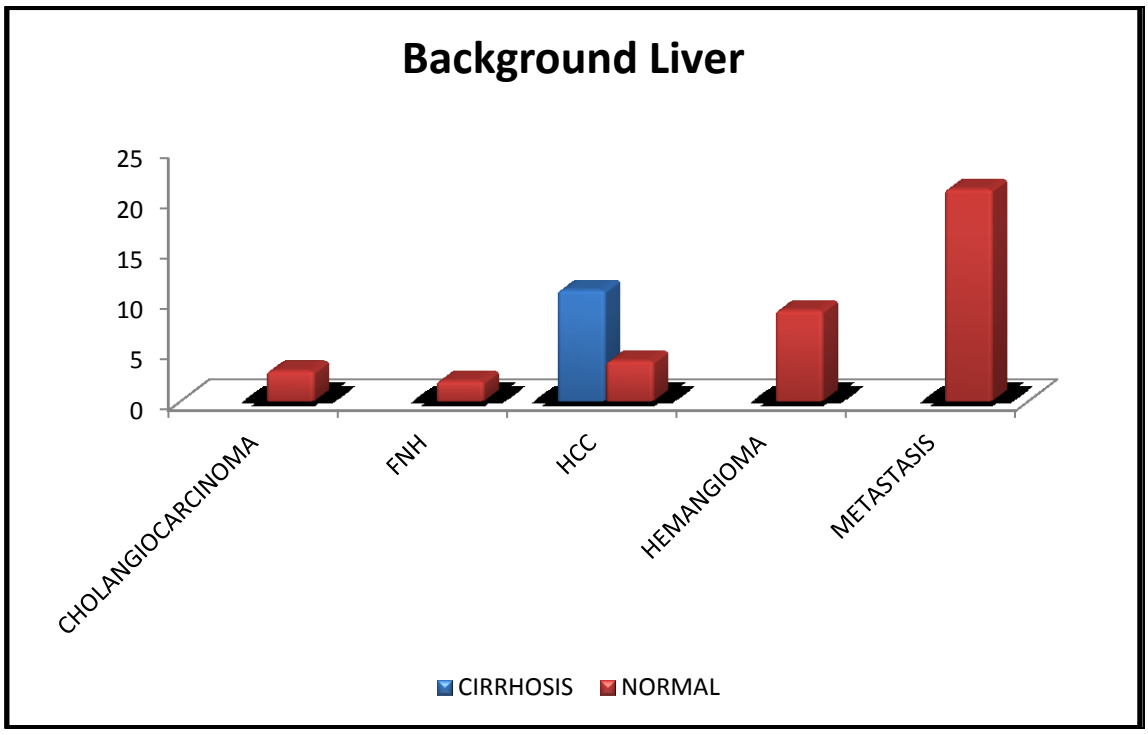

Fig.7.4.2. Bar diagram showing background liver in each group

Echogenicity of lesions in each group:

		LESION ECHOGENICITY			Total
		HETERO-ECHOIC	HYPER-ECHOIC	HYPO-ECHOIC	
CHOLANGIOCARCINOMA	Count	3	0	0	3
	%	100.0%	0.0%	0.0%	100.0%
FNH	Count	0	0	2	2
	%	0.0%	0.0%	100.0%	100.0%
HCC	Count	11	0	4	15
	%	73.3%	0.0%	26.7%	100.0%
HEMANGIOMA	Count	0	9	0	9
	%	0.0%	100.0%	0.0%	100.0%
METASTASIS	Count	21	0	0	21
	%	100.0%	0.0%	0.0%	100.0%

Table.7.4.3. Echogenicity of lesions in each group

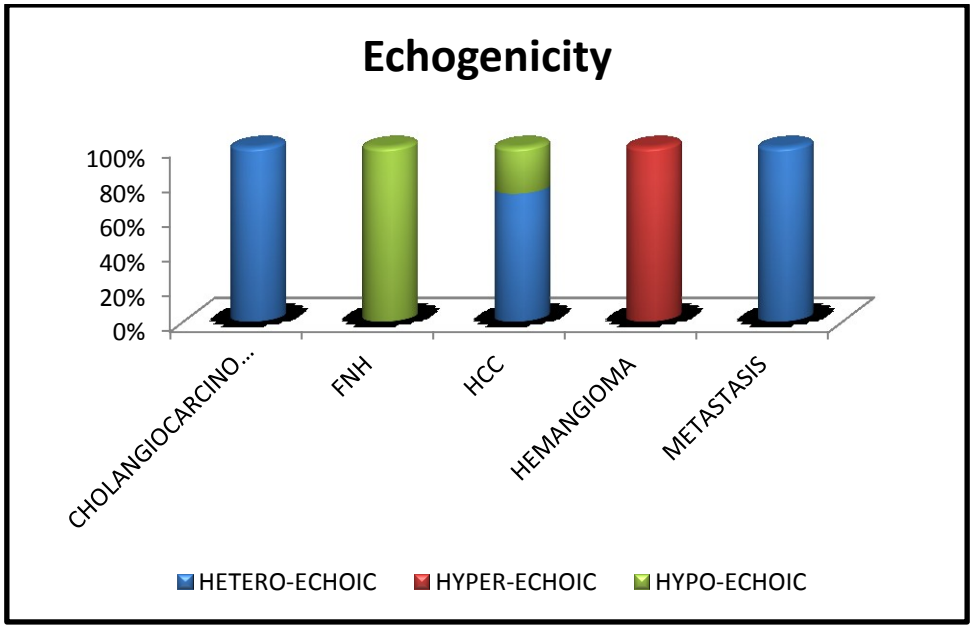

Fig.7.4.3. Bar diagram showing echogenicity of lesions in each group.

Vascularity of lesions in each group:

		VASCULARITY		Total
		INCREASED	NORMAL	
CHOLANGIOCARCINOMA	Count	0	3	3
	%	0.0%	100.0%	100.0%
FNH	Count	0	2	2
	%	0.0%	100.0%	100.0%
HCC	Count	11	4	15
	%	73.3%	26.7%	100.0%
HEMANGIOMA	Count	2	7	9
	%	22.2%	77.8%	100.0%
METASTASIS	Count	0	21	21
	%	0.0%	100.0%	100.0%

Table.7.4.4. Vascularity of lesions in each group.

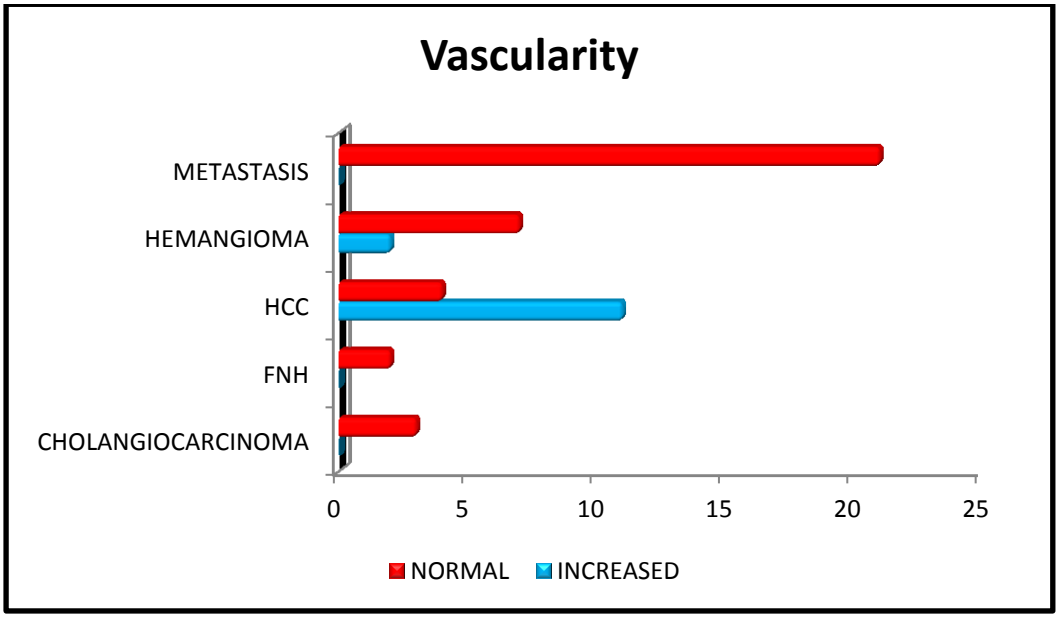

Fig.7.4.4. Bar diagram showing vascularity of lesions in each group.

Involvement of portal vein in each group:

		PORTAL VEIN THROMBOSIS		Total
		NO	YES	
CHOLANGIOCARCINOMA	Count	3	0	3
	%	100.0%	0.0%	100.0%
FNH	Count	2	0	2
	%	100.0%	0.0%	100.0%
HCC	Count	9	6	15
	%	60.0%	40.0%	100.0%
HEMANGIOMA	Count	9	0	9
	%	100.0%	0.0%	100.0%
METASTASIS	Count	21	0	21
	%	100.0%	0.0%	100.0%

Table.7.4.5. Portal vein involvement in each group

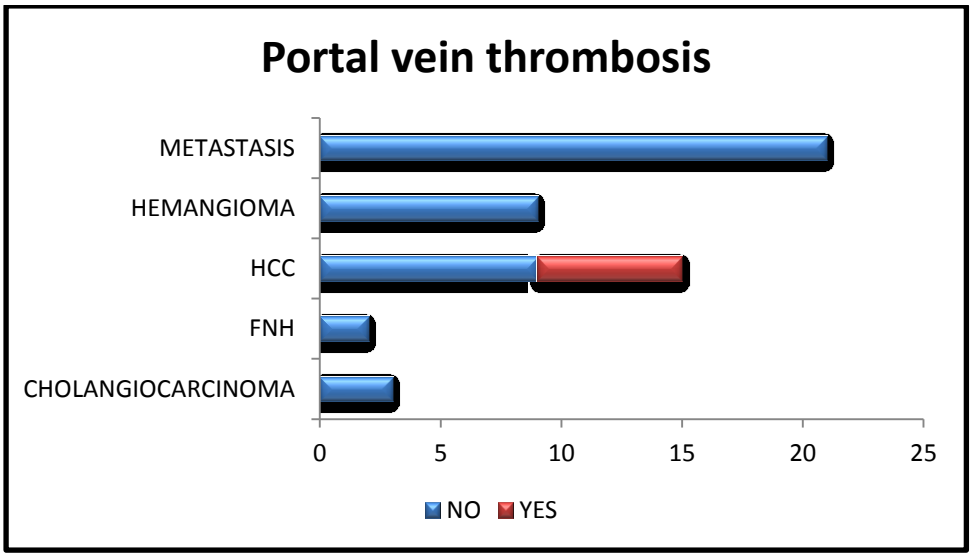

Fig.7.4.5. Bar diagram showing portal vein involvement in each group

7.5. MEAN VALUES OF ELASTOGRAPHIC PARAMETERS AMONG FLL

Among malignant lesions:

Group Statistics:

		N	Mean	Std. Deviation	Minimum	Maximum
STIFFNESS VALUE OF LESION(kPa)	HCC	15	37.7	18.7	15	82
	METASTASIS	21	28.0	16.1	7	68
	CHOLANGIOCARCINOMA	3	38.3	8.6	29	46
	Total	39	32.5	17.1	7	82
STIFFNESS RATIO	HCC	15	2.6	3.1	.3	11.9
	METASTASIS	21	4.1	2.5	1.1	9.7
	CHOLANGIOCARCINOMA	3	5.1	1.6	3.3	6.2
	Total	39	3.6	2.8	.3	11.9
SWV OF LESION	HCC	15	2.2	0.4	1.7	3.0
	METASTASIS	21	2.6	0.6	1.7	3.5
	CHOLANGIOCARCINOMA	3	2.5	0.4	2.1	2.8
	Total	39	2.5	0.5	1.7	3.5
STRAIN RATIO	HCC	15	3.3	0.7	2.75	5.50
	METASTASIS	21	3.3	0.3	2.85	3.89
	CHOLANGIOCARCINOMA	3	4.1	0.2	3.96	4.39
	Total	39	3.4	0.5	2.75	5.50

Table.7.5.1. Mean values of elastographic parameters among malignant liver lesions.

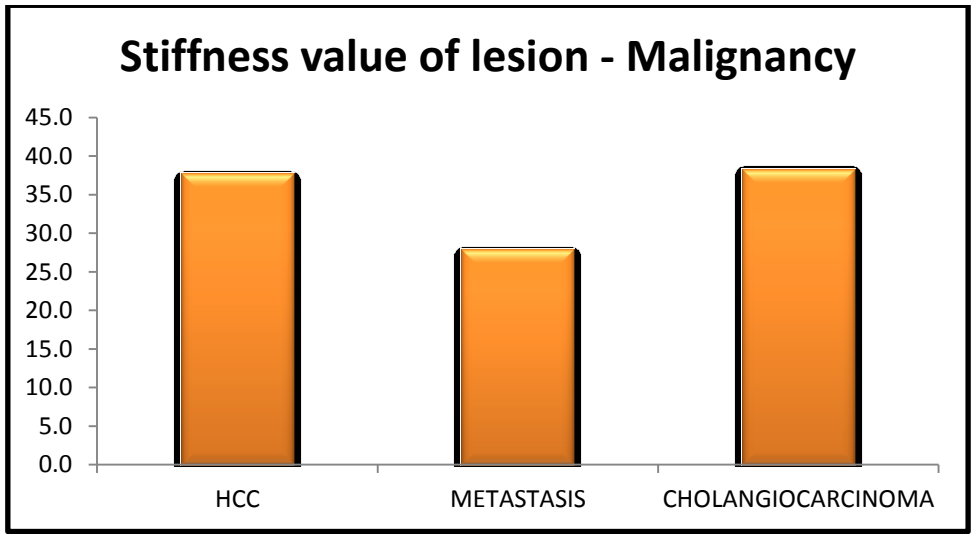

Fig.7.5.1. Bar diagram showing mean values of Stiffness value(kPa) among malignant liver lesions.

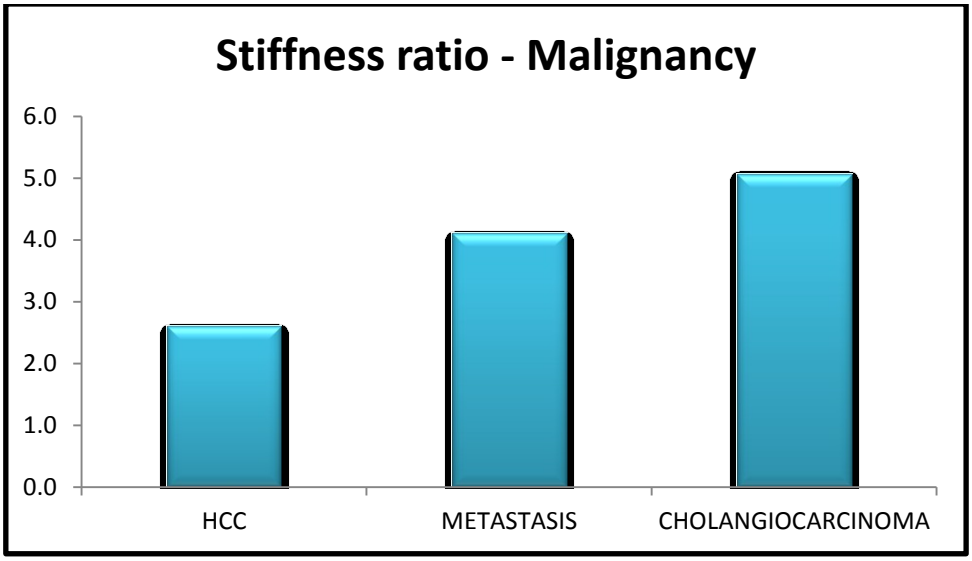

Fig.7.5.2. Bar diagram showing mean values of Stiffness ratio among malignant liver lesions.

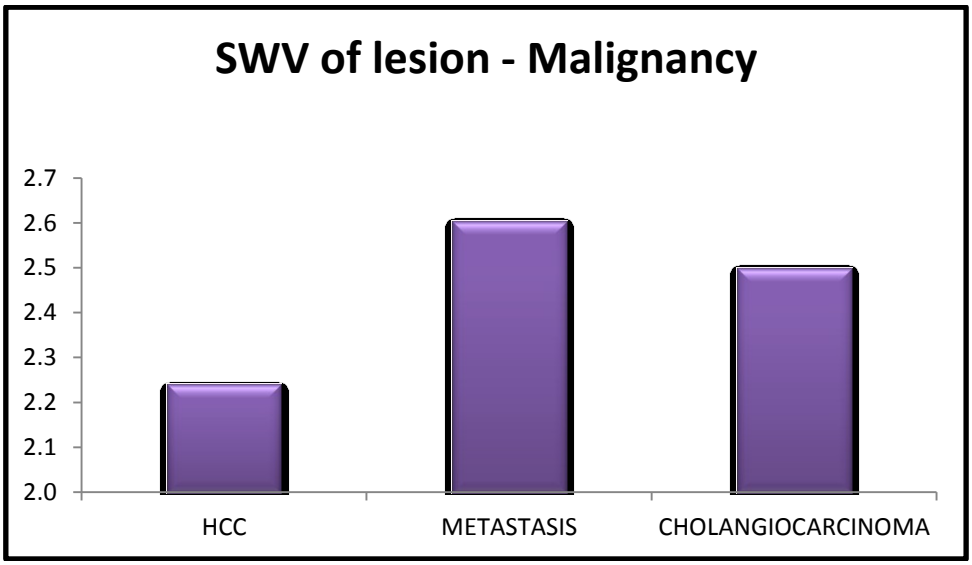

Fig.7.5.3. Bar diagram showing mean values of SWV(m/s) among malignant liver lesions.

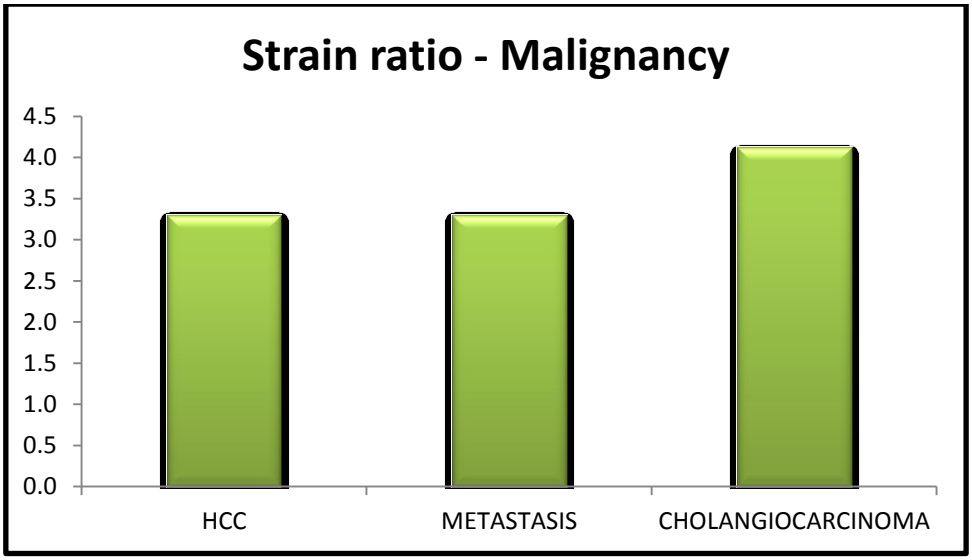

Fig.7.5.4. Bar diagram showing mean values of Strain Ratio among malignant liver lesions.

Test Statistics[a,b,c]

	Chi-Square	df	p-value
STIFFNESS VALUE OF LESION (kPa)	4.026	2	.134
STIFFNESS RATIO	7.557	2	.023
SWV OF LESION(m/s)	4.007	2	.135
STRAIN RATIO	8.229	2	.016

a. HPE = Malignancy

b. Kruskal Wallis Test

c. Grouping Variable: Groups

Table.7.5.2. Table showing statistical difference among elastographic parameters between malignant liver lesions.

Among benign lesions:

Group Statistics:

		N	Mean	Std. Deviation	Minimum	Maximum
STIFFNESS VALUE OF LESION(kPa)	HEMANGIOMA	9	11.4	4.876	6	19
	FNH	2	9.0	5.657	5	13
	Total	11	11.0	4.817	5	19
STIFFNESS RATIO	HEMANGIOMA	9	1.5	.5388	.7	2.4
	FNH	2	1.5	.8677	.9	2.1
	Total	11	1.5	.5547	.7	2.4
SWV OF LESION	HEMANGIOMA	9	1.4	.2991	1.0	1.8
	FNH	2	2.3	.2121	2.1	2.4
	Total	11	1.5	.4478	1.0	2.4
STRAIN RATIO	HEMANGIOMA	9	1.0	.17008	.82	1.34
	FNH	2	1.7	.16263	1.63	1.86
	Total	11	1.1	.35024	.82	1.86

Table.7.5.3. Mean values of elastographic parameters among benign liver lesions.

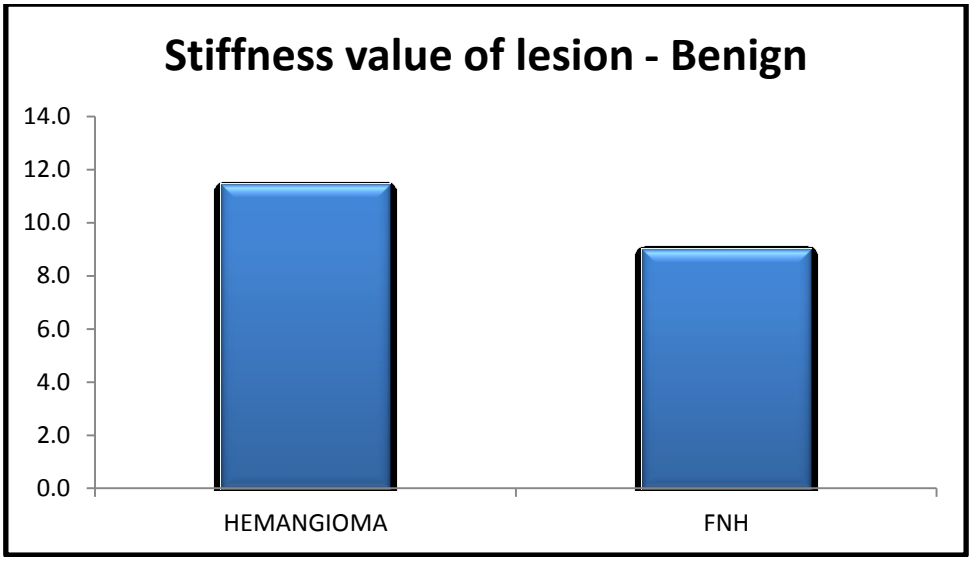

Fig.7.5.5.: Bar diagram showing mean values of Stiffness value(kPa) among benign liver lesions.

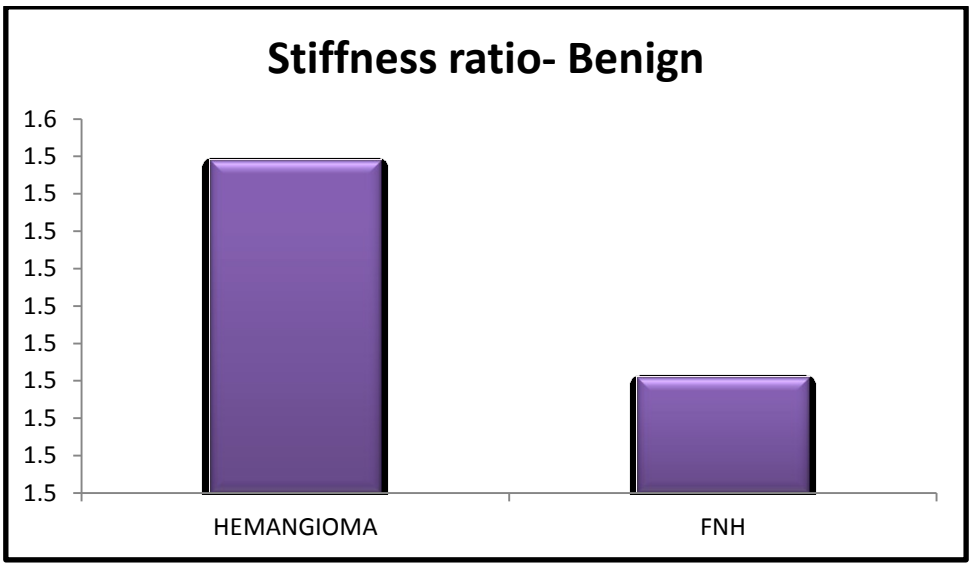

Fig.7.5.6. Bar diagram showing mean values of Stiffness ratio among benign liver lesions.

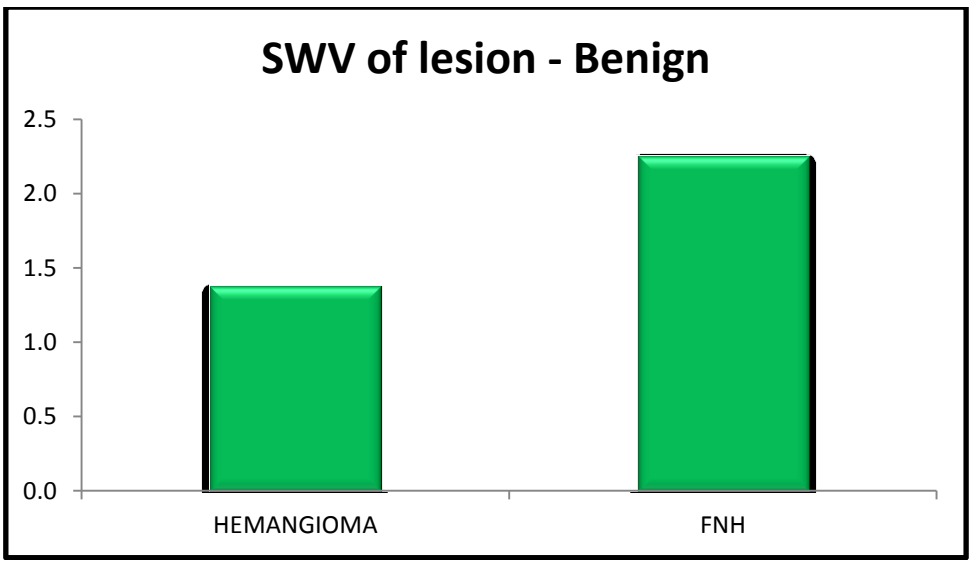

Fig.7.5.7. Bar diagram showing mean values of SWV(m/s) among benign liver lesions.

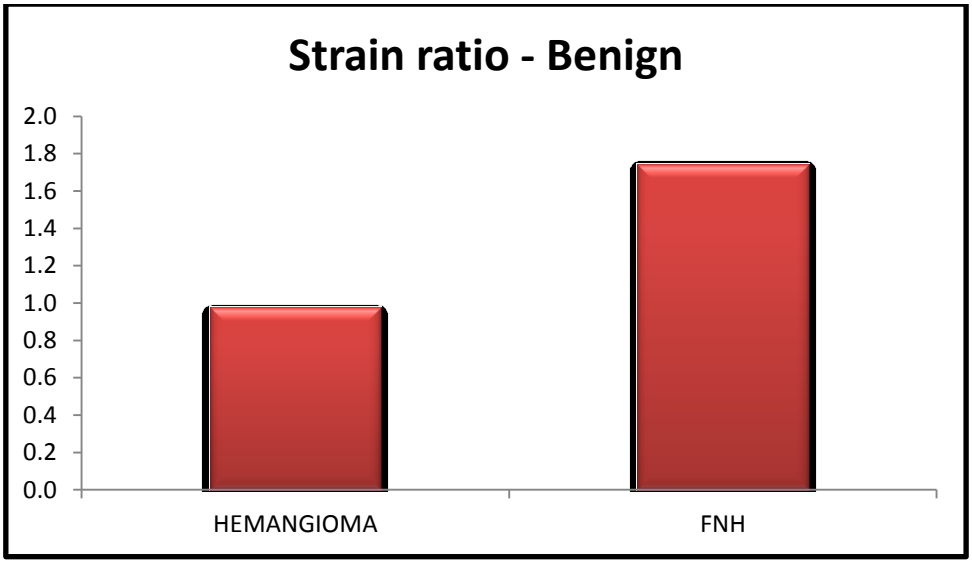

Fig.7.5.8.: Bar diagram showing mean values of Strain Ratio among benign liver lesions.

Test Statistics[a,b]

	Mann-Whitney U	Z	Asymp. Sig. (2-tailed)	p-value
STIFFNESS VALUE OF LESION (kPa)	6.000	-.715	.474	.582[c]
STIFFNESS RATIO	8.000	-.236	.813	.909[c]
SWV OF LESION	0.000	-2.131	.033	.036[c]
STRAIN RATIO	0.000	-2.121	.034	.036[c]

a. HPE = Benign

b. Grouping Variable: Groups

c. Not corrected for ties.

Table.7.5.4. Statistical difference among elastographic parameters between benign liver lesions.

P - Value	** Highly Significant at P ≤ .01
P - Value	* Significant at 0.01 < P ≤ .050
P -Value	# No Significant at P >.050

7.6. MEAN VALUES OF ELASTOGRAPHIC PARAMETERS BETWEEN MALIGNANT AND BENIGN FLL

Group Statistics

		N	Mean	Std. Deviation	Std. Error Mean
STIFFNESS VALUE OF LESION(kPa)	Malignancy	39	32.51	17.149	2.746
	Benign	11	11.00	4.817	1.452
STIFFNESS RATIO	Malignancy	39	3.595	2.7614	.4422
	Benign	11	1.539	.5547	.1672
SWV OF LESION	Malignancy	39	2.456	.5056	.0810
	Benign	11	1.536	.4478	.1350
STRAIN RATIO	Malignancy	39	3.3644	.52738	.08445
	Benign	11	1.1155	.35024	.10560

Table.7.6.1. Mean values of elastographic parameters between malignant and benign liver lesions.

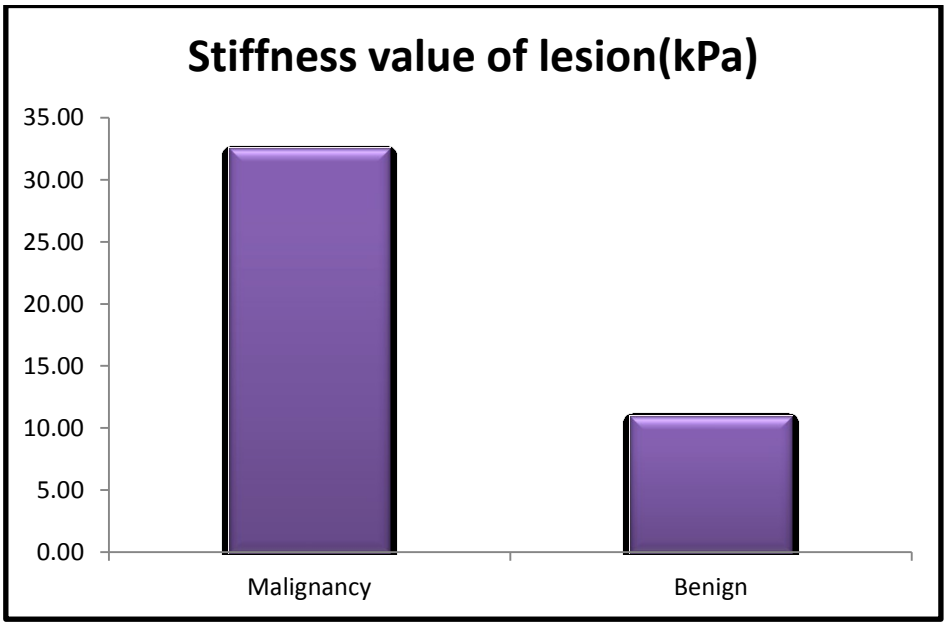

Fig.7.6.1. Bar diagram showing mean values of Stiffness value(kPa) between malignant and benign liver lesions.

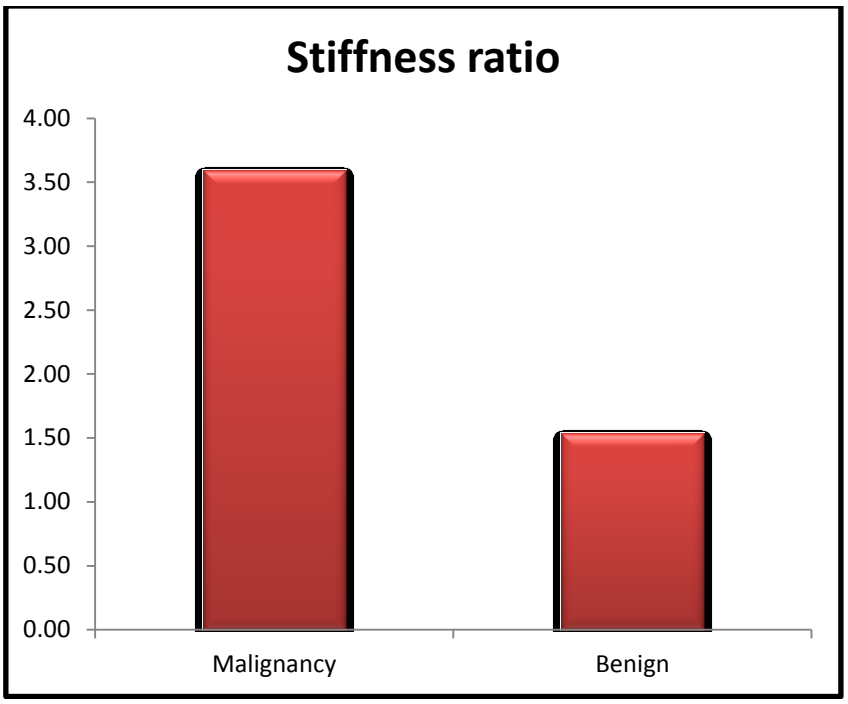

Fig.7.6.2. Bar diagram showing mean values of Stiffness ratio between malignant and benign liver lesions.

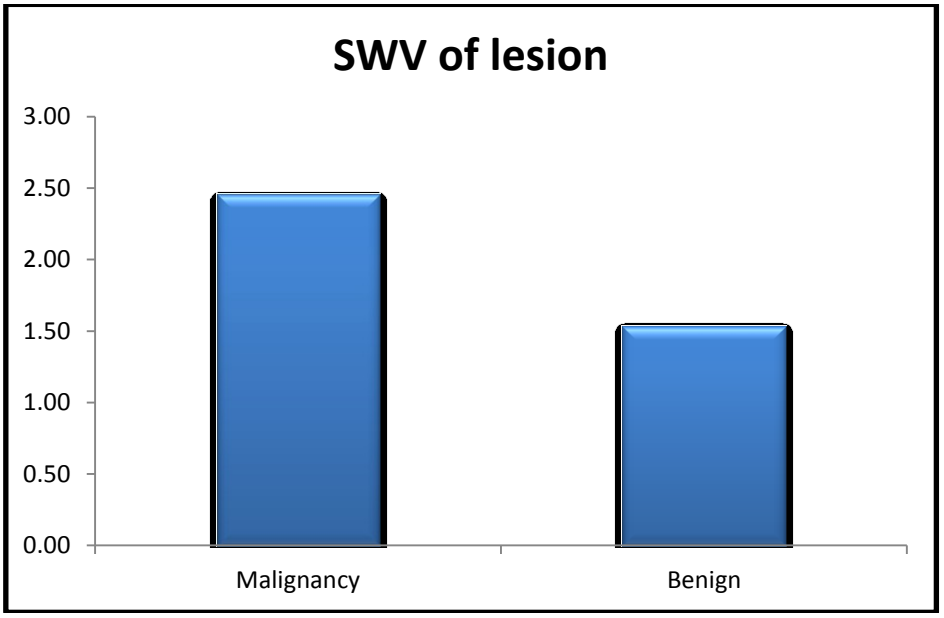

Fig.7.6.3. Bar diagram showing mean values of SWV(m/s) between malignant and benign liver lesions.

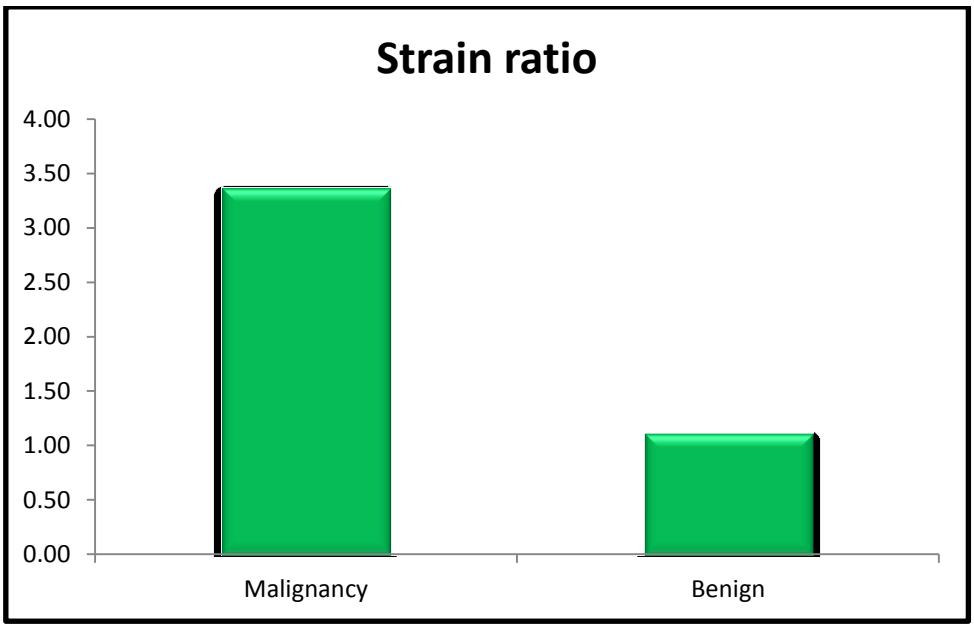

Fig.7.6.4. Bar diagram showing mean values of Strain Ratio between malignant and benign liver lesions

PARAMETER	t value	Sig.P-value
STIFFNESS VALUE	6.925	.0005
STIFFNESS RATIO	4.348	.0005
SWV	5.454	.0005
STRAIN RATIO	13.289	.0005

Table.7.6.2. Statistical difference among elastographic parameters between malignant and benign liver lesions.

7.7.ROC CURVE ANALYSIS (MALIGNANT AND BENIGN LIVER LESIONS) STIFFNESS VALUE OF THE LESION (kPa)

The cut off value of Stiffness value obtained by ROC curve analysis from our study along with the Sensitivity and Specificity to differentiate malignant and benign FLL are as below.

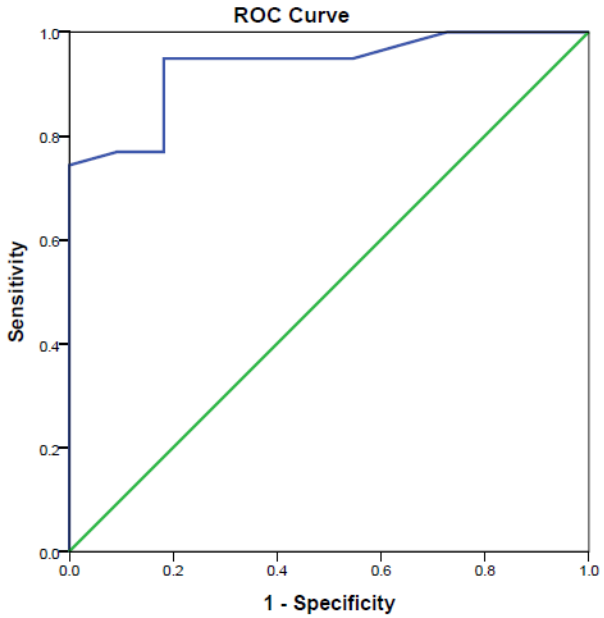

CUT OFF	16.5
SENSITIVITY	79.5%
SPECIFICITY	81.8%

Area Under the Curve

Test Result Variable(s): STIFFNESS VALUE OF LESION (kPa)

Area	Std. Error[a]	Asymptotic Sig.[b]	Asymptotic 95% Confidence Interval	
			Lower Bound	Upper Bound
.934	.036	.0005	.863	1.000

The test result variable(s): STIFFNESS VALUE OF LESION (kPa) has at least one tie between the positive actual state group and the negative actual state group. Statistics may be biased.

a. Under the nonparametric assumption

b. Null hypothesis: true area = 0.5

Fig.7.7.1. ROC Curve Analysis for Stiffness Value (Malignancy Vs Benign)

STIFFNESS RATIO

The cut off value of Stiffness Ratio obtained by ROC curve analysis from our study along with the Sensitivity and Specificity to differentiate malignant and benign FLL are as below.

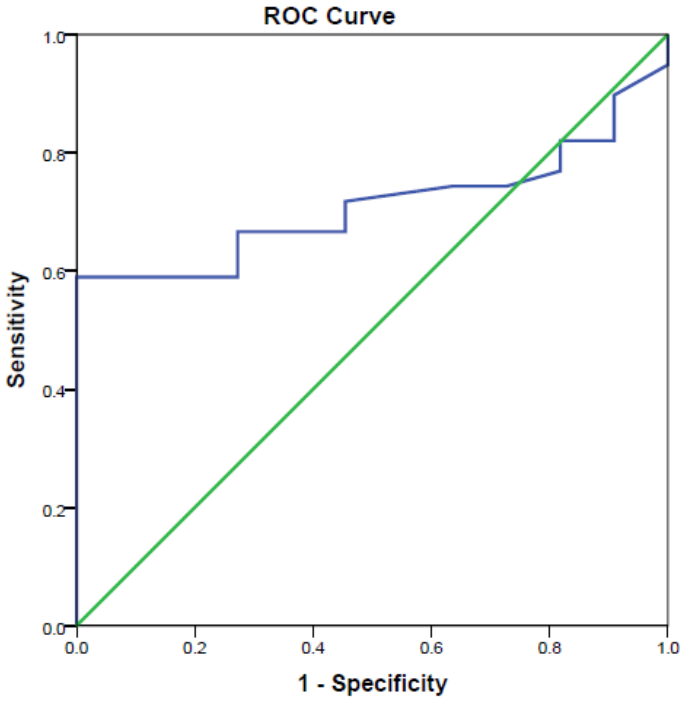

CUT OFF	1.75
SENSITIVITY	66.70%
SPECIFICITY	63.60%

Area Under the Curve

Test Result Variable(s): STIFFNESS RATIO

Area	Std. Error[a]	Asymptotic Sig.[b]	Asymptotic 95% Confidence Interval	
			Lower Bound	Upper Bound
.710	.070	.035	.573	.847

The test result variable(s): STIFFNESS RATIO has at least one tie between the positive actual state group and the negative actual state group. Statistics may be biased.

a. Under the nonparametric assumption

b. Null hypothesis: true area = 0.5

Fig.7.7.2. ROC Curve Analysis for Stiffness Ratio (Malignancy Vs Benign)

SHEAR WAVE VELOCITY(m/s)

The cut off value of Shear wave velocity (SWV) obtained by ROC curve analysis from our study along with the Sensitivity and Specificity to differentiate malignant and benign FLL are as below.

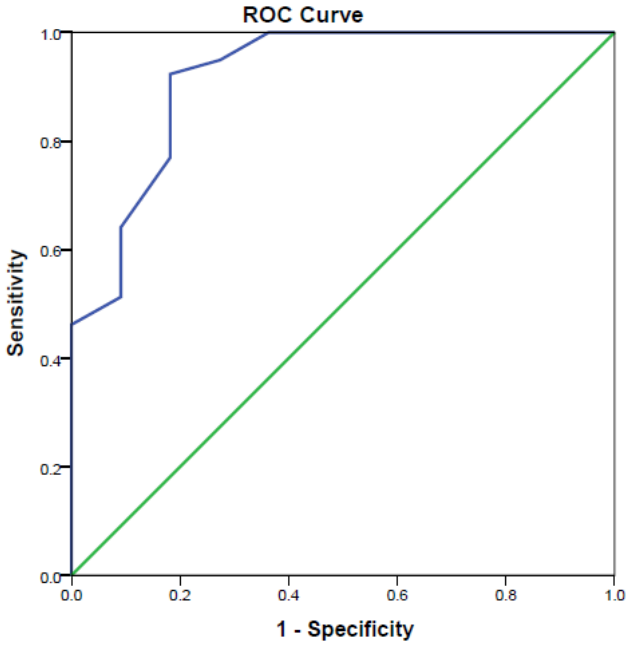

CUT OFF	1.95
SENSITIVITY	82.10%
SPECIFICITY	81.80%

Area Under the Curve

Test Result Variable(s): SWV OF LESION

Area	Std. Error[a]	Asymptotic Sig.[b]	Asymptotic 95% Confidence Interval	
			Lower Bound	Upper Bound
.918	.052	.0005	.817	1.000

The test result variable(s): SWV OF LESION has at least one tie between the positive actual state group and the negative actual state group. Statistics may be biased.

a. Under the nonparametric assumption

b. Null hypothesis: true area = 0.5

Fig.7.7.3. ROC Curve Analysis for Shear wave velocity (Malignancy Vs Benign)

STRAIN RATIO

The cut off value of Strain Ratio obtained by ROC curve analysis from our study along with the Sensitivity and Specificity to differentiate malignant and benign FLL are as below.

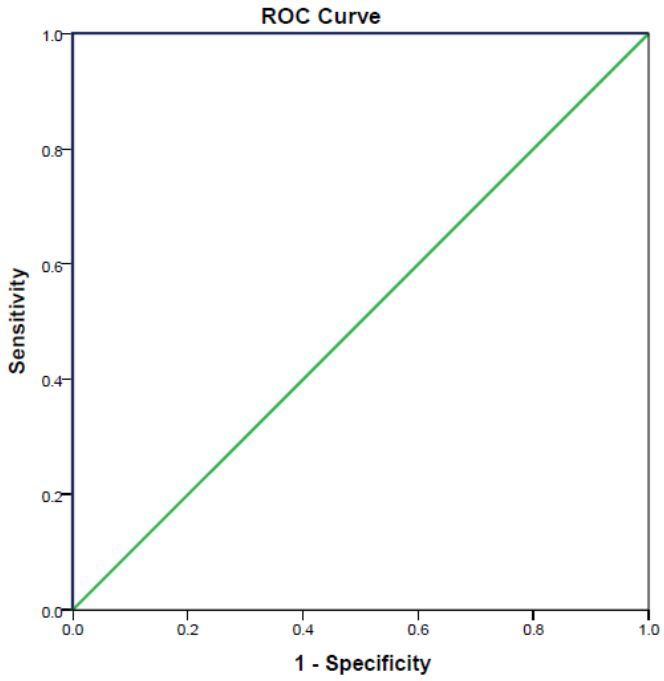

CUT OFF	2.3
SENSITIVITY	100%
SPECIFICITY	100%

Area Under the Curve

Test Result Variable(s): STRAIN RATIO

Area	Std. Error[a]	Asymptotic Sig.[b]	Asymptotic 95% Confidence Interval	
			Lower Bound	Upper Bound
1.000	0.000	.0005	1.000	1.000

a. Under the nonparametric assumption

b. Null hypothesis: true area = 0.5

Fig.7.7.4. ROC Curve Analysis for Strain Ratio (Malignancy Vs Benign)

7.8. FOCAL LIVER LESION vs BACKGROUND LIVER

STIFFNESS VALUE PROFILES IN FOCAL LIVER LESIONS AND BACKGROUND LIVER

Paired Samples Statistics			
Variable	Mean Stiffness Value of Lesion (kPa)	Mean Stiffness value of Background(kPa)	P value
HCC	37.73	29.07	.490
Metastasis	27.95	7.14	.0005
Cholangiocarcinoma	38.33	7.67	.109
Hemangioma	11.44	7.22	.021
FNH	9.00	5.50	.317

Table.7.8.1. Statistical difference in mean stiffness value(kPa) between FLL and background liver.

SHEAR WAVE VELOCITY PROFILES IN FOCAL LIVER LESIONS AND BACKGROUND LIVER

Variable	Mean Shear Wave Velocity of lesion (m/s)	Mean Shear Wave Velocity of Background (m/s)	P value
HCC	2.24	2.39	.245
Metastasis	2.605	2.057	.002
Cholangiocarcinoma	2.500	2.300	.109
Hemangioma	1.500	1.378	.027
FNH	2.250	1.950	.317

Table.7.8.2. Statistical difference in mean shear wave velocity(m/s) between FLL and background liver.

RESULTS OF COMPARISON OF ELASTOGRAPHIC PARAMETERS

Out of the 50 focal liver lesions among the study group, 39 were malignant (78%), 11 were benign (22%) lesions. Out of the 39 lesions which were found to be malignant, 21 were metastases (53.8%), 15 were HCC (38.5%) and 3 were cholangiocarcinoma (7.7%). And among the benign lesions, 9 were haemangiomas (81.8%) and 2 were FNH (18.2%).

Mean elastographic parameters (Stiffness value, Stiffness Ratio, Shear wave velocity & Strain Ratio) for focal liver lesions are summarized in the tables and bar charts above. The comparison among the elastographic parameters among various malignant and benign liver lesions showed the below results.

1. It was observed that highly significant difference existed among malignant liver lesions in the mean Strain Ratio (P value ≤ 0.01).
2. There was significant difference among malignant liver lesions in the mean Stiffness Ratio (P value ≤ 0.05).
3. Significant difference seen among benign liver lesions in the mean values of Shear wave velocity and Strain Ratio (P value ≤ 0.05).
4. No significant difference noted among malignant liver lesions in the mean values of Stiffness Value and Shear wave velocity (P value > 0.05).
5. No significant difference seen among benign liver lesions in the mean values of Stiffness value and Stiffness Ratio (P value > 0.05).

6. There was highly significant difference between mean values of all four elastographic parameters (Stiffness value, Stiffness Ratio, Shear wave velocity & Strain Ratio) between malignant and benign liver lesions (P value ≤ 0.01).
7. The Receiver Operator Characteristic (ROC) curve analysis of the elastographic parameters showed the following cut off values in discriminating malignant and benign liver lesions.
    a. 16.5kPa for Stiffness value with sensitivity of 79.50% and specificity of 81.80%.
    b. 1.75 for Stiffness Ratio with sensitivity of 66.70% and specificity of 63.60%.
    c. 1.95 m/s for Shear wave velocity with sensitivity of 82.10% and specificity of 81.80%.
    d. 2.3 for Strain Ratio with sensitivity of 100% and specificity of 100%.

    Strain Ratio was found to be a better parameter than the remaining three parameters helpful in differentiating between malignant and benign liver lesions.
8. Highly significant difference observed in mean stiffness value and mean shear wave velocity value between metastasis and background liver (P value ≤ 0.01). Metastatic lesions showed increased mean stiffness value and mean shear wave velocity, compared to the background liver.
9. Significant difference observed in mean stiffness value and mean shear wave velocity value between haemangioma and background liver (P value ≤ 0.05).

Haemangiomas showed increased mean stiffness value and mean shear wave velocity, compared to the background liver.

10. No significant difference seen in mean stiffness value and mean shear wave velocity value between tumour and background liver in hepatocellular carcinoma, cholangiocarcinoma and focal nodular hyperplasia (P value > 0.05).

8.DISCUSSION

Focal liver lesions (FLL) have been a common reason for consultation faced by gastroenterologists and hepatologists. Focal liver lesions can be classified into developmental, neoplastic, inflammatory and miscellaneous. Differentiation of focal liver lesions remains a major concern on imaging studies. Sonography, CT, and MRI have been used for this purpose. Gray-scale, colour, and spectral Doppler sonography have limited value in differential diagnosis of these lesions [107].

Imaging studies of focal liver lesions are usually required first to define the lesions as benign or malignant. Haemangiomas represent most frequently detected focal solid liver lesions in clinical practice and appear as hyperechoic solid lesions without vascularity on colour flow Doppler sonography. A centripetal enhancement pattern on dynamic CT and MRI is a characteristic imaging finding of haemangiomas. However, atypical haemangiomas may present as hypoechoic masses on gray-scale sonography with atypical contrast enhancement patterns on dynamic CT and MRI. Other types of focal liver lesions are usually diagnosed by dynamic CT and MRI or percutaneous liver biopsy [108].

Any pathologic process can change the tissue's internal architecture, and thus parenchyma elasticity of an organ. Direct mechanical measurements of resected liver samples have indicated that elastic contrast exists for many tumours in the liver [84]. Elastography aims to assess these elasticity differences in order to be able to characterize malignant and benign liver lesions [8].

Only a few authors have studied the utility of ultrasound elastography for the characterization of liver tumours and the differentiation between benign and malignant

tumours, in which various tumours were investigated and the elasticity parameters were compared.

Considering that ultrasound elastography is a promising method undergoing rapid development and active research, our study was conducted in a tertiary care teaching hospital in South India Among 50 people with focal liver lesions, 39 (78%) participants had malignant and 11 (22%) participants had benign lesions. Patients in the study were diagnosed based on biopsy / surgical excision and/or other imaging modalities. The average age of patients with malignant lesions was 62 years and that of patients with benign lesions was 38 years, with statistically significant difference (P-value ≤ 0.01) across these two groups. In both these groups, proportion of males was slightly higher.

Our study aimed at evaluating the usefulness of various elastographic parameters (Stiffness value, Stiffness Ratio, Shear wave velocity & Strain Ratio) in differentiation of both benign and malignant liver lesions.

Qiang Lu et al [106] reported the mean stiffness values and ranges expressed in kilopascals for patients with haemangioma, focal nodular hyperplasia (FNH), cirrhotic nodules, HCC, Cholangiocarcinoma, and metastasis were 9.3 (range, 3.1–41), 10 (range, 2.9–26), 11 (range, 4.4–49), 34 (range, 4.4–188), 25 (range, 5.5–79), and 30 (range, 4.7–64), respectively. In our study, the mean stiffness values and ranges obtained from patients with HCC, cholangiocarcinoma, metastasis, haemangioma and FNH were 37.73(range, 15-82), 38.33(range, 29-46), 27.95(range, 7-68), 11.44(range,6-19), and 9 (range, 5-13), respectively. Our results for these parameters

were slightly different and cannot be compared as such with the previous studies because of the differences in study population.

It was also demonstrated by Qiang Lu et al [106] that malignant tumours had significantly higher stiffness values and stiffness ratios than did benign lesions (P <.0001 and P = .0003, respectively;). For discrimination of malignant from benign lesions, diagnostic accuracy with use of the stiffness value was significantly higher than that with use of the stiffness ratio (AUC, 0.86 vs 0.69; P < .001). With a cut-off value of 13 kPa for the stiffness value, the sensitivity and specificity were 78% and 83%, respectively. With a cut-off value of 1.3 for the stiffness ratio, the sensitivity and specificity were 79% and 45%, respectively.

Our study showed the cut off value of 16.5kPa for Stiffness value with sensitivity of 79.50% and specificity of 81.80% and that of 1.75 for Stiffness Ratio with sensitivity of 66.70% and specificity of 63.60% in discriminating malignant and benign liver lesions (P value ≤ 0.01).

By using quantitative acoustic radiation force impulse imaging technology, Heide et al [107] showed statistically comparable stiffness values between 38 benign lesions and 24 malignant tumours (*P* = .28).

In comparison, Yu et al [104] showed a significant difference in the stiffness values between 41 benign and 64 malignant lesions (*P* < .001), with sensitivity and specificity of 68% (28 of 41) and 69% (44 of 64), respectively.

Park et al [97] demonstrated an AUC of 0.74 for discrimination of 39 malignant from eight benign liver lesions.

The results of the study done by Qiang Lu et al [106] confirmed that the stiffness value could be considered a non-invasive predictor for malignancy in focal liver lesions. For the differentiation of malignant and benign liver lesions with stiffness value, sensitivity and specificity results were 78% (156 of 159) and 83% (48 of 58), respectively.

Our study showed that the mean shear wave velocity of malignant lesions was 2.45±0.50 m/s and that of benign lesions was 1.53±0.44 m/s (P value ≤ 0.01). The cut-off value for SWV was 1.95 m/s with sensitivity of 82.10% and specificity of 81.80% in the differential diagnosis of malignant and benign masses.

Guo et al [99], evaluated the difference of the mean shear wave velocity of the mass among focal liver lesions. The mean shear wave velocity (SWV) of malignant and benign masses being 2.95 ± 1.00 m/s and 1.69 ± 0.89 m/s, respectively (p < 0.001). Those authors proposed cut-off values of 2.13 m/s for the SWV value in the differential diagnosis of malignant and benign masses. This was similar to our study, in which we found mean shear wave velocity values to be significantly higher in malignant liver lesions compared to benign liver lesions (P-Value < 0.01).

Onur et al [90] demonstrated that the mean strain ratio value of malignant liver lesions ± SD (2.82 ± 1.82) was significantly higher than that of benign liver lesions (1.45 ± 1.28; P< .0001). Our study showed that the mean strain ratio of malignant lesions was 3.36±0.52 and that of benign lesions 1.12±0.35(P<0.01). Both of these studies showed similar results that higher strain ratio seen in malignant liver lesions.

Study done by Qiang Lu et al [106] revealed that haemangioma, FNH, HCC, cholangiocarcinoma, and metastasis showed significantly higher stiffness values than

did background liver parenchyma (all, $P < .05$). Heide et al [107], reported that the HCC was softer than the background liver, whereas Gallotti et al [98] reported higher stiffness values in the lesions than in the background liver for patients with haemangioma, FNH, HCC, and metastasis.

In our study, Metastatic lesions showed increased mean stiffness value and mean shear wave velocity, compared to the background liver (P value $\leq$ 0.01). Haemangiomas showed increased mean stiffness value and mean shear wave velocity, compared to the background liver (P value $\leq$ 0.05). The discrepancy might be due to the regions of background liver used in the different studies.

Although, there was significant difference between mean values of elastographic parameters between benign and malignant liver lesions($P \leq 0.01$), strain ratio was found to be a better parameter than the remaining three parameters helpful in differentiating between malignant and benign liver lesions.

9.LIMITATIONS

Our study had some limitations which are listed below:

1. Out of the total 50 focal liver lesions, the subgroup of benign lesions included is relatively small(n=11), out of which 9 were haemangiomas and only 2 were FNH which might not be an adequate representation for interpretation of the results. Further large-scale confirmation studies with rare types of lesions are needed to validate our findings.
2. Generalizability of the study findings was limited, as the study was conducted in a single centre with limited catchment area.
3. The effect of distance between the transducer and region of interest measured on stiffness assessment was not directly evaluated.
4. Interobserver variability was not documented in the patient groups.
5. Finally, the USE showed some limitations. Poor compliance of the patients in holding their breath as requested. Sono-elastography is operator-dependent although it is non-invasive, easily performed and fast imaging technique.

10.CONCLUSION

Ultrasound elastography is a non-invasive, quantifiable, and feasible technique which allows the quantitative assessment of mechanical properties of the lesion.

Sono-elastography of the liver provides complementary information to conventional ultrasound by adding stiffness/strain as another measurable property to current ultrasonographic imaging technique that can be used to differentiate among various focal lesions of the liver.

This study, though it had some limitations, showed the feasibility of ultrasound elastography, in discriminating between malignant and benign liver lesions, which can be an aid in further management.

Significant differences in elastographic parameters among various benign and malignant liver lesions were apparent in this study. The mean values of elastographic parameters were significantly higher in malignant liver lesions compared to benign liver lesions. Among the elastographic parameters, Strain Ratio was found to be a better parameter to differentiate between focal liver lesions. These data may justify the more routine use of this technique in the characterisation and assessment of focal liver lesions.

Sono-elastography is an evolving imaging modality and in this recent era concerned with increased interest in active surveillance, further larger prospective studies with a stronger level of evidence are required to assess the potential role of this technique in discriminating the benign vs malignant nature of lesions and among different lesions.

To conclude, ultrasound elastography is a newer imaging technique which is non–contrast-enhanced and fast imaging method. Elastography can be incorporated onto a conventional ultrasound machine, which allows the combination, in one exam, of quantitative elastography assessment of the liver tumour after the morphological ultrasound examination of the liver and thus paving way to a better and more targeted approach and management.

REFERENCES

1. Bruix J, Sherman M, American Association for the Study of Liver. Management of hepatocellular carcinoma: an update. Hepatology 2011; 53: 1020 – 2.

2. Khan SA, Davidson BR, Goldin RD et al. Guidelines for the diagnosis and treatment of cholangiocarcinoma: an update. Gut 2012; 61: 1657 – 69.

3. European Association for The Study of Th e Liver; European Organisation for Research and Treatment of Cancer. EASL-EORTC clinical practice guidelines: management of hepatocellular carcinoma. J Hepatol 2012; 56: 908 – 43.

4. Gallotti A, DOnofrio M, Romanini L, Cantisani V, Pozzi Mucelli R. Acoustic radiation force impulse (ARFI) ultrasound imaging of solid focal liver lesions. Eur J Radiol 2012; 81(3): 451-5.

5. Bosch FX, Ribes J, Díaz M, Cléries R. Primary liver cancer: worldwide incidence and trends. Gastroenterology 2004; 127(5) Suppl 1: S5–S16

6. Ishak KG, Rabin L. Benign tumors of the liver. Med Clin North Am 1975; 59 (4):995–1013

7. Gandolfi L, Leo P, Solmi L, Vitelli E, Verros G, Colecchia A. Natural history of hepatic haemangiomas: clinical and ultrasound study. Gut 1991; 32(6):677– 680

8. Goertz RS, Amann K, Heide R, Bernatik T, Neurath MF, Strobel D. An abdominal and thyroid status with acoustic radiation force impulse elastometry feasibility study: acoustic radiation force impulse elastometry of human organs. Eur J Radiol 2011; 80(3): e226-30.

9. Ophir J, Céspedes I, Ponnekanti H, Yazdi Y, Li X. Elastography: a quantitative method for imaging the elasticity of biological tissues. Ultrason Imaging 1991; 13(2):111–134

10. Palmeri ML, Wang MH, Dahl JJ, Frinkley KD, Nightingale KR. Quantifying hepatic shear modulus in vivo using acoustic radiation force. Ultrasound Med Biol 2008; 34(4):546–558

11. Elias, H.; Bengelsdorf, H. (1 July 1952). "The Structure of the Liver in Vertebrates". Cells Tissues Organs. 14 (4): 297–337. doi:10.1159/000140715.

12. Abdel-Misih, Sherif R. Z.; Bloomston, Mark (2010). "Liver Anatomy". Surgical Clinics of North America. 90 (4): 643-53.

13. Tortora, Gerard J.; Derrickson, Bryan H. (2008). Principles of Anatomy and Physiology (12th ed.). John Wiley & Sons. p. 945. ISBN 978-0-470-08471-7.

14. Cotran, Ramzi S.; Kumar, Vinay; Fausto, Nelson; Nelso Fausto; Robbins, Stanley L.; Abbas, Abul K. (2005). Robbins and Cotran pathologic basis of disease (7th ed.). St. Louis, MO: Elsevier Saunders. p. 878. ISBN 0-7216-0187-1.

15. Renz, John F.; Kinkhabwala, Milan (2014). "Surgical Anatomy of the Liver". In Busuttil, Ronald W.; Klintmalm, Göran B. Transplantation of the Liver. Elsevier. pp. 23–39. ISBN 978-1-4557-5383-3

16. Kuntz, Erwin; Kuntz, Hans-Dieter (2009). "Liver resection". Hepatology: Textbook and Atlas (3rd ed.). Springer. pp. 900–3. ISBN 978-3-540-76839-5

17. Singh, Inderbir (2008). "The Liver Pancreas and Spleen". Textbook of Anatomy with Colour Atlas. Jaypee Brothers. pp. 592–606. ISBN 978-81-8061-833-8

18. McMinn, R. M. H. (2003). "Liver and Biliary Tract". Last's Anatomy: Regional and Applied. Elsevier. pp. 342–51. ISBN 978-0-7295-3752-0.

19. Skandalakis, Lee J.; Skandalakis, John E.; Skandalakis, Panajiotis N. (2009). "Liver". Surgical Anatomy and Technique: A Pocket Manual. pp. 497–531.

20. Kmieć Z (2001). "Cooperation of liver cells in health and disease". Adv Anat Embryol Cell Biol. 161: III–XIII, 1–151. PMID 11729749

21. Pocock, Gillian (2006). Human Physiology (Third ed.). Oxford University Press. p. 404.ISBN 978-0-19-856878-0

22. Human Anatomy & Physiology + New Masteringa&p With Pearson Etext. Benjamin-Cummings Pub Co. 2012. ISBN 9780321852120

23. Kawarada, Y; Das, BC; Taoka, H (2000). "Anatomy of the hepatic hilar area: the plate system". Journal of Hepato-Biliary-Pancreatic Surgery. 7 (6): 580–6.

24. Strunk, H.; Stuckmann, G.; Textor, J.; Willinek, W. (2003). "Limitations and pitfalls of Couinaud's segmentation of the liver in transaxial Imaging". European Radiology. 13 (11): 2472–82.

25. Uhlén, Mathias; Fagerberg, Linn; Hallström, Björn M.; Lindskog, Cecilia; Oksvold, Per; Mardinoglu, Adil; Sivertsson, Åsa; Kampf, Caroline; Sjöstedt, Evelina (2015-01-23)."Tissue-based map of the human proteome". Science. 347 (6220): 1260419.

26. Berg T, DeLanghe S, Al Alam D, Utley S, Estrada J, Wang KS (2010). "β-catenin regulates mesenchymal progenitor cell differentiation during hepatogenesis". J Surg Res. 164 (2): 276–85.

27. "β-catenin regulates mesenchymal progenitor cell differentiation during hepatogenesis". J Surg Res. 164 (2): 276–85.

28. Human Anatomy & Physiology + New Masteringa&p With Pearson Etext. Benjamin-Cummings Pub Co. 2012. p. 939.

29. Jelkmann, Wolfgang (2001). "The role of the liver in the production of thrombopoietin compared with erythropoietin". European Journal of Gastroenterology & Hepatology. 13(7): 791–801.

30. Shneider, Benjamin L.; Sherman, Philip M. (2008). Pediatric Gastrointestinal Disease. Connecticut: PMPH-USA. p. 751.

31. Schweitzer A, Horn J, Mikolajczyk RT, Krause G, Ott JJ (2015). "Estimations of worldwide prevalence of chronic hepatitis B virus infection: a systematic review of data published between 1965 and 2013". Lancet. 386 (10003): 1546–55.

32. "Global, regional, and national incidence, prevalence, and years lived with disability for 310 diseases and injuries, 1990-2015: a systematic analysis for the Global Burden of Disease Study 2015". Lancet. 388 (10053): 1545–1602. 2016.

33. Dény P (2006). "Hepatitis delta virus genetic variability: from genotypes I, II, III to eight major clades?". Curr. Top. Microbiol. Immunol. 307: 151–71.

34. Ghent, Cam N (2009). "Who should be performing liver biopsies?". Canadian Journal of Gastroenterology. 23 (6): 437–8.

35. Tietz PS, Larusso NF (May 2006). "Cholangiocyte biology". Current Opinion in Gastroenterology. 22 (3): 279–87.

36. Buell JF, Tranchart H, Cannon R, Dagher I. Management of benign hepatic tumors. Surg Clin North Am.2010; 90:719–735.

37. Kerlin P, Davis GL, McGill DB, Weiland LH, Adson MA, Sheedy PF. Hepatic adenoma and focal nodular hyperplasia: clinical, pathologic, and radiologic features. Gastroenterology. 1983; 84:994–1002.

38. Nguyen BN, Flejou JF, Terris B, Belghiti J, Degott C. Focal nodular hyperplasia of the liver: a comprehensive pathologic study of 305 lesions and recognition of new histologic forms. Am J Surg Pathol. 1999; 23:1441–1454.

39. Kondo F, Nagao T, Sato T, et al. Etiological analysis of focal nodular hyperplasia of the liver, with emphasis on similar abnormal vasculatures to nodular regenerative hyperplasia and idiopathic portal hypertension. Pathol Res Pract. 1998; 194:487–495.

40. Wanless IR, Mawdsley C, Adams R. On the pathogenesis of focal nodular hyperplasia of the liver. Hepatology.1985;5:1194–1200.

41. Weimann A, Ringe B, Klempnauer J, et al. Benign liver tumors: differential diagnosis and indications for surgery. World J Surg. 1997; 21:983–990.

42. Reimer P, Rummeny EJ, Shamsi K, et al. Phase II clinical evaluation of Gd-EOB-DTPA: dose, safety aspects, and pulse sequence. Radiology. 1996; 199:177–183

43. Zech CJ, Grazioli L, Breuer J, Reiser MF, Schoenberg SO. Diagnostic performance and description of morphological features of focal nodular hyperplasia in Gd-EOB-DTPA-enhanced liver magnetic resonance imaging: results of a multicenter trial. Invest Radiol. 2008; 43:504–511.

44. Brodsky RI, Friedman AC, Maurer AH et-al. Hepatic cavernous hemangioma: diagnosis with 99mTc-labeled red cells and single-photon emission CT. AJR Am J Roentgenol. 1987;148 (1): 125-9.

45. Vilanova JC, Barceló J, Smirniotopoulos JG et-al. Hemangioma from head to toe: MR imaging with pathologic correlation. Radiographics. 24 (2): 367-85.

46. John T. G.; et al. (1994). "Superior staging of liver tumors with laparoscopy and laparoscopic ultrasound". Ann. Surg. 220 (6): 711–719.

47. Mayo Clinic. Liver Hemangioma. 2013. http://www.mayoclinic.org/diseases-conditions/liver-hemangioma/basics/risk-factors/con-20034197

48. Bengmark S, Hafstrom L, Olssen A, et al. The natural history of primary and secondary liver tumours. V. The prognosis for conventionally treated patients with liver metastases. Digestion. 1972; 6:321-329.

49. American Cancer Society. Cancer Facts and Figures, 1999. Atlanta, Ga: American Cancer Society; 1999.

50. Hollett MD, Jeffrey RB Jr, Nino-Murcia M, et al. Dual-phase helical CT of the liver: value of arterial phase scans in the detection of small (< or = 1.5cm) malignant hepatic neoplasms. AJR Am J Roentgenol. 1995; 164:879-884.

51. Bonaldi VM, Bret PM, Reinhold C, et al. Helical CT of the liver: value of an early hepatic arterial phase. Radiology. 1995; 197:357-363.

52. Isozaki T, Numata K, Kiba T, et al. Differential diagnosis of hepatic tumors by using contrast enhancement patterns at US. Radiology. 2003; 229:798-805. Epub 2003 Oct 16

53. Bluemke DA, Soyer PA, Chan BW, et al. Spiral CT during arterial portography: technique and applications. Radiographics. 1995; 15:623-639. Erratum in: Radiographics. 1995; 15:1190.

54. Bhattacharjya S, Bhattacharjya T, Baber S, et al. Prospective study of contrast-enhanced computed tomography, computed tomography during arterioportography, and magnetic resonance imaging for staging colorectal liver metastases for liver resection. Br J Surg. 2004; 91:1361-1369.

55. Vogl TJ, Schwarz W, Blume S, et al. Preoperative evaluation of malignant liver tumors: comparison of unenhanced and SPIO (Resovist)-enhanced MR imaging with biphasic CTAP and intraoperative US. Eur Radiol. 2003; 13:262-272.

56. Tsaitas C, Semertzidou A, Sinakos E (April 2014). "Update on inflammatory bowel disease in patients with primary sclerosing cholangitis". World Journal of Hepatology.6 (4): 178–87.

57. Kobayashi M, Ikeda K, Saitoh S, Suzuki F, Tsubota A, Suzuki Y, Arase Y, Murashima N, Chayama K, Kumada H (June 2000). "Incidence of primary cholangiocellular carcinoma of the liver in Japanese patients with hepatitis C virus-related cirrhosis". Cancer. 88 (11): 2471–7.

58. Yamamoto S, Kubo S, Hai S, Uenishi T, Yamamoto T, Shuto T, Takemura S, Tanaka H, Yamazaki O, Hirohashi K, Tanaka T (July 2004). "Hepatitis C virus infection as a likely etiology of intrahepatic cholangiocarcinoma". Cancer Science. 95 (7): 592–5.

59. Lu H, Ye MQ, Thung SN, Dash S, Gerber MA (December 2000). "Detection of hepatitis C virus RNA sequences in cholangiocarcinomas in Chinese and American patients". Chinese Medical Journal. 113 (12): 1138–41.

60. Shaib YH, El-Serag HB, Davila JA, Morgan R, McGlynn KA (March 2005). "Risk factors of intrahepatic cholangiocarcinoma in the United States: a case-control study". Gastroenterology. 128 (3): 620–6.

61. Sorensen HT, Friis S, Olsen JH, Thulstrup AM, Mellemkjaer L, Linet M, Trichopoulos D, Vilstrup H, Olsen J (October 1998). "Risk of liver and other types of cancer in patients with cirrhosis: a nationwide cohort study in Denmark". Hepatology. 28 (4): 921–5.

62. Lipsett PA, Pitt HA, Colombani PM, Boitnott JK, Cameron JL (November 1994)."Choledochal cyst disease. A changing pattern of presentation". Annals of Surgery.220 (5): 644.

63. Dayton MT, Longmire WP, Tompkins RK (January 1983). "Caroli's Disease: a premalignant condition?". American Journal of Surgery. 145 (1): 41–8.

64. Mecklin JP, Järvinen HJ, Virolainen M (March 1992). "The association between cholangiocarcinoma and hereditary nonpolyposis colorectal carcinoma". Cancer. 69 (5): 1112–4.

65. Lee SS, Kim MH, Lee SK, Jang SJ, Song MH, Kim KP, Kim HJ, Seo DW, Song DE, Yu E, Lee SG, Min YI (February 2004). "Clinicopathologic review of 58 patients with biliary papillomatosis". Cancer. 100 (4): 783–93.

66. Lee CC, Wu CY, Chen GH (September 2002). "What is the impact of coexistence of hepatolithiasis on cholangiocarcinoma?". Journal of Gastroenterology and Hepatology. 17(9): 1015–20.

67. Su CH, Shyr YM, Lui WY, P'Eng FK (July 1997). "Hepatolithiasis associated with cholangiocarcinoma". British Journal of Surgery. 84 (7): 969–73.

68. Donato F, Gelatti U, Tagger A, Favret M, Ribero ML, Callea F, Martelli C, Savio A, Trevisi P, Nardi G (December 2001). "Intrahepatic cholangiocarcinoma and hepatitis C and B virus infection, alcohol intake, and hepatolithiasis: a case-control study in Italy". Cancer Causes & Control. 12 (10): 959–64.

69. Saini S (June 1997). "Imaging of the hepatobiliary tract". New England Journal of Medicine. 336 (26): 1889–94.

70. Sharma MP, Ahuja V (1999). "Aetiological spectrum of obstructive jaundice and diagnostic ability of ultrasonography: a clinician's perspective". Tropical Gastroenterology. 20 (4): 167–9.

71. Bloom CM, Langer B, Wilson SR (1999). "Role of US in the detection, characterization, and staging of cholangiocarcinoma". Radiographics. 19 (5): 1199–218.

72. Forner A, Llovet JM, Bruix J (2012). "Hepatocellular carcinoma". The Lancet. 379(9822): 1245–1255.

73. Kumar V, Fausto N, Abbas A, eds. (2015). Robbins & Cotran Pathologic Basis of Disease (9th ed.). Saunders. pp. 870–873.

74. Colli, A; Fraquelli, M; Casazza, G; Massironi, S; Colucci, A; Conte, D; Duca, P (March 2006). "Accuracy of ultrasonography, spiral CT, magnetic resonance, and alpha-fetoprotein in diagnosing hepatocellular carcinoma: a systematic review". The American Journal of Gastroenterology. 101 (3): 513–23.

75. El-Serag HB, Marrero JA, Rudolph L, Reddy KR (May 2008). "Diagnosis and treatment of hepatocellular carcinoma". Gastroenterology. 134 (6): 1752–63.

76. Kitagawa K, Matsui O, Kadoya M, et al: Hepatocellular carcinomas with excessive copper accumulation: CT and MR findings. Radiology 180:623–628, 1991

77. Miyayama S, Matsui O, Ueda K, et al: Hemodynamics of small hepatic focal nodular hyperplasia: Evaluation with single-level dynamic CT during hepatic arteriography. AJR Am J Roentgenol 174:1567–1569, 2000.

78. Ueda K, Matsui O, Kawamori Y, et al: Differentiation of hypervascular hepatic pseudolesions from hepatocellular carcinoma: Value of single-level dynamic CT during hepatic arteriography. J Comput Assist Tomogr 22:703–708, 1998

79. Ueda K, Matsui O, Kawamori Y, et al: Hypervascular hepatocellular carcinoma: Evaluation of hemodynamics with dynamic CT during hepatic arteriography. Radiology 206:161–166, 1998.

80. Gennisson JL, Deffieux T, Fink M, Tanter M. Ultrasound elastography: principles and techniques. Diagnostic and interventional imaging. 2013; 94: 487-95.

81. Cho SH, Lee JY, Han JK, Choi BI. Acoustic radiation force impulse elastography for the evaluation of focal solid hepatic lesions: preliminary findings. Ultrasound Med Biol 2010; 36:202–208.

82. Morikawa H, Fukuda K, Kobayashi S, Fujii H, Iwai S, Enomoto M, et al. Real-time tissue elastography as a tool for the noninvasive assessment of liver stiffness in patients with chronic hepatitis C. Journal of gastroenterology. 2011; 46: 350-8.

83. Yeh WC, Li PC, Jeng YM, et al. Elastic modulus measurements of human liver and correlation with pathology. Ultrasound Med Biol 2002; 28:467– 474.

84. Nightingale K. Acoustic Radiation Force Impulse (ARFI) Imaging: a Review. Current medical imaging reviews. 2011; 7: 328-39.

85. Tang A, Cloutier G, Szeverenyi NM, Sirlin CB. Ultrasound Elastography and MR Elastography for Assessing Liver Fibrosis: Part 1, Principles and Techniques. American journal of roentgenology. 2015; 205: 22-32.

86. Barr RG, Ferraioli G, Palmeri ML, Goodman ZD, Garcia-Tsao G, Rubin J, et al. Elastography Assessment of Liver Fibrosis: Society of Radiologists in Ultrasound Consensus Conference Statement. Radiology. 2015; 276: 845-61.

87. Ferraioli G, Filice C, Castera L, Choi BI, Sporea I, Wilson SR, et al. WFUMB Guidelines and Recommendations for Clinical Use of Ultrasound Elastography: Part 3: Liver. Ultrasound in medicine & biology. 2015; 41: 1161-79.

88. Itokawa F, Itoi T, Sofuni A, Kurihara T, Tsuchiya T, Ishii K, et al. EUS elastography combined with the strain ratio of tissue elasticity for diagnosis of solid pancreatic masses. J Gastroenterol 2011;46(6):843—53.

89. Onur MR, Poyraz AK, Ucak EE, Bozgeyik Z, Ozercan IH, Ogur E. Semiquantitative strain elastography of liver masses. J Ultrasound Med 2012;31(7):1061—7.

90. Zhang Y, Tang J, Li YM, Fei X, Lv FQ, He EH, et al. Differentiation of prostate cancer from benign lesions using strain index of transrectal real-time tissue elastography. Eur J Radiol 2012;81(5):857—62.

91. Zhao QL, Ruan LT, Zhang H, Yin YM, Duan SX. Diagnosis of solid breast lesions by elastography 5-point score and strain ratio method. Eur J Radiol 2012;81(11):3245—9.

92. Xing P, Wu L, Zhang C, Li S, Liu C, Wu C. Differentiation of benign from malignant thyroid lesions: calculation of the strain ratio on thyroid sonoelastography. J Ultrasound Med 2011;30(5):663—9.

93. Palmeri ML, Nightingale KR. What challenges must be overcome before ultrasound elasticity imaging is ready for the clinic? Imaging in medicine. 2011; 3: 433-44.

94. Cosgrove D, Piscaglia F, Bamber J, Bojunga J, Correas JM, Gilja OH, et al. EFSUMB guidelines and recommendations on the clinical use of ultrasound elastography. Part 2: Clinical applications. Ultraschall in der Medizin. 2013; 34: 238-53.

95. Tang A, Cloutier G, Szeverenyi NM, Sirlin CB. Ultrasound Elastography and MR Elastography for Assessing Liver Fibrosis: Part 2, Diagnostic Performance, Confounders, and Future Directions. American journal of roentgenology. 2015; 205: 33-40.

96. Park H, Park JY, Kim do Y, Ahn SH, Chon CY, Han KH, Kim SU. Characterization of focal liver masses using acoustic radiation force impulse elastography. World J Gastroenterol 2013; 19: 219-226.

97. Guo LH, Wang SJ, Xu HX, Sun LP, Zhang YF, Xu JM, Wu J, Fu HJ, Xu XH. Differentiation of benign and malignant focal liver lesions: value of virtual touch tissue quantification of acoustic radiation force impulse elastography. Med Oncol 2015; 32: 68.

98. Zhang P, Zhou P, Tian SM, Qian Y, Deng J, Zhang L. Application of acoustic radiation force impulse imaging for the evaluation of focal liver lesion elasticity. Hepatobiliary Pancreat Dis Int 2013; 12: 165-170.

99. Ronot M, Di Renzo S, Gregoli B, Duran R, Castera L, Van Beers BE, Vilgrain V. Characterization of fortuitously discovered focal liver lesions: additional information provided by shearwave elastography. Eur Radiol 2015; 25: 346-358.

100. Shuang-Ming T, Ping Z, Ying Q, Li-Rong C, Ping Z, Rui-Zhen L. Usefulness of acoustic radiation force impulse imaging in the differential diagnosis of benign and malignant liver lesions. Acad Radiol 2011; 18(7): 810-5.

101. Yu H, Wilson SR. Differentiation of benign from malignant liver masses with acoustic radiation force impulse technique. Ultrasound Q 2011; 27(4): 217-23.

102. Kapoor A, Kapoor A, Mahajan G, Sidhu BS, Lakhanpal VP. Real-time elastography in differentiating metastatic from nonmetastatic liver nodules. Ultrasound Med Biol 2011; 37(2): 207-13.

103. Lu Q, Ling W, Lu C, et al. Hepatocellular carcinoma: stiffness value and ratio to discriminate malignant from benign focal liver lesions. Radiology 2015; 275(3): 880-8.

104. Heide R, Strobel D, Bernatik T, Goertz RS. Characterization of focal liver lesions (FLL) with acoustic radiation force impulse (ARFI) elastometry. Ultraschall Med 2010;31(4):405—9.

105. Davies G, Koenen M. Acoustic radiation force impulse elastography in distinguishing hepatic haemangiomata from metastases: preliminary observations. Br J Radiol 2011;84(1006): 939—43.

106. Frulio N, Laumonier H, Carteret T, Laurent C, Balabaud C, Bioulac-Sage P, et al. Evaluation of liver tumors using ARFI (acoustic radiation force impulse imaging) elastography and correlation with histology. J Ultrasound Med 2013; 32:121—30.

107. Leen E, Ceccotti P, Kalogeropoulou C, Angerson WJ, Moug SJ, Horgan PG. Prospective multicenter trial evaluating a novel method of characterizing focal liver lesions using contrast-enhanced sonography. AJR Am J Roentgenol 2006; 186:1551–1559.

108. Hardie AD, Naik M, Hecht EM, et al. Diagnosis of liver metastases: value of diffusion-weighted MRI compared with gadolinium-enhanced MRI. Eur Radiol 2010; 20:1431–1441.

ABBREVIATIONS

USG	-	Ultrasonography
CT	-	Computed Tomography
MDCT	-	Multi Detector Computed Tomography
CECT	-	Contrast Enhanced Computed Tomography
MRI	-	Magnetic Resonance Imaging
SPECT	-	Single Photon Emission Computed Tomography
CEUS	-	Contrast Enhanced Ultrasound
FLL	-	Focal Liver Lesion
FNH	-	Focal nodular hyperplasia
HCC	-	Hepatocellular carcinoma
CCC	-	Cholangiocellular Carcinoma
HPE	-	Histopathological Examination
lb	-	pounds
ROI	-	Region of Interest
RBC	-	Red blood cells

GD-DTPA	-	Gadolinium- Diethylene Triamine Penta Acetic acid
T1W	-	T1 weighted
T2W	-	T2 weighted
TE	-	Echo time
GIT	-	Gastro Intestinal Tract
CTAP	-	Computed Tomography during Arterial Portography
CTHA	-	Computed Tomography during Hepatic Arteriography
DWI	-	Diffusion Weighted Imaging
ADC	-	Apparent Diffusion Coefficient
HBV	-	Hepatitis B Virus
HCV	-	Hepatitis C Virus
AFP	-	Alpha Fetoprotein
NASH	-	Non-Alcoholic Steato Hepatitis
USE	-	Ultrasound Elastography
Eqn	-	Equation

SWI	-	Shear Wave Imaging
1DTE	-	One Dimensional Transient Elastography
pSWE	-	Point Shear Wave Elastography
2DSWE	-	2-Dimensional Shear Wave Elastography
SE	-	Strain Elastography
ARFI	-	Acoustic Radiation Force Impulse
SWV	-	Shear Wave Velocity
VTTQ	-	Virtual Touch Tissue Quantification
MHz	-	Mega Hertz
ROC	-	Receiver Operator Characteristic Curve
AUC	-	Area Under the Curve
kPa	-	kilopascals
m/s	-	meter per second
n	-	sample

PROFORMA

"EFFICACY OF ULTRASOUND ELASTOGRAPHY IN CHARACTERIZING FOCAL LIVER LESIONS WITH HISTOPATHOLOGIC CORRELATION"

SI. No:

Name:

Age/Sex:

Occupation:

Address:

Presenting Complaints:

Past H/O:

Clinical Examination:

Other Investigations:

USG /CT/MRI Findings:

IMAGING FINDINGS:

B MODE		STIFFNESS VALUE (kPa)	SWV (m/s)	STRAIN INDEX
BACKGROUND LIVER				
Normal	Cirrhosis			
LESION				
No. of lesions				
Echogenicity				
Vascularity				
Portal vein Involvement				

HPE REPORT:

PATIENT INFORMATION SHEET

We are conducting a study on "**EFFICACY OF ULTRASOUND ELASTOGRAPHY IN CHARACTERIZING FOCAL LIVER LESIONS WITH HISTOPATHOLOGIC CORRELATION**"

- Your cooperation would be valuable for the same
- The privacy of patients in the research will be maintained throughout the study. In the event of any publication or presentation resulting from the research, no personally identifiable information will be shared.
- Taking part of the study is voluntary. You are free to decide whether to participate in this study or to withdraw at any time. Your decision will not result in any loss of benefits to which you are otherwise entitled.
- The result of the special study may be intimated to you at the end of the study period or during the study if anything is found abnormal which may aid in the management or treatment.

Signature of the Investigator Signature of Participant

(Dr.K.B. NAGARAJAN)

Date:

PATIENT INFORMED CONSENT FORM

Title of the study**:** "**EFFICACY OF ULTRASOUND ELASTOGRAPHY IN CHARACTERIZING FOCAL LIVER LESIONS WITH HISTOPATHOLOGIC CORRELATION"**

Name of the Participant: DATE:

AGE: SEX: ID NO:

I have read the information in this form (or it has been read to me).

I have read and understood this consent form and the information provided to me.

I have had the consent document explained to me.

I have been explained about the nature of the study.

I have been explained about my rights and responsibilities by the investigator.

I have been explained that there are no risks associated with my participation in this study. *

I am aware of the fact that I can opt out of the study at any time without having to give any reason and this will not affect my future treatment in this hospital. *

I am also aware that the investigator may terminate my participation in the study at any time, for any reason, without my consent. *

I hereby give permission to the investigators to release the information obtained from me as result of participation in this study. I understand that they are publicly presented.

I have understood that my identity will be kept confidential.

I have had my questions answered to my satisfaction.

I have decided to be in the research study.

By signing this consent form I attest that the information given in this document has been clearly explained to me and understood by me, I will be given a copy of this consent document.

Name _____

Signature_____

ஆராய்ச்சி தகவல் தாள்

கல்லீரல் கட்டிகளின் திசுப்பரிசோதனை முடிவுகளுடன் ஒப்பிட்டு, அல்ட்ரா சவுண்ட் எலாஸ்டோக்ராபி முறை மூலம் அவற்றின் கடின அளவைக் கொண்டு, அவற்றின் தன்மையைக் கண்டறிதல்

மேற்கண்ட ஆராய்ச்சியானது, சென்னை மருத்துவக் கல்லூரியில், அல்ட்ரா சவுண்ட் ஸ்கேன் மூலம் கண்டறியப்பட்ட கல்லீரல் கட்டி இருக்கும் நபர்களிடம் மேற்கொள்ளப்படுகிறது.

அல்ட்ரா சவுண்ட் ஸ்கேன் மூலம் கல்லீரல் கட்டி இருப்பதாக கண்டறியப்பட்ட நபர்கள், அல்ட்ரா சவுண்ட் எலாஸ்டோக்ராபி ஸ்கேன் எனப்படும் பரிசோதனைக்கு உட்படுத்தப்படுவர். அதன் மூலம் பெறப்படும் துப்புகள், சதை பரிசோதனையின் முடிவுகளோடு ஒப்பிட்டுப்பார்க்கப்படும். இந்த தகவல்கள் கல்லீரல் கட்டியின் தன்மையை பற்றி அறிய உதவும். கல்லீரல் கட்டியின் தன்மையை முன்னரே அறிவதன் மூலம் அதற்கான சிகிச்சை முறைகளையும், சிகிச்சை பலன்களையும் முன் கணிக்க முடியும். தங்களுடைய பங்களிப்பும் ஒத்துழைப்பும் ஆராய்ச்சி நன்முறையில் வெற்றி பெற பெரிதும் உதவியாக அமையும்.

நீங்களும் இந்த ஆராய்ச்சியில் பங்கேற்க நாங்கள் விரும்புகிறோம் . இந்த ஆராய்ச்சியில் உங்களுக்கு பரிசோதனைகள் செய்து அதன் தகவல்களை ஆராய்வோம் .அதனால் தங்களது நோயின் ஆய்வறிக்கையோ அல்லது சிகிச்சையோ பாதிப்பு ஏற்படாது என்பதையும் தெரிவித்துகொள்கிறோம் .

முடிவுகளை அல்லது கருத்துகளை வெளியிடும்போதோ அல்லது ஆராய்ச்சியின் போதோ தங்களது பெயரையோ அல்லது அடையாளங்களையோ வெளியிட மாட்டோம் என்பதையும் தெரிவித்து கொள்கிறோம் .

இந்த ஆராய்ச்சியில் பங்கேற்பது தங்களுடைய விருப்பத்தின் பேரில் தான் இருக்கிறது . மேலும் நீங்கள் எந்நேரமும் இந்த ஆராய்ச்சியிலிருந்து பின்வாங்கலாம் என்பதையும் தெரிவித்துக் கொள்கிறோம் .

இந்த சிறப்பு பரிசோதனையின் முடிவுகளை ஆராய்ச்சியின்போது அல்லது ஆராய்ச்சியின் முடிவின் போது தங்களுக்கு அறிவிக்கப்படும் என்பதையும் தெரிவித்துக் கொள்கிறோம் .

ஆராய்ச்சியாளர் கையொப்பம் **பங்கேற்பாளர் கையொப்பம்**

நாள் :

இடம் :

<u>ஆராய்ச்சி ஒப்புதல் கடிதம்</u>

ஆராய்ச்சி தலைப்பு

<u>கல்லீரல் கட்டிகளின் திசுப்பரிசோதனை முடிவுகளுடன் ஒப்பிட்டு, அல்ட்ரா சவுண்ட் எலாஸ்டோக்ராபி முறை மூலம் அவற்றின் கடின அளவைக் கொண்டு, அவற்றின் தன்மையைக் கண்டறிதல்</u>

பெயர் :

வயது :

பாலினம் :

இந்த ஆய்வு , அல்ட்ரா சவுண்ட் எலாஸ்டோக்ராபி முறை மூலம் கல்லீரல் கட்டிகளின் கடின அளவைக் கொண்டு, அவற்றின் தன்மையை அறுவை சிகிச்சைக்கு முன்னரே அறிய உதவும் என்பதை அறிவேன் .

இந்த ஆராய்ச்சியின் விவரங்களும் அதன் நோக்கங்களும் முழுமையாக எனக்கு தெளிவாக விளக்கப்பட்டது . எனக்கு விளக்கப்பட்ட விஷயங்களை நான் புரிந்துகொண்டு எனது சம்மதத்தை தெரிவிக்கிறேன் .

இந்த ஆராய்ச்சியில் பிறரின் நிர்பந்தமின்றி என் சொந்த விருப்பத்தின் பேரில் பங்கு பெறுகின்றேன் .

நான் என்னுடைய சுய நினைவுடனும் மற்றும் முழு சுதந்திரத்துடனும் இந்த மருத்துவ ஆராய்ச்சியில் என்னை சேர்த்துக்கொள்ள சம்மதிக்கிறேன் .

தேதி : **பங்கேற்பாளர் கையொப்பம்**

MASTER CHART

S.NO	AGE	SEX	HPE REPORT	NO. OF LESIONS	LESION ECHOGENECITY	VASCULARITY	BACKGROUND LIVER	PORTAL VEIN INVOLVEMENT	STIFFNESS VALUE OF LESION(kPa)	STIFFNESS VALUE OF BACKGROUND LIVER(kPa)	STIFFNESS RATIO	SWV OF LESION	SWV OF BACKGROUND	STRAIN RATIO
1	56	M	HCC	SINGLE	HYPO-ECHOIC	NORMAL	CIRRHOSIS	NO	14.6	44.2	0.3	2.3	2.9	2.83
2	59	M	HCC	SINGLE	HETERO-ECHOIC	INCREASED	CIRRHOSIS	NO	63.9	67.9	0.9	1.9	2.3	2.75
3	48	M	HCC	SINGLE	HYPO-ECHOIC	NORMAL	NORMAL	NO	28.9	7.5	3.9	2.6	2.4	3.46
4	61	M	HCC	SINGLE	HETERO-ECHOIC	INCREASED	CIRRHOSIS	NO	26.7	31.3	0.9	3.0	2.1	3.11
5	45	M	HCC	SINGLE	HETERO-ECHOIC	INCREASED	CIRRHOSIS	YES	24.9	45.8	0.5	2.6	2.0	3.24
6	67	M	HCC	SINGLE	HETERO-ECHOIC	INCREASED	CIRRHOSIS	YES	37.9	18.9	2.0	2.1	2.8	2.94
7	70	M	HCC	MULTIPLE	HETERO-ECHOIC	INCREASED	CIRRHOSIS	NO	56.8	12.1	4.7	2.2	2.7	5.5
8	58	M	HCC	MULTIPLE	HYPO-ECHOIC	NORMAL	CIRRHOSIS	NO	43.7	45.9	1.0	1.8	2.1	3.15
9	55	M	HCC	MULTIPLE	HETERO-ECHOIC	INCREASED	CIRRHOSIS	NO	22.8	30.5	0.7	1.7	2.4	2.85
10	49	M	HCC	SINGLE	HETERO-ECHOIC	INCREASED	CIRRHOSIS	NO	37.9	38.1	1.0	2.4	2.0	3.56
11	52	M	HCC	SINGLE	HETERO-ECHOIC	INCREASED	NORMAL	YES	38.6	6.7	5.8	2.0	2.9	3.64
12	63	M	HCC	SINGLE	HETERO-ECHOIC	INCREASED	NORMAL	YES	24.9	6.8	3.7	2.3	2.1	2.84
13	45	M	HCC	SINGLE	HETERO-ECHOIC	INCREASED	CIRRHOSIS	YES	14.9	21.1	0.7	1.9	2.5	3.38
14	35	M	HEMANGIOMA	MULTIPLE	HYPER-ECHOIC	NORMAL	NORMAL	NO	5.6	7.9	0.7	1.1	1.4	0.89
15	47	M	HEMANGIOMA	MULTIPLE	HYPER-ECHOIC	NORMAL	NORMAL	NO	11.6	6.9	1.7	1.6	1.7	0.82
16	28	M	HEMANGIOMA	SINGLE	HYPER-ECHOIC	NORMAL	NORMAL	NO	12.9	8.9	1.4	1.2	1.2	1.01
17	38	M	HEMANGIOMA	SINGLE	HYPER-ECHOIC	INCREASED	NORMAL	NO	8.93	6.2	1.4	1.0	1.2	0.86
18	50	M	HEMANGIOMA	SINGLE	HYPER-ECHOIC	NORMAL	NORMAL	NO	18.6	7.9	2.4	1.8	1.7	1.34
19	45	M	HEMANGIOMA	SINGLE	HYPER-ECHOIC	INCREASED	NORMAL	NO	17.5	9.7	1.8	1.1	1.2	0.88
20	36	M	HEMANGIOMA	SINGLE	HYPER-ECHOIC	NORMAL	NORMAL	NO	12.6	5.6	2.3	1.3	1.5	0.83
21	72	M	METASTASIS	MULTIPLE	HETERO-ECHOIC	NORMAL	NORMAL	NO	8.98	7.9	1.1	3.1	1.9	3.67
22	64	M	METASTASIS	MULTIPLE	HETERO-ECHOIC	NORMAL	NORMAL	NO	23.8	12.3	1.9	3.5	1.7	2.89
23	77	M	METASTASIS	MULTIPLE	HETERO-ECHOIC	NORMAL	NORMAL	NO	54.2	5.6	9.7	1.9	1.9	3.45
24	59	M	METASTASIS	MULTIPLE	HETERO-ECHOIC	NORMAL	NORMAL	NO	16.4	5.3	3.1	2.4	2.3	2.89
25	75	M	METASTASIS	MULTIPLE	HETERO-ECHOIC	NORMAL	NORMAL	NO	22.6	7.6	3.0	2.6	2.1	3.02
26	66	M	METASTASIS	MULTIPLE	HETERO-ECHOIC	NORMAL	NORMAL	NO	29.4	5.1	5.8	2.3	2.0	3.31
27	53	M	METASTASIS	MULTIPLE	HETERO-ECHOIC	NORMAL	NORMAL	NO	43.6	6.2	7.0	3.4	1.8	2.92
28	49	M	METASTASIS	MULTIPLE	HETERO-ECHOIC	NORMAL	NORMAL	NO	26.8	7.2	3.7	2.7	2.2	2.86
29	58	M	METASTASIS	MULTIPLE	HETERO-ECHOIC	NORMAL	NORMAL	NO	67.5	8.1	8.3	2.1	2.3	3.46
30	65	M	METASTASIS	MULTIPLE	HETERO-ECHOIC	NORMAL	NORMAL	NO	44.2	6.2	7.1	1.7	1.8	3.27
31	58	M	METASTASIS	MULTIPLE	HETERO-ECHOIC	NORMAL	NORMAL	NO	26.2	6.1	4.3	2.0	2.1	3.08
32	73	M	METASTASIS	MULTIPLE	HETERO-ECHOIC	NORMAL	NORMAL	NO	33.6	7.6	4.4	1.9	2.4	3.21
33	68	M	METASTASIS	MULTIPLE	HETERO-ECHOIC	NORMAL	NORMAL	NO	29.6	6.2	4.8	3.5	2.1	3.66
34	61	M	METASTASIS	MULTIPLE	HETERO-ECHOIC	NORMAL	NORMAL	NO	13.5	5.4	2.5	2.6	2.2	3.52
35	78	M	METASTASIS	MULTIPLE	HETERO-ECHOIC	NORMAL	NORMAL	NO	18.6	9.6	1.9	3.0	2.0	2.97
36	60	M	CHOLANGIOCARCINOMA	SINGLE	HETERO-ECHOIC	NORMAL	NORMAL	NO	28.6	8.6	3.3	2.6	2.4	4.01
37	66	M	CHOLANGIOCARCINOMA	SINGLE	HETERO-ECHOIC	NORMAL	NORMAL	NO	46.4	8.2	5.7	2.1	2.0	4.39
38	31	F	FNH	SINGLE	HYPO-ECHOIC	NORMAL	NORMAL	NO	4.6	5.1	0.90	2.40	1.80	1.86
39	55	F	METASTASIS	MULTIPLE	HETERO-ECHOIC	NORMAL	NORMAL	NO	16.4	10.1	1.6	2.6	2.4	2.85
40	68	F	METASTASIS	MULTIPLE	HETERO-ECHOIC	NORMAL	NORMAL	NO	16.8	6.1	2.8	2.9	1.9	3.33
41	53	F	METASTASIS	MULTIPLE	HETERO-ECHOIC	NORMAL	NORMAL	NO	13.6	8.6	1.6	2.2	1.8	3.69
42	74	F	METASTASIS	MULTIPLE	HETERO-ECHOIC	NORMAL	NORMAL	NO	19.7	5.9	3.3	2.1	2.0	3.77
43	80	F	METASTASIS	MULTIPLE	HETERO-ECHOIC	NORMAL	NORMAL	NO	6.8	5	1.4	2.8	2.1	3.65
44	67	F	METASTASIS	MULTIPLE	HETERO-ECHOIC	NORMAL	NORMAL	NO	52.4	7.7	6.8	3.4	2.2	3.89
45	75	F	HCC	SINGLE	HETERO-ECHOIC	INCREASED	NORMAL	YES	82.1	6.9	11.9	2.1	2.1	3.01
46	58	F	HCC	SINGLE	HYPO-ECHOIC	NORMAL	CIRRHOSIS	NO	44.9	52.2	0.9	2.7	2.6	3.23
47	35	F	HEMANGIOMA	SINGLE	HYPER-ECHOIC	NORMAL	NORMAL	NO	6.9	5.8	1.2	1.6	1.8	1.04
48	27	F	HEMANGIOMA	SINGLE	HYPER-ECHOIC	NORMAL	NORMAL	NO	5.7	5.1	1.1	1.7	1.8	1.11
49	66	F	CHOLANGIOCARCINOMA	SINGLE	HETERO-ECHOIC	NORMAL	NORMAL	NO	39.7	6.4	6.2	2.8	2.5	3.96
50	45	F	FNH	SINGLE	HYPO-ECHOIC	NORMAL	NORMAL	NO	13.2	6.2	2.13	2.10	2.10	1.63

ETHICS COMMITTEE APPROVAL LETTER

INSTITUTIONAL ETHICS COMMITTEE
MADRAS MEDICAL COLLEGE, CHENNAI 600 003

EC Reg.No.ECR/270/Inst./TN/2013
Telephone No.044 25305301
Fax: 011 25363970

CERTIFICATE OF APPROVAL

To
Dr.K.B.Nagarajan
Post Graduate in MDRD
Department of Radio-Diagnosis
MMC/RGGGH
Chennai 600 003

Dear Dr.K.B.Nagarajan,

The Institutional Ethics Committee has considered your request and approved your study titled **"EFFICACY OF ULTRASOUND ELASTOGRAPHY IN CHARACTERIZING FOCAL LIVER LESIONS WITH HISTOPATHOLOGIC CORRELATION" - NO.08122017**

The following members of Ethics Committee were present in the meeting hold on **05.12.2017** conducted at Madras Medical College, Chennai 3

1. Prof.P.V.Jayashankar :Chairperson
2. Prof.R.Narayana Babu,MD.,DCH., Dean,MMC,Ch-3 : Deputy Chairperson
3. Prof.Sudha Seshayyan,MD., Vice Principal,MMC,Ch-3 : Member Secretary
4. Prof.N.Gopalakrishnan,MD,Director,Inst.of Nephrology,MMC,Ch : Member
5. Prof.S.Mayilvahanan,MD,Director,Inst. of Int.Med,MMC, Ch-3 : Member
6. Prof.A.Pandiya Raj,Director, Inst. of Gen.Surgery,MMC : Member
7. Prof.Shanthy Gunasingh, Director, Inst.of Social Obstetrics,KGH : Member
8. Prof.Rema Chandramohan,Prof.of Paediatrics,ICH,Chennai : Member
9. Prof. Susila, Director, Inst. of Pharmacology,MMC,Ch-3 : Member
10. Prof.K.Ramadevi,MD., Director, Inst. of Bio-Chemistry,MMC,Ch-3 : Member
11. Prof.Bharathi Vidya Jayanthi,Director, Inst. of Pathology,MMC,Ch-3: Member
12. Thiru S.Govindasamy, BA.,BL,High Court,Chennai : Lawyer
13. Tmt.Arnold Saulina, MA.,MSW., :Social Scientist
14. Thiru K.Ranjith, Ch- 91 : Lay Person

We approve the proposal to be conducted in its presented form.

The Institutional Ethics Committee expects to be informed about the progress of the study and SAE occurring in the course of the study, any changes in the protocol and patients information/informed consent and asks to be provided a copy of the final report.

Member Secretary - Ethics Committee

URKUND

Urkund Analysis Result

Analysed Document:	Nagarajan Thesis Final for Plagiarism.docx (D42484153)
Submitted:	10/12/2018 3:23:00 PM
Submitted By:	nagarajankb@yahoo.in
Significance:	4 %

Sources included in the report:

ELASTOGRAPHY CERVICL LYMPH NODES.docx (D31102745)
https://www.researchgate.net/publication/271591677_Hepatocellular_Carcinoma_Stiffness_Value_and_Ratio_to_Discriminate_Malignant_from_Benign_Focal_Liver_Lesions

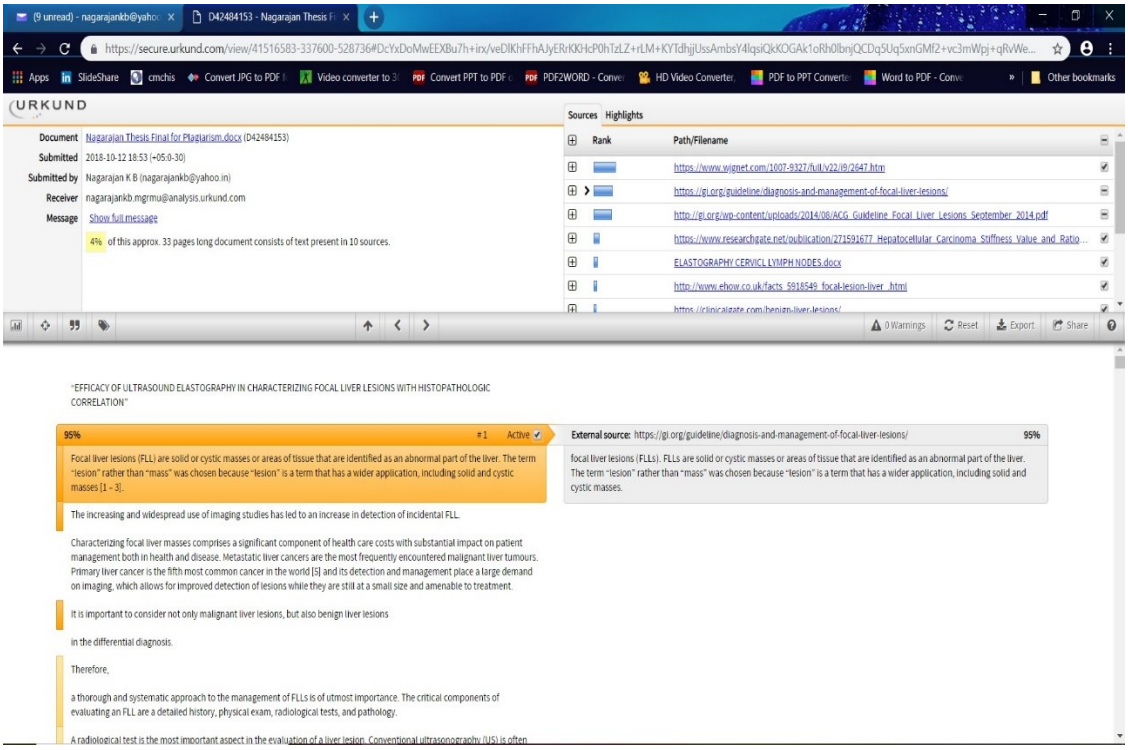

PLAGIARISM CERTIFICATE

This is to certify that this dissertation work titled **"EFFICACY OF ULTRASOUND ELASTOGRAPHY IN CHARACTERIZING FOCAL LIVER LESIONS WITH HISTOPATHOLOGIC CORRELATION"** of the candidate **Dr.NAGARAJAN.K.B.** with registration Number **201618003** for the award of **M.D RADIODIAGNOSIS** in the branch of **VIII**. I personally verified the urkund .com website for the purpose of plagiarism check. I found that the uploaded thesis file contains from introduction to conclusion pages and result shows **4 percentage** of plagiarism in the dissertation.

Guide & Supervisor sign with Seal